The Role of Gamma-Synuclein in Mammary Gland Tumourigenesis

Essam Sharfeddin

Submitted for the award of Doctor of Philosophy,

December 2012

Declaration

This work has not been submitted in substance for any other degree or award at this or any other university or place of learning, nor is being submitted concurrently in candidature for any degree or other award.

Signed  Date: 21/12/2012

STATEMENT 1

This thesis is being submitted in partial fulfillment of the requirements for the degree of PhD.

Signed  Date: 21/12/2012

STATEMENT 2

This thesis is the result of my own independent work/investigation, except where otherwise stated. Other sources are acknowledged by explicit references. The views expressed are my own.

Signed  Date: 21/12/2012

STATEMENT 3

I hereby give consent for my thesis, if accepted, to be available for photocopying and for inter-library loan, and for the title and summary to be made available to outside organizations.

Signed  Date: 21/12/2012

Acknowledgement

I am deeply grateful to my supervisor Prof Vladimir Buchman for his wise scientific guidance, encouragement and patience. I am also indebt to Dr Natalia Ninkina for her excellent supervising and teaching of laboratory techniques needed throughout. Special thanks are also due to Dr Richard Clarkson for providing helpful discussions, insights and continuous support.

I would like to thank Dr Trevor Hay for help with tumour samples, Mr Derek Scarborough for help with histology work and all people on the 4th and 5th floors of the Biosciences Building for their patience and support.

I am forever grateful to all my family members, specially my parents, who endlessly supported me throughout my life and made me the man I am today. I am especially grateful to my wife for years of devotion and endless support, and for standing by me during the good times and bad. I cannot adequately express my feelings towards my beloved children Sharfeddin, Shadar, Suad and Ibrahim for their love and support, and for putting a smile on my face and making me a proud father.

Abstract

γ-synuclein is the third and last discovered member of the synuclein family, it is expressed mostly in the nervous system and its physiological function is still unknown. γ-synuclein has been claimed to play a role in mammary gland tumourigenesis as its overexpression in cancer cells was shown to inhibit apoptosis and stimulate growth, proliferation, survival, motility and metastasis. However, the role of endogenous γ-synuclein in mammary gland tumourigenesis has not been studied in an appropriate *in vivo* model. The results obtained in this study show that γ-synuclein is not required for the normal development of the mammary gland at any developmental stage - embryonic, pubertal or reproductive. Furthermore, ablation of γ-synuclein did not prevent induction of mammary gland tumours by activated ErbB2 transgene in mammary gland epithelium. Unexpectedly, transgenic activated ErbB2 hemizygous, γ-synuclein knockout female mice developed slightly more tumours with a significantly shorter tumour latency than the wild type littermates. These animals also exhibited similar tumour growth rates and metastases to the lungs, and a slightly shorter survival. Overall, a trend for accelerated tumourigenesis in the absence of γ-synuclein was observed. Thus, it is feasible that the aberrant expression of γ-synuclein reported in advance-stage tumours and metastases reflects activation of pathways aimed at repressing rather than enhancing tumourigenesis, as widely thought. Future studies will clarify the role of γ-synuclein in ErbB2-induced mammary gland tumourigenesis.

Contents

List of figures and tables

Abbreviations

AD	Alzheimer’s disease
AP1	activator protein 1
ATF3	activating transcription factor 3
ATGL	adipose triglyceride lipase
BAD	Bcl2-associated death promoter
BAK	Bcl-2 homologous antagonist/killer
Bax	Bcl-2–associated X protein
Bcl-2	B-cell lymphoma 2
Bcl-2L11/Bim	Bcl2-like protein 11
BCSG1	breast cancer-specific gene1
BMP4	bone morphogenetic protein 4
BMPR1A	bone morphogenetic protein receptor1A
C/EBP-β	CCAAT/enhancer binding protein-β
Cat-D	cathepsin D
Ccnd1	cyclin-D1
CDC42	cell division control protein 42
c-MAF	V-maf musculoaponeurotic fibrosarcoma oncogene homolog
CNS	central nervous system
CREB-1	c-AMP responsive element binding protein 1
CSP-α	cysteine-string protein alpha
Cx26	connexin-26

DA	dopamine
DAG	diacylglycerol
DFS	disease-free survival
DHA	docosahexaenoic acid
DLB	dementia with Lewy bodies disease
DNMT3B	DNA methyl transferase3B
E	estrogen
E2	estradiol
ECM	extracellular matrix
EGF	epidermal growth factor
eGFP	enhanced green fluorescent protein
EGFR	epidermal growth factor receptor
ER	endoplasmic reticulum
ERK	extracellular-regulated kinase
ER-α	estrogen receptor-α
ER-β	estrogen receptor -β
ESCC	esophageal squamous cell carcinoma
FACS	fluorescence-activated cell sorting
FasL	TNF (tumour necrosis factor) Fas ligand
FGF	fibroblast growth factor
FGFR2b	FGF receptor 2b
GATA3	GATA DNA sequence-binding proteins

GPCR	G protein-coupled receptor
GRK	GPCR kinases
hDAT	human presynaptic dopamine transporter
Hey1	hairy/enhancer-of-split related with YRPW motif protein 1
HFD	high fat diet
HGF	hepatocyte growth factor
Hh	hedgehog
Hsp	heat shock protein
IGF-2	insulin growth factor 2
IGFBP5	insulin-like growth factor binding protein 5
IKK-β	inhibitor of nuclear factor kappa-B kinase subunit beta
IL13	interleukin 13
IL4	interleukin 4
IP3	inositol 1,4,5 trisphosphate
JNK	c-Jun N-terminal kinase
KO	knockout
Lef1	lymphoid enhancer-binding factor 1
LFD	low fat diet
LIF	leukaemia inhibitory factor
MAP2	microtubule-associated protein 2
MAPK	mitogen-activated protein kinase
MEC	mammary epithelial cells

MECP2	methyl CpG binding protein 2
MEF	mouse embryonic fibroblasts
MEK1/2	mitogen-activated protein kinase kinase
MFGE-8	milk fat globule-EGF factor 8
MMP	matrix metalloproteinases
MMTV	mouse mammary tumour virus
MSA	multiple system atrophy
NAC	non-amyloid component
NEFA	non-esterified fatty acids
NET	norepinephrine transporter
NF-κB	nuclear factor kappa-light-chain-enhancer of activated B cells
NICD	notch intracellular domain
Nrg3	neuregulin3
OS	overall survival
p63	tumour protein p63
PD	Parkinson’s disease
Pg	progesterone
PgR	progesterone receptor
PIP2	phosphatidylinositol 4,5-bisphosphate
PKB/AKT	protein kinase B
PKC	protein kinase C
PLCβ2	phospholipase Cβ2

PMCA2	plasma membrane Ca^{2+}-ATPase
PNP-14	phosphoneuroprotein-14
PPARγ	peroxisome proliferator-activated receptor-gamma
Prl	prolactin
PrlR	prolactin receptor
PtdEtn	phosphatidylethanolamine
PtdSer	phosphatidylserine
PTHrP	parathyroid hormone-related protein
RAC	ras-related C3 botulinum toxin substrate
RankL	receptor activator of nuclear factor kappa-B ligand
ROBO1	roundabout homolog protein 1
SCAT	subcutaneous adipose tissue
SERT	serotonin transporter
SGP2	clusterin/sulphated glycoprotein-2
shRNA	short hairpin RNA
SLIT2	slit homolog 2 protein
SNARE	N-ethylmaleimide–sensitive factor attachment protein receptor
SNPs	single nucleotide polymorphisms
Socs5	suppressor of cytokine signalling 5
STAT6	signal transducer and activator of transcription 6
TAG	triacylglycerol
TCEA1	transcription elongation factor A protein 1

TEB	terminal end bud
TF	transcription factor
TFF1/PS2	trefoil factor 1
TGF-β1	transforming growth factor β1
TH	tyrosine hydroxylase
Th1/Th2	T helper 1/T helper 2 cells
TNF	tumour necrosis factor
TNFR1	tumour necrosis factor receptor
TRAIL	TNF-related apoptosis-inducing ligand
TWEAK	TNF-like weak inducer of apoptosis
VAMP2	vesicle-associated membrane protein 2
VAT	visceral adipose tissue
WAT	white adipose tissue
WKY	Wistar-Kyoto
Wnt	wingless/integrin
Wt	wild type
α/β-synuclein KO	α- and β-synuclein double-KO mice

Chapter 1. General Introduction

1.1. Breast cancer facts

Breast cancer is the most common type of cancer in women worldwide. Approximately 1.38 million women were diagnosed in the year 2008, accounting for nearly 23% of all diagnosed cancers. In the UK alone, 48788 cases were diagnosed in the year 2009 (48417 in women and 371 in men), accounting for nearly 16% of all cancers. In the year 2010, breast cancer killed 11556 women and 77 men (CancerResearchUK, 2012). Combating the disease includes different types of treatments. Some treatments are general in the sense that they are directed against any tumour for the purpose of either surgically removing or killing the mass of uncontrollably dividing cancerous cells. These include surgical intervention, chemotherapy, radiotherapy or, as often the case is, a combination of these. Other treatments are directed against certain types of breast tumours. Hormonal therapy is aimed at tumours that are hormone positive, namely estrogen receptor (ER) and progesterone receptor (PR) expressing tumours, e.g, tamoxifen and aromataze inhibitors. Immunotherapy is directed against tumours that express certain molecules, such as the monoclonal antibody Trastuzumab that targets ErbB2 positive tumours and Bevacizumab that targets VEGF positive tumours (Widakowich et al., 2007).

Despite the moderate success achieved in the overall survival rates, most patients undergo recurrence largely due to resistance that tumours eventually develop to drugs. Moreover, these drugs give rise to side effects that may complicate the treatment and limit the advantages to certain people than others. Needless to say, success in improving the effectiveness of the existing treatments, developing better ones and hopefully curing cancer would ultimately come from increased knowledge of the disease, especially at the cellular and molecular levels. Intensive research in

basic and cancer biology has identified many key molecules involved in the development of cancer, some of which led to the development of new targeted therapies as exemplified above. One possible target claimed by some researchers to play a role in breast cancer is a small cytosolic protein called gamma-synuclein (γ-synuclein) that belongs to the synuclein family. Before reviewing available literature on the possible role of γ-synuclein in mammary gland tumourigenesis, and to provide better context for this thesis, an overview to both the mammary gland and the synuclein family will be presented first.

1.2. An overview of mammary gland structure and development

The mammary gland is thought to have evolved from an ancient apocrine gland for the ultimate function of nourishing the newborn mammal through the production and secretion of milk (Oftedal, 2002). The lactating mammary gland also contributes immune factors in milk it produces in order to help protect the young against infection. In addition, breast feeding provides a close physical contact between the young and the mother which provides developmental benefits (Peaker, 2002). Structurally, the mammary gland is a complex secretory organ that is composed of a network of branching ducts of epithelial cells residing in a structurally and functionally supporting stroma. The ducts consist of two types of epithelial cells: basal, contractile myoepithelial cells and luminal cells. The myoepithelial cells form a contractile outer layer that helps expel the milk secreted by the underneath luminal cells. This cell layer also produces the basement membrane which forms a boundary with the surrounding complex stroma. The luminal cells form the inner cell layer in the ducts and alveoli that produce and secrete the nourishing milk during lactation (Watson and Khaled, 2008).

The stroma does not just act as a scaffold that supports the branching ducts for proper functioning. It houses a heterogenous group of cells including adipocytes that form most of the fat pad, mesenchymal cells, fibroblasts, endothelial cells forming the blood vessels and many types of immune cells (Watson and Khaled, 2008). These stromal components hold bidirectional interactions with the ductal epithelial cells to orchestrate the complex developmental processes that drive mammary gland development. Figure 1.1 below shows the morphology of a bifurcating terminal end

bud (TEB) and a trailing duct with a forming side-branch. The role of TEBs in the elongation and proliferation of ducts will be discussed later.

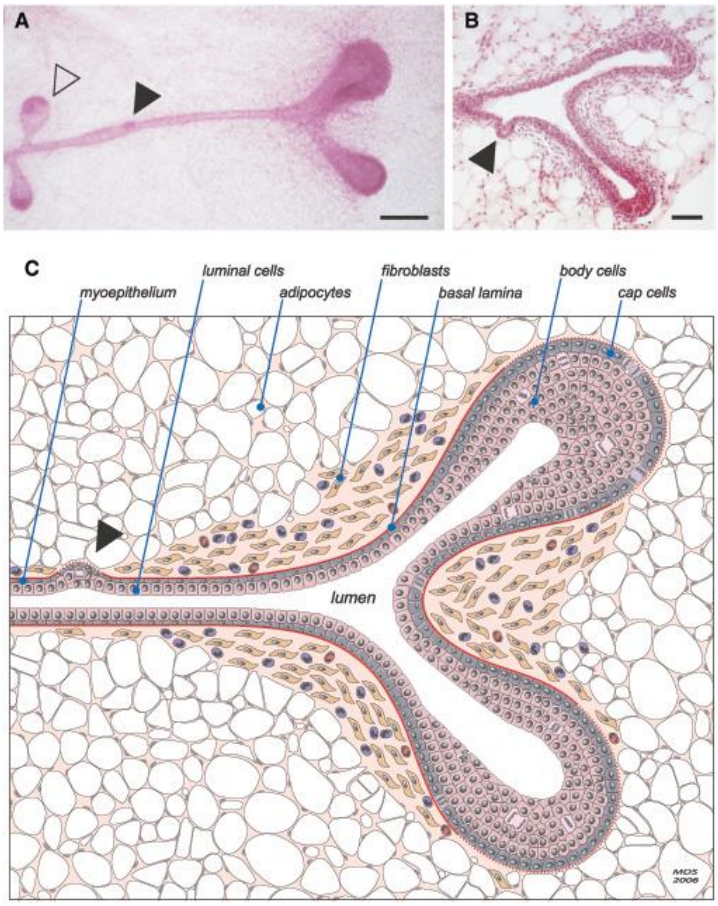

Figure 1.1. Murine TEB and duct morphology. A: carmine alum whole mount of a bifurcating TEB forming two new primary ducts. Two new secondary side-branches (open arrowhead) and a possible lateral bud (closed arrowhead) are also shown. Scale bar: 200 µm. B: H&E-stained section of a bifurcating TEB showing a side-branch in the trailing duct (closed arrowhead). Scale bar: 100 µm. C: schematic diagram of a bifurcating TEB and trailing duct. The single layer-cap cells and multilayer-body cells are highly proliferative and give rise to the myoepithelial cells and luminal cells of branching ducts. The collagen-, fibroblast- and immune cell-rich collar structure at the neck of the TEB serves stromal-epithelial interactions for bifurcation and elongation. A forming side-branch is indicated (closed arrowhead), as is the basal lamina and the stromal adipocytes. Adopted from (Sternlicht et al., 2006).

The mammary gland develops through a detailed and complex developmental program involving interactions between different types of cells, both epithelial and stromal. These intricate interactions are governed by many signalling pathways involving hormones and growth factors that are temporally and spatially co-ordinately regulated. When such factors and molecular mechanisms are perturbed, either because of genetic abnormalities or environmental influences, aberrant proliferation and consequently breast cancer may develop. The mammary gland, both in humans and rodents, develops through three basic stages: embryonic, pubertal and adult (reproductive). A brief overview of these three developmental stages in the mouse will be presented, with those in humans and other mammals sharing similar processes.

1.2.1. Embryonic development of the mammary gland

Fetal mammary gland development is first notable by embryonic day 10.5 (E10.5) with the appearance of two ectodermal, multi-cell-layered ridges. These run anteroposteriorly on the ventral side between the fore and hind limbs and are commonly referred to as the “milk (mammary) lines” (Hens and Wysolmerski, 2005). By E11.5, five pairs of disk-shaped “placodes” form along the milk lines at certain reproducible locations. These placodes give rise to bulbs of epithelial cells which, by E13.5, will have invaginated into the underlying subdermal mesenchyme and become the “mammary buds”. The mesenchymal cells surrounding the buds are induced to condense and differentiate into a few-cell-layered “mammary mesenchyme” arranged radially around the buds. By E15.5, the epithelial cells proliferate and further penetrate into the subdermal fat pad precursors and become the “mammary sprouts”, concurrently forming a lumen with an opening to the skin marked by the “nipple sheath”. At E18.5, end of embryogenesis, the mammary

sprout sinks deeper still and forms a main duct that, through the process of branching morphogenesis, branches into about 10 to 15 secondary branches, forming the “rudimentary mammary gland (anlage)”. At this point, development essentially ceases until the onset of puberty (Watson and Khaled, 2008; Hens and Wysolmerski, 2005).

As already stated, embryonic development of the mammary gland involves complex interactions between the ectoderm and the underlying mesenchyme, governed by many signalling pathways and molecules that are temporally and spatially co-ordinately regulated. These molecular mechanisms include wingless/integrin (Wnt), hedgehog (Hh), epidermal growth factor receptor (EGFR), fibroblast growth factor (FGF), GATA DNA sequence-binding proteins (GATA3) and parathyroid hormone-related protein (PTHrP) signalling. These signalling pathways involve many transcription factors and effector molecules including bone morphogenetic protein 4 (BMP4) and its receptor BMP receptor1A (BMPR1A), homeobox protein MSX-2, T-box 3, zinc finger protein Gli3, lymphoid enhancer-binding factor 1 (Lef1), FGF10 and its receptor FGF receptor 2b (FGFR2b), neuregulin3 (Nrg3) and EGFR4 (ErbB4), among others. Abnormal mammary gland development occurs if these factors and signalling pathways are perturbed. Such perturbations may include mutations, up/down-regulations and spatial and temporal alterations in the expression or availability of key molecules. Abnormalities in the mammary gland include misplaced placodes, absence of some or all placodes, mammary hypoplasia and nipple loss, supernumerary glands and absence of ductal branching (reviewed in (Hens and Wysolmerski, 2005; Watson and Khaled, 2008)).

1.2.2. Pubertal development of the mammary gland

Mammary gland development continues postnatally but in a commensurate manner with body growth. With this allometric growth, terminal end buds (TEB) form at the end of the growing epithelial ducts that invade the fat pad (figure 1.2-A) (Watson and Khaled, 2008). Figure 1.2 below shows a schematic diagram of ductal and lobuloalveolar development of the murine mammary gland at different pubertal and reproductive stages.

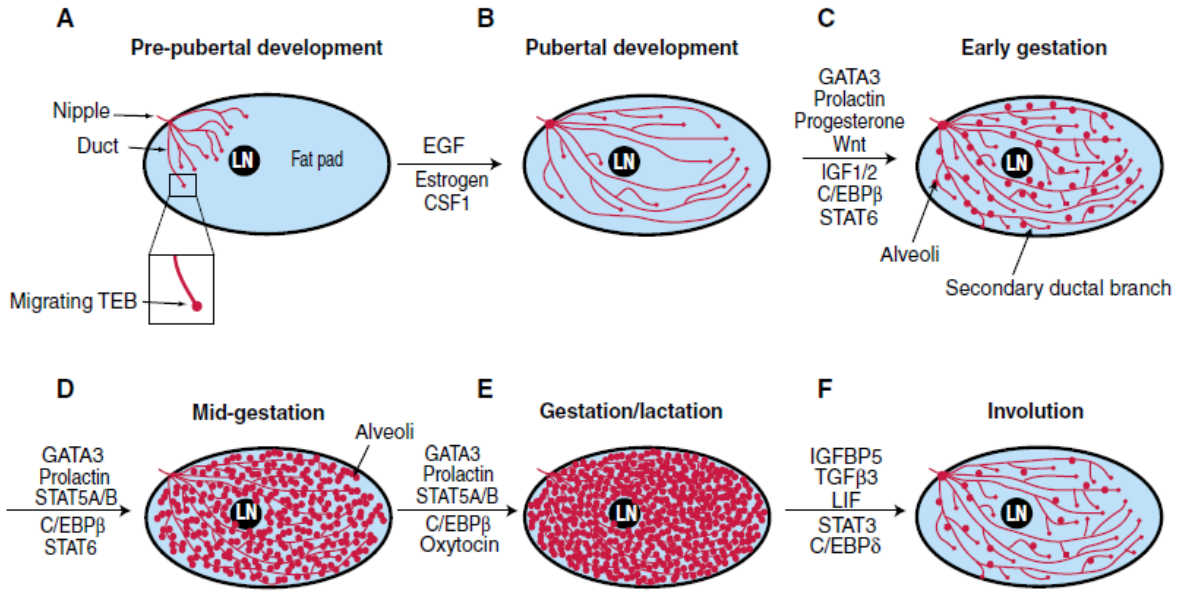

Figure 1.2. Schematic diagram of murine adult mammary gland development. A (pre-pubertal development): allometric growth of epithelial ducts led by migrating terminal end buds (TEB) (LN: lymph node). B (pubertal development): ductal morphogenesis extends throughout the fat pad to create an “open” architecture. C-E (early gestation-lactation): robust lobuloalveolar development produces secondary and tertiary branches, and alveoli differentiate to fill the entire fat pad. F (Involution): post-lactational regression of surplus epithelia returns the mammary gland to a pre-pregnant state. Adopted from (Watson and Khaled, 2008).

Robust branching morphogenesis begins with the rising levels of serum estrogens at puberty which induce the formation of TEBs at the distal ends of ducts (figure 1.2-B). TEBs, made up of an outer layer of progenitor cap cells and an inner multicellular layer of body cells, are the sites of active cellular proliferation and differentiation during ductal morphogenesis. They respond to estrogens and proliferate to elongate the ducts and undergo a bifurcation process to form new primary branches (Hinck and Silberstein, 2005). Secondary side-branches sprout laterally from the trailing ducts. It is believed that apoptosis occurs in the body cells to create the luminal space. Ductal branching continues until an age of about 8-10 weeks, when the margins of the fat pad are reached and the TEBs disappear. With each oestrus cycle in the mature virgin mammary gland, side-branching and apoptosis occur (Sternlicht, 2006). In mice devoid of white adipose tissue (WAT), ductal morphogenesis is severely limited (only 3-4 short ducts appear at E18) and TEBs are absent, highlighting a crucial role of adipocytes in this developmental process (Couldrey et al., 2002). It is important that pubertal development creates an “open” architecture of ductal trees, open in the sense of leaving most of the fatty pad epithelium-free for the massive branching and development of milk-secreting alveoli during gestation and lactation (Sternlicht et al., 2006).

This complex process of branching morphogenesis is regulated by a multitude of factors which are expressed by both the epithelium and stromal components to provide global and positional cues. These include growth factors and hormones, such as estrogen (E) and its receptors (ER-α and ER-β), progesterone (Pg) and its receptor (PgR), prolactin (Prl) and its receptor (PrlR), epidermal growth factor (EGF), hepatocyte growth factor (HGF), epimorphin/syntaxin2 and transforming growth factor β1 (TGF-β1), as well as extracellular matrix molecules and metalloproteinases

(MMPs), adipocytes and immune cells (reviewed in (Sternlicht et al., 2006; Watson and Khaled, 2008)). Disturbances to these factors and associated signalling pathways, whether of genetic or environmental origins, lead to defects in the developing mammary gland and may result eventually in tumourigenesis.

ER-α-null mice did not differ from Wt mice up to puberty, at which time their ducts showed no TEBs and failed to invade the fatty stroma (Mallepell et al., 2006). Mice with conditional KO of ER-α in the mammary epithelium at different developmental stages have revealed that ER-α signalling is required for both proper ductal branching during puberty and normal lobuloalveolar development during late gestation and lactation (Feng et al., 2007). Furthermore, tissue geometry and morphogenetic gradients of locally secreted inhibitors in the microenvironment of the mammary epithelium were shown to be critical for the process of branching morphogenesis (Nelson et al., 2006). TGF-β1 inhibited tubule elongation at tips and side-branching in nearby tubules, suggesting a role in creating the “open” ductal architecture important for optimal alveologenesis. This *in vitro* study suggested that the geometry of the elongating duct and its location relative to neighbouring ducts may determine the position of branching. The same group also revealed that signal intensity and duration have a profound effect on ductal branching. They showed that TGFα is sufficient for induction of ductal branching and that the duration of an active extracellular signal–regulated kinase 1/2 (ERK1/2) signal is important (Fata et al., 2007).

Lumen formation is also crucial to mammary gland development and function, and is thought to occur through apoptosis. The pro-apoptotic protein Bcl2-like protein 11 (Bcl-2L11/Bim) was found to be essential for lumen formation in the TEB during puberty (Mailleux et al., 2007). The axonal guidance proteins roundabout homolog

protein 1 (ROBO1), slit homolog 2 protein (SLIT2) and netrin1 were also reported to affect lumen formation in the TEBs. Mice null for these proteins exhibited disorganized, occluded TEBs and ducts, and had spaces between the cap and body cells resulting in separated layers, as opposed to normal bi-layered epithelium (Strickland et al., 2006). These results point to a role of these axonal guidance proteins in maintaining the integrity of the epithelium bi-layer. Moreover, enlarged ducts with reduced secondary branching were observed in virgin mice lacking the transcription factor CCAAT/enhancer binding protein-β (C/EBP-β) (Seagroves et al., 1998). These mutant mammary glands also displayed limited ductal side-branching and lobuloalveolar development when stimulated with E and Pg.

1.2.3. Reproductive development of the mammary gland

1.2.3.1. Gestation, lobuloalveolar development and lactation

To prepare for nourishment of the newborn during lactation, a gestating mammary gland undergoes massive tissue remodelling involving extensive proliferation of the epithelial ducts and differentiation of alveoli, the specialized luminal cells that synthesize and secrete milk. Concomitant with the massive proliferation of epithelia and to make room for such development, remodelling features the dedifferentiation of adipocytes whereby they lose their lipid droplets and become long projections scattered among the lobuloalveoli. Remodelling also includes expansion of the blood vasculature to meet the demands for ample nutrients, such as amino acids, sugars and other solutes needed for milk synthesis (Anderson et al., 2007).

Extensive side-branching and alveologenesis are induced by the ovarian steroid hormone Pg which, in association with the pituitary hormone Prl, promotes the differentiation of alveoli (Oakes et al., 2006). Prl stimulates Pg and upregulates the

transcription of PgR, and likewise Pg upregulates PrlR. This synergism provides for the required levels of both hormones for proper development of the mammary gland. Brisken and colleagues found that mammary transplants devoid of PgR in the epithelium, but not stroma, lacked side-branching and alveoli (Brisken et al., 1998). PrlR-null mammary glands transplanted into Wt pregnant females developed normal side branching and produced alveolar buds, but failed to develop lobuloalveolar structures (Brisken et al., 1999). Figure 1.2(C-E) depicts schematically the process of ductal morphogenesis and lobuloalveolar development.

Canonical Wnt signalling through β-catenin is one of many mediators that can affect PgR-promoted alveologenesis. Constitutive activation of Wnt/β-catenin signalling in the luminal cells induced precocious differentiation of lobuloalveoli and resulted in adenocarcinomas. Likewise, targeted activation of β-catenin in the basal cells induced precocious formation of lateral buds and differentiation of lobuloalveoli during pregnancy, increased proliferation during lactation and increased involution (Teuliere et al., 2005). In addition, the nulliparous transgenic females in this study developed mammary hyperplasia comprised of undifferentiated basal cells and reported invasive basal-type carcinomas. In another study, alveologenesis in mice null for PgR during gestation can be rescued by activated β-catenin (Hiremath et al., 2007). Notably, only cells at the tips of ducts were inherently responsive and developed alveoli. This is due to the regulation of lineage commitment and cell fate mechanisms in the progenitor cells. Interestingly, T helper cell (Th) signalling, important for determination of Th1/Th2 cell lineage, is also involved in mammary luminal lineage determination and maintenance of the differentiated state of luminal cells (Hiremath et al., 2007).

Th2 signalling factors, including signal transducer and activator of transcription 6 (STAT6), interleukin 4 (IL4), IL13, GATA3 and V-maf musculoaponeurotic fibrosarcoma oncogene homolog (c-MAF) have been shown to be involved in luminal lineage determination and alveologenesis (Khaled et al., 2007). These Th2 signalling factors were found to be up-regulated while, concomitantly, the Th1 signalling factors were down-regulated upon induction of differentiation of mammary epithelial cells (MEC) towards luminal lineage by a lactogenic cocktail. By day 5 of gestation, phosphorylation of STAT6 increases and correlates with the expression of IL4 and GATA3 in the epithelium, and later in gestation with c-MAF expression. Also, $IL4^{-/-}$ /$IL13^{-/-}$ double KO mice and mice lacking the transcription factor STAT6 both show about 70% reduction in the numbers of differentiated alveoli which correlates with reduced epithelial proliferation (Khaled et al., 2007). On the other hand, precocious differentiation of alveoli occurred when the suppressor of cytokine signalling 5 (Socs5), a negative regulator of STAT6, was deleted. Moreover, conditional deletion of GATA3 in alveolar cells during gestation expanded the pool of undifferentiated epithelial cells and blocked alveologenesis and lactation, indicating that GATA3 is required for alveolar luminal differentiation. Thus, the IL-4/IL13-STAT6-GATA3 Th2 signalling pathway is important for luminal alveolar lineage. It is worth noting that GATA3 is over-expressed in the luminal A subtype of breast cancer (Asselin-Labat et al., 2007).

Canonical Notch signalling is also required for the proliferation of luminal cells, as well as for the maintenance, but not establishment, of their differentiated status (Buono et al., 2006). The DNA-binding protein RBPJk regulates this signalling pathway by binding and repressing promoters of target genes. Upon activation of Notch signalling, the Notch intracellular domain (NICD) translocates to the nucleus

and binds RBPJk. This releases repression and allows the transcription of target genes such as hairy/enhancer-of-split related with YRPW motif protein 1 (Hey1), a transcriptional repressor itself. Mice with conditional deletion of RBPJk in mammary epithelial cells during pregnancy expressed and accumulated tumour protein p63 in their luminal cells, resulting in transdifferentiation to basal type. This was evidenced by suppressing of luminal features in favour of inducing more basal characteristics including the expression of keratin5. These mutant mice also exhibited increased rates of basal cell proliferation (Buono et al., 2006).

PgR-promoted alveologenesis is also mediated by receptor activator of nuclear factor kappa-B ligand (RankL)/nuclear factor kappa-light-chain-enhancer of activated B cells (NF-κB) pathway, resulting in the transcription of G1/S-specific cyclin-D1 (Ccnd1). Gestating mammary glands in mice lacking RankL or its receptor Rank undergo normal ductal morphogenesis but, later on in pregnancy, do not form lobuloalveolar structures, resulting in neonatal death of pups due to lack of milk (Fata et al., 2000). The alveolar buds of these mutant mice were characterized by lack of proliferation, enhanced cell death and failed activation of protein kinase B (PKB/AKT) signalling. RankL co-localises with PgR as the serum levels of the endocrines progesterone and estrogen rise in pregnancy. Estrogen synergizes with progesterone to increase the transcription of Ccnd1 and thereby increase the rate of epithelial cell proliferation and lobuloalveolar development during pregnancy (Said et al., 1997). It has also been reported that Ccnd1 levels may be up-regulated through insulin growth factor 2 (IGF-2) independent of RankL (Brisken et al., 2002). This work revealed that Prl induces IGF-2 expression which in turn induces Ccnd1. All three factors are overexpressed in mammary tumours. As already mentioned, the ovarian steroid hormones estrogen and progesterone and the pituitary hormone

prolactin all synergise to produce a highly proliferated epithelium with differentiated lobuloalveoli in preparation for lactation.

Many genes critical for mammary gland development during early pregnancy were revealed through transcript profiling of PrlR-null mammary glands. Two collagen members and laminin were identified, which are cell adhesion components of the extracellular matrix known to regulate stromal-epithelial interactions crucial for gene expression and lobuloalveolar differentiation (Fata et al., 2004). Signalling of these molecules may be mediated by the luminal epithelial surface cell receptor "β-1 integrin". Conditional ablation of β-1 integrin during early and late gestation revealed a critical role in lobuloalveolar formation and functional differentiation. The luminal cells detached from the extracellular matrix but remained connected to one another and did not undergo apoptosis. Moreover, these mice showed major deficits in milk protein and fat synthesis as well as in STAT5 activation, indicating a role in Prolactin signalling (Naylor et al., 2005).

Also identified through transcript profiling of PrlR-null mammary glands were the tight junction proteins caludin-3 and claudin-7 which were down-regulated. These play a crucial role in the closure of tight junctions that regulate the establishment of cell polarity, a process required for proper alveologenesis (Ormandy et al., 2003). Connexin-26 (Cx26), a gap junction protein involved in ion and metabolite exchange, was also identified in this study. Conditional KO of the Cx26 gene at different stages of mammary development showed it to play an essential role in lobuloalveolar development as well as in preventing apoptosis of alveoli in early, but not late, gestation (Ormandy et al., 2003).

Furthermore, all aspects of mammary gland development are crucially mediated by the receptor tyrosine kinases of EGFR family and their ligands. The family has four known members: EGFR/ErbB/HER1; ErbB2/HER2/Neu; ErbB3/HER3; ErbB4/HER4. These are activated by many ligands upon which they dimerize and cross phosphorylate to initiate a signalling cascade that has different outcomes depending on the ligand and receptors involved (Stern, 2003). Expression of a non-functional ErbB2 protein had no effect in transgenic mice till late gestation and postpartum, when lactationally active, distended lobuloalveoli did not form (Jones and Stern, 1999). Mice null for ErbB4 exhibited a phenotype of reduced alveologenesis starting at mid-pregnancy and leading to reduced expression of milk genes and failure to nurse pups. Investigations of the mammary epithelia revealed reduction of alveolar proliferation, lack of functional phosphorylated form of STAT5 and reduced expression of β-casein and whey acidic protein (Long et al., 2003). Moreover, mice lacking the ErbB4 ligand Neuregulin-α exhibit a similar phenotype to that of ErbB4 null mice, with attenuated alveolar proliferation and differentiation evidenced by dramatic reduction in β-casein expression (Li et al., 2002b).

Alveolar cell differentiation begins around mid-pregnancy to initiate the secretory phase. For full differentiation of lobuloalveoli, a contact between the luminal cells and the basement membrane/extracellular matrix is needed (Oakes et al., 2006). This contact is enabled by the discontinuity of the myoepithelium around the secretory luminal cells. Lobuloalveolar differentiation is marked by the expression of genes required for the synthesis and secretion of milk proteins, lactose and lipids. Milk secretion is critical to the survival of the newborn mammal as it provides the sole nutrients for nourishment.

1.2.3.2. Post-lactational involution

Upon weaning and milk stasis, the lactating mammary gland undergoes an intricately coordinated process of epithelial regression, or involution, and returns to a pre-pregnant state. The involution process occurs through an exquisitely controlled program of cell death with concomitant tissue remodelling (Watson and Kreuzaler, 2011). It involves clearing of the debris of dead cells and milk components upon a surge of macrophages and other types of immune cells, degradation of the extracellular matrix (ECM), remodelling of the vasculature and re-differentiation of adipocytes to regenerate the fat pad. It has been reported that the mammary gland microenvironment during involution may promote metastasis of tumourous cells (McDaniel et al., 2006).

Morphologically, the process of involution may be divided into two phases: a first reversible phase that extends for approximately 48 hrs in the mouse, and a second phase that involves tissue remodelling and recycling of the gland back to the pre-pregnant state (Watson and Kreuzaler, 2011). In the first phase, the lumens of the alveoli become distended due to the accumulation of milk. It also witnesses shedding of dying epithelial cells and infiltration of neutrophils. In the second phase, matrix metalloproteinases (MMPs) increase their levels and begin to digest the extracellular matrix (ECM). Concomitantly, adipocytes re-differentiate, macrophages and other immune cells infiltrate and blood vessels and the rest of stromal components remodel. Many signalling pathways and genes involved in involution have been identified through genetic manipulations of cell lines and living models (mostly mice), as well as through transcription profiling studies.

Involution is triggered mainly by milk stasis, possibly due to a resultant mechanical stretch of epithelial cells and/or an accumulation of factors secreted in the milk (Li et

al., 1997; Quaglino et al., 2009). Early in involution, the plasma membrane Ca^{2+}-ATPase (PMCA2) is down-regulated as a result of changes in the shapes of mammary epithelial cells. In contrast, the expression of this ion transporter is increased several hundred-fold in the apical surface of lactating mammary epithelial cells as it transports about 60-70 % of milk calcium (VanHouten et al., 2010). This study revealed that mammary epithelial cells devoid of PMCA2 were sensitized to apoptosis as a consequence of the elevated intracellular calcium levels.

Furthermore, the cytokines leukaemia inhibitory factor (LIF) and TGF-β3 are secreted factors that have been implicated in involution. LIF was concluded to be a physiological activator of STAT3, a transcription factor that is a key mediator of cell death in the mammary gland (Kritikou et al., 2003). In this study, phosphorylated STAT3 was not observed and its target C/EBP-δ was not up-regulated. Like STAT3-null mammary glands, LIF-null mammary glands reported delayed involution and reduced apoptosis, and unlike Wt glands, showed no up-regulation of insulin-like growth factor binding protein 5 (IGFBP5) (Chapman et al., 1999). These glands also had increased levels of the pro-apoptotic p53 and p21, most likely as a compensatory mechanism for inducing the delayed involution observed. Moreover, C/EBP-δ was shown to be a crucial mediator for the expression of some pro-apoptotic genes in mammary epithelia. Its deletion caused delaying of involution and halting of expression of the pro-apoptotic genes coding for p53, Bcl-2 homologous antagonist/killer (BAK), IGFBP5 and clusterin/sulphated glycoprotein-2 (SGP2). Deletion of C/EBP-δ also prevented the repression of the anti-apoptotic genes coding for BFL-1 and Ccnd1 (Thangaraju et al., 2005). Moreover, another STAT3 target, TGF-β3, was shown to be up-regulated in the mammary epithelium immediately after weaning and before cell death, and its expression was found to be

induced by milk stasis and not by hormonal cues. Upon milk stasis, TGF-β3-null mammary gland transplants showed significant inhibition of cell death relative to wild type (Wt) mice (Nguyen and Pollard, 2000).

Furthermore, delay in involution and remodelling occurred when the NF-kappa B upstream regulator “inhibitor of nuclear factor kappa-B kinase subunit beta (IKK-β)” was conditionally deleted. This phenotype was associated with significant down-regulation of the death receptor ligands TNF-like weak inducer of apoptosis (TWEAK) and tumour necrosis factor (TNF) and the TNF receptor (TNFR1), and with prevention of caspase-3 cleavage (Baxter et al., 2006). In addition, many other factors involved in apoptosis were shown to contribute to mammary epithelial involution. These include the death receptor ligands FasL and TNF-related apoptosis-inducing ligand (TRAIL) which are up-regulated during involution, and the Bcl-2 family of apoptosis regulators Bcl-2–associated X protein (Bax) and B-cell lymphoma 2 (Bcl-2) (Song et al., 2000; Sohn et al., 2001; Schorr et al., 1999; Walton et al., 2001). These studies and others suggest the existence of crosstalk between these signalling pathways, and that efficient involution and remodelling requires this crosstalk to be under tight regulation.

For involution and remodelling to proceed normally, the dead cells and milk components have to be removed. Milk fat globule-EGF factor 8 (MFGE-8) was found to play an important role in this process. Mice null for the MFGE-8 glycoprotein exhibited reduced phagocytosis, developed inflammation and reported failed lactation in subsequent pregnancies (Atabai et al., 2005). Upon completion of involution, the lactating mammary gland with massive ductal and lobuloalveolar epithelia returns to a pre-pregnant state with minimum epithelia. The mammary gland is unique in that most of its development, including its full differentiation,

occurs in adulthood, and in that it may repeat its complete development of gestation/lactation/involution with cycles of successive pregnancies.

1.3. The synuclein family

The synuclein family includes three highly homologous members that are conserved throughout vertebrates. These are α-synuclein, β-synuclein and γ-synuclein. They are heat stable, small, soluble cytoplasmic proteins with an inherently unfolded structure, and are expressed mostly in neural tissues (Clayton and George, 1998). α- and β-synucleins are expressed largely in the central nervous system (CNS), while γ-synuclein is expressed predominantly, although not exclusively, in the peripheral nervous system, in the axons and cell bodies of primary sensory neurons, sympathetic neurons and motor neurons (Buchman et al., 1998b). They share 3 modular domains: a lipid binding domain at a highly conserved N-terminus, a hydrophobic central domain and a less conserved acidic C-terminal domain. They are also characterized by the absence of cysteines and tryptophans (George, 2002; Clayton and George, 1998). Figure 1.3 below shows a diagram illustrating the common modular structure in the three highly homologous members. The physiological function of the synucleins is not known but they have been shown to possess chaperone-like activity (Souza et al., 2000), which points to potential roles in the regulation/modulation of some cellular processes through interaction with relevant molecules.

1.3.1. α-synuclein

α-synuclein is the most widely studied member of this family due to its implication in Parkinson's disease (PD), Alzheimer's disease (AD), Dementia with Lewy bodies disease (DLB), Multiple System Atrophy (MSA) and other neurodegenerative diseases. It is linked to PD both genetically and histopathologically.

In some affected kindreds, molecular genetic studies established linkage to early-onset PD by identifying the missense autosomal-dominant point mutations A53T (Polymeropoulos et al., 1997), A30P (Kruger et al., 1998) and E46K (Zarranz et al., 2004), as well as gene dosage duplications (Ibanez et al., 2004; Chartier-Harlin et al., 2004) and triplication (Singleton et al., 2004). Moreover, at least four independent genome-wide association studies linked single nucleotide polymorphisms (SNPs) in α-synuclein gene to the disease (Edwards et al., 2010; Pankratz et al., 2009; Satake et al., 2009; Simon-Sanchez et al., 2009). A haplotype spanning about 15.3 kb of the α-synuclein gene promoter was also linked to the disease (Pals et al., 2004).

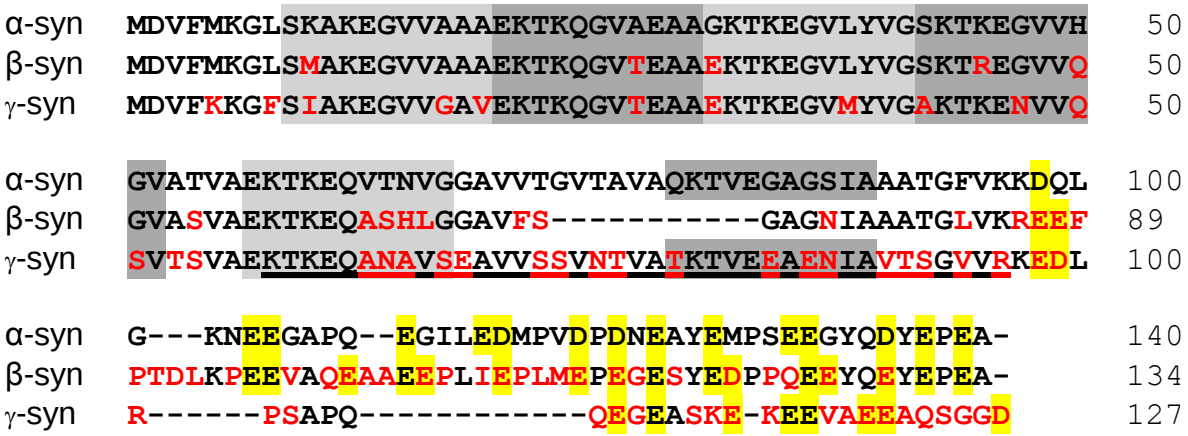

Figure 1.3. Aligned sequences of human α-, β- and γ-synucleins using Clustalw2 software. Red letters indicate differences from α-synuclein sequence. Light and dark grey-boxed sequences represent the imperfect 11 amino acid repeats containing the consensus KTKEGV (of note is the absence in β-synuclein of an imperfect repeat in the NAC peptide region). The underlined region marks the highly hydrophobic central NAC region. Negatively charged amino acids in the acidic C-terminal tail are highlighted in yellow. The UniProtKB/Swiss-Prot accession numbers for α-, β- and γ-synucleins are P37840.1, Q16143.1 and O76070.2, respectively. Assignment of repeat motifs and NAC region is based on Sung, et al 2007.

1.3.1.1. α-synuclein structure

α-synuclein was first isolated from the pacific electric ray fish *Torpedo californica* using antisera raised against purified cholinergic synaptic vesicles. Expression screening of a cDNA library constructed from the electromotor nucleus resulted in the isolation of a cDNA clone encoding a 143 amino acid protein of an approximately 17 kDa size. This protein localized to the inner nuclear envelope and presynaptic nerve terminals and was hence named synuclein (Maroteaux et al., 1988). Also, this group used the same antisera to screen and isolate from a rat brain cDNA library a clone that coded for a highly homologous 140 amino acid protein. In humans, the α-synuclein orthologue was first isolated as the precursor of the non-amyloid component of AD amyloid plaque (NACP) (Ueda et al., 1993). The brain cDNA library was screened and a cDNA was cloned encoding a protein of approximately 19 kDa.

Maroteaux's group analysis of the electric rays' α-synuclein revealed the presence of an 11 amino acid imperfect repeat motif within the N-terminal 93 amino acids. This motif repeated 6 times and contained the consensus sequence KTKEGV. The motif region is conserved in the synuclein family and is similar to the apolipoprotein class-A2 helix. It is believed to endue the synucleins with a reversible phospholipid–binding property, a characteristic that supports a role for α-synuclein in presynaptic vesicle release (Clayton and George, 1998). Indeed, using site-directed mutagenesis, the *in vitro* binding of α-synuclein to phospholipid vesicles was shown to involve the N-terminal repeat domain. Notably, the binding induced a large shift in secondary structure from about 3% to nearly 80% α-helix, a finding that lent further strength to the proposed role in presynaptic function (Perrin et al., 2000; Davidson et al., 1998). The protein is found enriched at presynaptic nerve terminals and

particularly in the synaptic vesicle fraction of various brain neurons, including neurons of the hippocampus, amygdala, olfactory tubercle, striatum, thalamus and cerebral cortex (Giasson et al., 2001; Iwai et al., 1995; Li et al., 2002a; Mori et al., 2002).

Unlike the N-terminus, the C-terminus tail is the least conserved between the synuclein members and contains many acidic amino acids. It is believed to acquire no secondary structure when the protein is lipid-bound. The more hydrophobic central region contains the 35-amino acid-NAC peptide which is thought to render the protein susceptible to aggregation (Maroteaux et al., 1988; Clayton and George, 1998; Lavedan, 1998). The α-synuclein-encoding gene was mapped to chromosome 4q21.3-q22 and was shown to have 6 exons, 5 of which are coding (Spillantini et al., 1995; Chen et al., 1995; Touchman et al., 2001). Three human isoforms of α-synuclein have been described as a result of alternative splicing (Xia et al., 2001).

1.3.1.2. α-synuclein function.

The physiological function of α-synuclein, as well as β- and γ-synuclein, is not clear yet, but it has been proposed to play a role in the regulation of synaptic vesicle release and plasticity (Clayton and George, 1998; Lavedan, 1998), in the biosynthesis and metabolism of dopamine (Al-Wandi et al., 2010; Lee et al., 2001; Perez et al., 2002) and in promoting the assembly of N-ethylmaleimide–sensitive factor attachment protein receptor (SNARE) complexes, proteins mediating vesicle fusion with the cell membrane (Burre et al., 2010).

Of the early findings pointing to a role for α-synuclein in the regulation of synaptic vesicle release and plasticity is a study by Jenco and co-workers (Jenco et al., 1998). They purified from a bovine brain a factor that inhibited phospholipase D2

activity *in vitro,* which appeared to be a mixture of α- and β-synucleins. Phospholipase-D is known to be involved in the production of phosphatidic acid, which is thought to be a key factor in the synthesis and fusion of synaptic vesicles. Further probing into the function of α-synuclein found structural and functional homology with the 14-3-3 proteins, a family of chaperones that are, like α-synuclein, abundant in the cytoplasm of neurons (Ichimura et al., 1988; Ostrerova et al., 1999). This prompted the investigation of α-synuclein for binding 14-3-3 as well as proteins known to bind 14-3-3 proteins.

Immunoprecipitation studies using homogenized rat brain tissue demonstrated that α-synuclein is associated with 14-3-3 proteins. It also bound protein kinase C (PKC) and inhibited its activity, but did not affect its translocation to the cell membrane (Ostrerova et al., 1999). This study also demonstrated that, in rat cortex homogenate and HEK 293 cells, α-synuclein protein associated with the extracellular-regulated kinase (ERK) and dephosphorylated Bcl2-associated death promoter (BAD), suggesting a possible role in regulating ERK cascade and apoptosis. Moreover, over-expressing the wild type or mutant A53T or A30P α-synuclein proteins in HEK 293 cells resulted in cytotoxicity and induced apoptosis, with the mutant proteins having a much more pronounced effect.

Furthermore, α-synuclein was investigated for physical association and functional relation to the tyrosine hydroxylase (TH), the rate-limiting enzyme in the biosynthesis of dopamine (DA) (Ichimura et al., 1988). α-synuclein was found to co-immunoprecipitate with TH from homogenates of rat striatum and MN9D dopaminergic cells (Perez et al., 2002). Immunoelectron microscopy on MN9D cells confirmed co-localization of α-synuclein with TH on or near mitochondria and vesicular membranes. To probe the functional aspect of this association, authors

over-expressed α-synuclein in MN9D cells and demonstrated a significant reduction in TH activity accompanied by a decrease in DA levels. The reduced TH activity was shown to result from a reduced level of phosphorylated enzyme rather than reduced total TH levels or increased DA degradation (Perez et al., 2002). This reduced phosphorylation may be due to α-synuclein interacting with TH thereby inhibiting/reducing a kinase's ability to phosphorylate TH, or inducing/enhancing a phosphatase enzyme to remove added phosphates.

Another evidence for a role for α-synuclein in DA metabolism came from studies of α-synuclein interaction with the human presynaptic dopamine transporter (hDAT). hDAT is a presynaptic transmembrane protein known to mediate the reuptake of DA upon release at the synaptic terminals of substantia nigral neurons. Using the yeast two hybrid system, this interaction was shown to involve the NAC domain of α-synuclein and the C-terminus of hDAT. Immunoprecipitation showed this binding to occur in both rat striatum and Ltk^- cells co-transfected with plasmids expressing human α-synuclein and hDAT. Also, confocal immunofluorescent microscopy confirmed co-localization of the two proteins in cultured human precursor cells of substantia nigra neurons. Further investigation of the co-transfected Ltk^- cells revealed that the binding facilitates clustering of DAT at the cell membrane surface and thereby accelerates the rate of cellular DA uptake (Lee et al., 2001).

The implication of α-synuclein in DA metabolism was further supported by observations made on α-synuclein knockout (KO) mice (Abeliovich et al., 2000). These mice were viable, fertile, displayed no severe morphological or histological abnormalities, and showed a normal complement of dopaminergic neurons. However, they showed increased release of dopamine at the nigrostriatal presynaptic terminals when paired electrical stimuli were applied. Concurrent with

this altered DA release, striatal dopamine content was lower (by about 18%) and DA-dependent locomotor response to amphetamine was attenuated compared to the Wt littermates. Accordingly, the authors postulated that α-synuclein may act as a presynaptic negative regulator of DA neurotransmission.

However, a later study conducted by Cabin and co-workers did not find any difference in amphetamine-induced locomotor response between Wt and α-synuclein KO mice (Cabin et al., 2002). This discrepancy may be due to background strain differences as it has been reported that different strains may respond differently to amphetamine (Ralph et al., 2001). This same study, however, reported significant impairments in hippocampal synaptic response following prolonged, repetitive electrical stimulation. Closer investigation revealed ultrastructural differences where the number of reserve-resting pool of synaptic vesicles in the hippocampus was significantly reduced in the KO mice, as well as in cultured hippocampal neurons obtained from 17.5 day *post coitum* KO embryos (Cabin et al., 2002). Similar ultrastructural difference was also observed in cultured rat primary hippocampal neurons in which α-synuclein levels were down-regulated by about 50% using antisense oligonucleotides (Murphy et al., 2000).

Further discrepancy was added by results obtained in studies of α- and β-synuclein double-KO mice (α/β-synuclein KO) (Chandra et al., 2004). These mice showed normal basic brain function and normal survival. Moreover, unlike some of the above data, no changes in the ultrastructure of synapses and no decrease in the size of synaptic vesicle pools were found. Nevertheless, authors recorded a statistically significant 18% reduction in brain striatal dopamine levels compared to Wt mice, whereas the α- and β-synuclein single-KOs had only slight reductions compared to the Wt mice. This hinted towards functional redundancy in maintaining normal

dopamine levels in the striatum. Nevertheless, the reduced levels of dopamine did not result in any significant alterations in the release and reuptake of the neurotransmitter. In addition, quantitative alterations in four small synaptic proteins were reported: about 50% increase in γ-synuclein, 30% increase in 14-3-3-ζ, 30% reduction in 14-3-3-ε and 30% reduction in complexin proteins. These alterations may reflect functional relationships between these proteins and α and β-synucleins: up-regulation of the homologous family member γ-synuclein may serve a compensatory role; 14-3-3 proteins are known to interact with synucleins (Ostrerova et al., 1999); complexins regulate neurotransmitter release by binding to assembled soluble N-ethylmaleimide–sensitive factor attachment protein receptor (SNARE) complexes, proteins mediating vesicle fusion with the cell membrane (Brose, 2008; Reim et al., 2001).

Indeed, α-synuclein was shown, both *in vivo* and *in vitro*, to bind synaptic vesicle-associated membrane protein 2 (VAMP2)/synaptobrevin-2 and promote SNARE complex assembly (Burre et al., 2010). Furthermore, age-dependent neurological deficits exhibited by α-/β-/γ-synuclein triple-KO mice were characterized by decreased SNARE complex assembly and resulted in premature death of the mice. This led to the conclusion that the synucleins may provide chaperoning activity required for maintaining SNARE complex assembly during increased synaptic activity, synaptic injury and aging (Burre et al., 2010). In an earlier study, transgenic overexpression of α-synuclein unexpectedly rescued cysteine-string protein alpha (CSP-α) KO mice from progressive lethal neurodegeneration, while ablation of the endogenous α-synuclein gene accelerated this process. CSP-α is an abundant synaptic protein thought to have co-chaperoning activity essential for neuronal survival. Deletion of CSP-α induces neurodegeneration by compromising proper

SNARE complex assembly and consequently neurotransmitter release, and it has been suggested that transgenic overexpression of α-synuclein partially corrected formation of these complexes by acting downstream of CSP-α (Chandra et al., 2005). It has also been demonstrated that for rescuing this type of neurodegeneration α-synuclein should be able to bind phospholipids of synaptic vesicle membranes. However, in another study no changes in SNARE complex assembly were observed in the striatum of triple-KO mice, suggesting that in dopaminergic synaptic terminals the loss of α- and other synucleins function can be efficiently compensated (Anwar et al., 2011).

1.3.2. β-synuclein

1.3.2.1. β-synuclein structure

β-synuclein was initially isolated from bovine brain as a 134 amino acid residue phosphoneuroprotein-14 (PNP-14), and found to be phosphorylated on serine residues by Ca^{2+} calmodulin-dependent protein kinase II (Nakajo et al., 1990; Nakajo et al., 1993). The human orthologue was later identified and found to have 61% sequence homology with the 140 amino acid long α-synuclein, and was therefore renamed β-synuclein (Jakes et al., 1994). It shares with the other two members, α- and γ-synucleins, the three modular domains shown above in Figure 1.3 with a deletion of 11 amino acids overlapping the last repeat motif occurring within the hydrophobic NAC region. This renders it, relative to α- and γ-synucleins, less predisposed to forming secondary alpha helical structures in this part of its lipid binding domain, more prone to extending structures at the acidic tail, and thus less prone to aggregation (Sung and Eliezer, 2007). The β-synuclein gene has been

mapped to chromosome 5q35, with 6 exons, five of which are coding (Spillantini et al., 1995).

1.3.2.2. β-synuclein function

Like α- and γ-synuclein, the physiological function of β-synuclein is still eluding. The pattern of expression is very similar to that of α-synuclein, being predominantly expressed in the CNS and enriched at presynaptic terminals (Jakes et al., 1994). This co-expression points to some degree of functional redundancy.

As mentioned above, Jenco and co-workers purified from a bovine brain a factor that inhibited phospholipase D2 activity *in vitro*. This factor was analysed to be a mixture of α- and β-synucleins (Jenco et al., 1998). Phospholipase D is known to be involved in the production of phosphatidic acid, a factor thought to be involved in the synthesis and fusion of synaptic vesicles. Thus, β-synuclein may be involved in the synthesis and fusion of synaptic vesicles, suggesting some functional redundancy with α-synuclein. β-synuclein may also be involved in dopamine synthesis, as evidenced in Chandra's group observations on α-/β-synuclein double-KO mice summarized above (Chandra et al., 2004): these mice recorded a statistically significant 18% reduction in brain striatal dopamine levels compared to Wt mice, whereas the α- and β-synuclein single-KOs had only slight reductions compared to the Wt mice. This indicates functional redundancy in maintaining normal dopamine levels in the striatum.

Interestingly, β-synuclein has been reported to have a cell protecting role against cytotoxicity induced by α-synuclein aggregation. It was found to inhibit the protofibril formation of α-synuclein *in vitro* (Park and Lansbury, 2003), and to completely inhibit α-synuclein fibril formation, as was γ-synuclein, at a 4:1 molar excess ratio (Uversky

et al., 2002). Moreover, human (h) α-/β-synuclein double transgenic mice show ameliorated motor deficits and reduced hα-synuclein aggregation in the brain compared to hα-synuclein monotransgenic ones (Hashimoto et al., 2001). This work also demonstrated that α- and β-synuclein co-immunoprecipitated in the brains of double transgenics as well as when co-expressed in HEK 293 cells, and that β-synuclein inhibited the aggregation of α-synuclein *in vitro*. This suggested that β-synuclein may act as a chaperone negative regulator of α-synuclein fibrillation and aggregation, and thus protects against cytotoxicity and neurodegeneration.

1.3.3. γ-synuclein

1.3.3.1. γ-synuclein structure

γ-synuclein is the last to be discovered and the least studied member of the synuclein family. Its gene was independently identified by several laboratories in rat, mouse and human genomes (Akopian and Wood, 1995; Buchman et al., 1998b; Ji et al., 1997; Lavedan et al., 1998). One group named it breast cancer-specific gene1 (BCSG1) because it was found to be aberrantly expressed in a large percentage of advanced infiltrating breast carcinomas, compared to normal tissue and benign tumours where its levels were absent or hardly detectable (Ji et al., 1997). Other groups called it synuclein-like protein (Akopian and Wood, 1995; Lavedan et al., 1998) or persyn (Buchman et al., 1998b). The gene maps to chromosome 10q23.2-q23.3, spans about 5.0 Kb, is composed of five exons all of which are coding and transcribes into approximately 1.0 Kb mRNA (Lavedan, 1998; Ninkina et al., 1998).

The human protein is 127 amino acids long, shows 56% and 54% sequence identity with α- and β-synuclein, respectively, and was therefore renamed γ-synuclein (Lavedan et al., 1998; Clayton and George, 1998). The γ-synuclein protein shares

the family's three modular domain structure mentioned above and shown in Figure 1.3. It is the least conserved of the family members and is largely divergent at the acidic C-terminal domain where it notably lacks the tyrosine-rich signature of α- and β-synucleins. γ-synuclein has a free-state residual secondary structure similar to that of α-synuclein, accounting for the tendency of both proteins to aggregate *in vitro* and form fibrils. However, the transient lipid-bound structure of γ-synuclein is more comparable to that of β-synuclein. This underlies the ability of both proteins to prevent the aggregation of α-synuclein, albeit β-synuclein is much more efficient at this due to its more extended structure in the NAC region caused by the 11 amino acid deletion (Sung and Eliezer, 2007).

1.3.3.2. γ-synuclein tissue distribution and subcellular localization

γ-synuclein is expressed predominantly, although not exclusively, in the peripheral nervous system, in the axons, presynaptic terminals and to less extent in cell bodies of primary sensory neurons, sympathetic neurons and motor neurons (Buchman et al., 1998b). It is highly expressed in certain areas of the central nervous system including the substantia nigra, thalamus, subthalamic nucleus, caudate nucleus, hippocampus, amygdala, and retina and is moderately expressed in the corpus callosum (Surguchov et al., 1999; Lavedan et al., 1998). Furthermore, it was shown to be expressed in the stratum granulosum of neonatal and adult mice epidermis (Ninkina et al., 1999). It is also highly expressed in cells of the wall of small diameter blood vessels (see below). Low levels of expression were also detected in heart, skeletal muscle, pancreas, kidney, lung, testis, ovary and colon (Ji et al., 1997; Lavedan et al., 1998), but these results might reflect expression of this gene in neurons of the autonomic nervous system and in cells of the wall of small diameter

blood vessels. γ-synuclein is also expressed in adipocytes of subcutaneous and visceral fat where it is found to be overexpressed in obese people (Oort et al., 2008) and adipocytes of the mouse mammary gland, as will be shown later in this work.

To reveal domains responsible for subcellular localization, recombinant deletion mutants of α- and γ-synucleins were expressed as fusion proteins with enhanced green fluorescent protein (eGFP) in hippocampal neurons (Specht et al., 2005). The results showed that the N-terminal and core region of α-synuclein directed presynaptic targeting and caused nuclear exclusion, whereas the C-terminal domain supported nuclear localization. In γ-synuclein, the more conserved N-terminal domain favoured cytoplasmic localization as in α-synuclein, but the divergent C-terminal domain did not support nuclear localization. However, another group using neuronal and nonneuronal cells from ocular tissue concluded that γ-synuclein has a dynamic localization and may associate with subcellular structures (Surguchov et al., 2001). By immunocytochemical staining, they showed that in primary human optic nerve astrocytes, bovine retinal epithelial cells and human retinoblastoma Y79 cells during the interphase, γ-synuclein localized to the perinuclear space and bound to centrosomes. They also found the protein bound to the spindle poles in the mitotic Y79 cells. In human astrocytoma cell line U373 and melanoma cells OM431 and C8161, the protein was observed to lose the association with centrosomes and redistribute to the midbody in the telophase. This group also showed that, in mouse photoreceptor cell line 661W and human melanoma cells OM431 and C8161, stress conditions (incubation at 42°C for 12 hrs) effected translocation of γ-synuclein to the nucleus (Surgucheva et al., 2006).

1.3.3.3. γ-synuclein function

Like α-synuclein and β-synuclein, the physiological function of γ-synuclein is still elusive but it has been associated with some cellular processes including chaperone-like activity (Souza et al., 2000), regulation of neurofilament network integrity (Buchman et al., 1998a), regulation of microtubules (Zhang et al., 2010), cell division and cytokinesis (Surgucheva et al., 2006), regulation/modulation of some signalling pathways (Golebiewska et al., 2012; Surguchov et al., 1999; Surguchov et al., 2001), energy homeostasis and obesity (Guschina et al., 2010; Oort et al., 2008), and progression of cancer (Ahmad et al., 2007; Hibi et al., 2009; Ji et al., 1997).

1.3.3.3.1. γ-synuclein possesses chaperone-like activity

γ-synuclein, as well as α- and β-synucleins, were shown to possess chaperone-like activity. They prevented the thermally-induced aggregation of alcohol dehydrogenase at 45°C and the chemically-induced aggregation of insulin at 25°C, two assays routinely used in the determination of chaperone-like activities of proteins (Souza et al., 2000; Smulders et al., 1996; Manna et al., 2001). As mentioned above, one interesting role proposed for γ-synuclein and especially β-synuclein is the inhibition of α-synuclein fibrillation *in vivo*, acting effectively as chaperones to minimize the aggregation of α-synuclein. This is thought to occur through the incorporation of γ-synuclein and β-synuclein into the forming α-synuclein intermediates resulting in their stabilization, as it is these partially folded intermediate structures that are believed to lead to fibrillation (Uversky et al., 2002). The possession of such chaperone-like activity points to a potential role in the regulation/modulation of some cellular processes through interaction with relevant molecules.

1.3.3.3.2. γ-synuclein and regulation of the cytoskeleton

A role in the regulation of neurofilament network was postulated for γ-synuclein (Buchman et al., 1998a). This conclusion was drawn when γ-synuclein overexpression in cultured trigeminal ganglion neurons resulted in a dramatic decrease in the levels of neurofilaments (NF) fluorescence staining. Immunofluorescent staining of other cytoskeletal filaments, namely microfilaments, microtubules and peripherin, did not exhibit any changes. The effect on neurofilaments was largely suppressed by the addition of calpeptin, an inhibitor of Ca^{2+}-dependent proteases. Western blotting revealed NF-H to be degraded, but not NF-M, NF–L or the intermediate protein peripherin. This observation suggested that γ-synuclein might have a role in the regulation of neurofilament network integrity through increasing the susceptibility of NF-H to Ca^{2+}-dependent proteases (Buchman et al., 1998a).

Nevertheless, another study reported a role for γ-synuclein in the regulation of microtubules (Zhang et al., 2010). *In vitro* assays demonstrated that γ-synuclein promoted tubulin polymerization and bound to preformed microtubules. It also reduced the aggregation of small microtubule bundles induced by microtubule-associated protein 2 (MAP2) and promoted longer and thicker bundles of microtubules in a dose-dependent manner. This binding of γ-synuclein to microtubules was also confirmed *in vivo*, in human breast cancer cell line T47D and HeLa cells. Using immunocytochemistry, γ-synuclein was shown to colocalize with microtubules in HeLa cells and to reduce the aggregation and rigidity of microtubule bundles promoted by paclitaxel. It was also found to cause microtubule-dependent clustering of mitochondria in the perinuclear space in the ovarian cancer cell line

A2780. Thus, γ-synuclein, at least under certain cellular conditions, may act as a microtubule-associated protein that regulates microtubule-related cellular processes such as trafficking of mitochondria and vesicles (Zhang et al., 2010), cell division and cytokinesis (Surgucheva et al., 2006) and, if aberrantly expressed, increases resistance of cancer cells to apoptosis induced by anti-microtubule drugs such as paclitaxel and vinblastine (Zhou et al., 2006; Pan et al., 2002).

1.3.3.3.3. γ-synuclein and signal transduction

γ-synuclein has been shown to modulate key molecules involved in signal transduction. Overexpression of the protein in the retinoblastoma Y79 cell line led to significant increases in the levels of both isoforms of mitogen-activated protein kinase (MAPK), Erk1 and Erk2, as well as the levels of the phosphorylated form of the coactivator, transcription factor (TF) Elk1 (Surguchov et al., 2001; Surguchov et al., 1999). Using fluorescence-activated cell sorting (FACS) analysis of cell cycle progression, Y79 cells overexpressing γ-synuclein exhibited a greater percentage of cells in the G2/M phase and a corresponding lower percentage in the G1 phase. Y79 cells overexpressing γ-synuclein were also confirmed to have a higher percentage of cells undergoing mitosis by cell counting upon staining with anti-α-tubulin antibody. In search of other transcription factors as targets of γ-synuclein, TransSignal TF Protein Arrays (Panomics) were used to detect possible *in vitro* binding of the protein to some TFs (Surgucheva and Surguchov, 2008). This resulted in the identification of the following potential targets: JunB, methyl CpG binding protein 2 (MECP2), c-AMP responsive element binding protein 1 (CREB-1), peroxisome proliferator-activated receptor-gamma (PPARγ), transcription elongation factor A protein 1 (TCEA1) and

activating transcription factor 3 (ATF3). Some of these will be discussed later in connection with mammary gland tumourigenesis and adipocytes.

The involvement of the synuclein proteins in signal transduction extends to G protein-coupled receptor (GPCR) signalling pathways. All three synucleins were found to be *in vitro* substrates for different types of GPCR kinases (GRK) (Pronin et al., 2000). In the presence of phospholipids, the GRK5 isozyme produced a phosphorylation pattern that reduced the electrophoretic mobility of γ-synuclein. This was detected as two heavier, additional bands in the western blot. Mutation of serine 124 abolished the lighter band while the two heavier ones associated with phospholipids' addition remained. This suggests that GRK5 phosphorylates γ-synuclein in at least another site. This study by Pronin et al further reported that GRK2 and GRK5 were also able to phosphorylate α-synuclein *in vivo*.

Furthermore, γ-synuclein may modulate G proteins signalling through interaction with phospholipase Cβ2 (PLCβ2) (Golebiewska et al., 2012). G proteins activate PLC which in turn catalyses the hydrolysis of Phosphatidylinositol 4,5-bisphosphate (PIP2) into the two second messengers diacylglycerol (DAG) and inositol 1,4,5 trisphosphate (IP3). IP3 may then diffuse into the cytosol and bind calcium channels in the endoplasmic reticulum (ER) and cause the release of Ca^{2+}. This released Ca^{2+} allows DAG to activate PKC, leading to further signal transduction and eventual changes in cellular processes depending on incoming signal and cell type. In this study, γ-synuclein co-immunoprecipitated and colocalized with PLCβ2 in two cultured breast cancer cell lines, MCF10A and MDA-MB-231. This cellular association of the two proteins was confirmed *in vitro* and found to involve the C-terminal region of PLCβ2. Functionally, this interaction was shown to inhibit the *in vitro* enzymatic

activity of PLCβ2 as evidenced by a 4-fold decrease in the production of IP3 from PIP2 hydrolysis. This enzymatic inhibition was thought to result from inhibition of product release through stabilizing a conformation of PLCβ2 that binds the product more strongly. The activated G proteins Gαq and Gβγ bind to PLCβ2 and relieve the inhibition by γ-synuclein and thus activate the enzyme. The inhibition of PLCβ2 by γ-synuclein is thought to have no significant cellular effects as the basal enzymatic activity of the enzyme is low. However, it may serve to create a more robust effect as the G proteins both release the inhibition of basal activity and at the same time activate the stimulated activity of PLCβ2 (Golebiewska et al., 2012).

1.3.3.3.4. γ-synuclein and modulation of monoamine transporters

There is growing body of evidence that synucleins may play a role in monoamine homeostasis including synthesis, release and reuptake (Oaks and Sidhu, 2011). Knocking down of endogenous γ-synuclein in the nucleus accumbens of experimental Wistar rats reduced the locomotor response to cocaine by about 47% compared to control animals, whereas overexpression of the protein had no effect. On the other hand, overexpressing the protein along with DAT increased the cocaine-induced locomotor response by about 52%. This led to the conclusion that γ-synuclein and DAT exert a synergistic effect, possibly through a direct interaction between the two proteins (Boyer and Dreyer, 2008).

Moreover, γ-synuclein was implicated in the modulation of norepinephrine transporter (NET). It was found to be upregulated and α-synuclein to be concomitantly downregulated in the frontal cortex of an animal model of depression, Wistar-Kyoto (WKY) rats, compared to control parent strain Wistar. This was believed to result in altered interactions with NET and microtubule cytoskeleton, leading to the observed

reduction in cell membrane-surface NE levels. However, chronic treatment with the NET-selective antidepressant Desipramine reduced γ-synuclein levels while increased α-synuclein and NET levels. In addition, synaptosomes prepared from frontal cortex of WKY rats showed no sensitivity to the microtubule-destabilizing drug nocodazole, possibly due to the increased expression of γ-synuclein as it has been known to effect resistance of cancer cells to such chemotherapeutic drugs (Inaba et al., 2005). However, treatment of synaptosomes from Desipramine-treated WKY experimental rats with nocodazole led to increased [^{3}H]-NE uptake. Taken together, these results suggest a role for both γ- and α-synucleins in the modulation of NET trafficking, with a possible baseline optimal ratio to maintain normal NET cell membrane levels. The authors also postulated that, contrary to α-synuclein, γ-synuclein negatively modulates NET trafficking in a microtubule-independent manner (Jeannotte et al., 2009).

γ-synuclein was also found to negatively modulate serotonin transporter (SERT) (Wersinger and Sidhu, 2009). In this study, co-immunoprecipitation showed γ- or α-synuclein to complex with SERT, a finding confirmed by immunocytochemistry showing colocalization of either synuclein with SERT in rat primary raphae nuclei neurons. Cotransfection of Ltk$^-$ cells with either γ- or α-synuclein and SERT results in the reduction of [^{3}H]-SER uptake compared to transfection with SERT alone. This reduced SERT reuptake activity was partial in the case of γ-synuclein, with about 27% maximal reduction in activity even at increasing expression levels of γ-synuclein. α-synuclein, on the other hand, reduced SERT activity by about 65% at the expression level matching that for γ-synuclein. Thus, γ-synuclein may exert a partial negative modulation on SERT distribution to the cell membrane and activity.

1.3.3.3.5. γ-synuclein and lipid metabolism

γ-synuclein was postulated to play an important role in adipocyte physiology (Oort et al., 2008). Its mRNA levels were significantly upregulated in mature 3T3-L1 adipocytes compared to trace levels found in preadipocytes, suggesting a role in the physiology/maintenance of the differentiated state. Short term treatment (18 h) of fully mature 3T3-L1 adipocytes with the peroxisome proliferator-activated receptor-gamma (PPARγ) agonist GW1929 reduced γ-synuclein mRNA levels by about 50%. This reduction was qualitatively paralleled by leptin mRNA expression levels, suggesting that the respective genes may share PPARγ response elements that repress the genes upon PPARγ activation in adipocytes. Moreover, γ-synuclein mRNA levels were found to be differentially upregulated in white adipose tissue (WAT) from obese versus nonobese subjects from different groups, and was higher in subcutaneous (SC) than visceral adipose tissue (VAT). Again, leptin mRNA levels were changed co-ordinately with levels of γ-synuclein mRNA, with a Pearson correlation coefficient of 0.887. Also, WAT γ-synuclein mRNA levels were downregulated upon a 3 week-fasting regimen in obese individuals (Oort et al., 2008). This data points to a role for γ-synuclein in fat metabolism and adipocyte physiology.

The fact that γ-synuclein is strongly expressed in both WAT (adipocytes) and the peripheral nervous system hints to the sharing of some functional pathways in these two different tissues. A role for γ-synuclein in lipid metabolism in the nervous system was suggested by observations in γ-synuclein KO mice (Guschina et al., 2010). In these mice, lipid composition was examined in two brain regions, midbrain and cerebral cortex that normally have high and substantially lower γ-synuclein

expression levels, respectively. Compared to Wt mice, γ-synuclein KO mice reported a significant increase in the relative proportion of phosphatidylserine (PtdSer) in the midbrain region, but not in the cerebral cortex in which the relative proportions of membrane polar lipids were unchanged. Moreover, alterations in fatty acid patterns were reported in the cerebral cortex of KOs where the levels of docosahexaenoic acid (DHA) in PtdSer and phosphatidylethanolamine (PtdEtn) were modified. PtdSer and DHA are known to have important roles in cell signalling, apoptosis, enzyme regulation, SNARE complex formation and function of acetylcholine receptor, among others (Mozzi et al., 2003; Walczewska et al., 2011). Therefore, γ-synuclein may play an indirect role in such vital neuronal processes through modulation of lipid metabolism and phospholipid fatty acid composition.

1.3.3.3.6. γ-synuclein and diet-induced obesity

A role for γ-synuclein in diet-induced obesity was investigated in this lab (Millership et al., 2012). Unless otherwise referenced, this section summarizes some of the findings from a PhD project undertaken at this lab by Steven Millership and supervised by Prof. Vladimir Buchman. In this study, γ-synuclein KO and Wt mice were used to study a role of this protein in the development of high fat diet (HFD)-induced obesity. As in obese people, in Wt C57Bl6J mice WAT γ-synuclein expression was nutritionally regulated - the HFD-fed mice exhibited increased mRNA and protein levels compared to the control low fat diet (LFD)-fed mice. This increase could be reversed upon fasting or changing to LFD. Moreover, expression of γ-synuclein was restricted to the mature adipocytes and localized to the cytosol but not the lipid droplets. It has also been demonstrated that γ-synuclein is not required for adipocyte differentiation as the KO mice developed mature WAT adipocytes. This

has been confirmed in experiments with mouse embryonic fibroblasts (MEF) isolated from KO and Wt mice that revealed no effect of γ-synuclein expression on differentiation of preadipocytes *in vitro*, as cells of both genotypes differentiated into adipocytes with similar efficiencies and kinetics.

However, the ablation of γ-synuclein protected mice from HFD-induced obesity and associated metabolic disturbances. The HFD-fed KO mice gained only 16% of their original body weight compared to a 33% weight gain in the HFD-fed Wt mice, with no difference observed in weight between Wt and KO mice fed LFD. This attenuated weight gain was at least partly attributed to the reduced adipocyte hypertrophy as the KO mice accumulated less WAT that was characterized by smaller size adipocytes compared to adipocytes in HFD-fed Wt mice.

The HFD-fed KO mice were also protected from metabolic disturbances associated with obesity. Plasma insulin levels were only increased in the HFD-fed Wt mice (~3 fold increase), with the HFD-fed KO mice retaining similar levels to those in the LFD-fed mice. Likewise, hepatic and plasma Triacylglycerol (TAG) levels were only increased in the HFD-fed Wt mice, with the HFD-fed KO mice retaining similar levels to those in the LFD-fed mice. Also, no steatosis was observed in the liver of the HFD-fed KO mice. However, in contrast to mice on LFD, both KO and Wt mice on HFD reported increased plasma leptin levels, but less significantly so in the KO mice (~2.9 fold increase versus ~5.5 fold increase, respectively). In addition, the HFD-fed KO mice exhibited increased whole-body lipid utilization and energy expenditure, with increased lipid oxidation and reduced carbohydrate oxidation compared to the HFD-fed Wt mice.

The decreased lipid storage and increased lipid utilization mentioned above in the HFD-fed KO mice were suggested to be due to increased lipolytic capacity of WAT adipocytes lacking γ-synuclein. This suggestion was supported by the increased levels of non-esterified fatty acids (NEFA), as well as ~1.8 fold increase in the protein levels of adipose triglyceride lipase (ATGL) observed in epididymal WAT of the HFD-fed KO mice. Also, this tissue displayed ~1.9 fold increase in the protein levels of phosphorylated extra cellular regulated kinase (ERK, Thr202/Tyr204), a key protein kinase intracellular signalling molecule in the ERK signalling pathway involved in many basic cellular processes including cell cycle, cell proliferation and cell differentiation, including adipocyte differentiation (Bost et al., 2005). The nature of this increased phosphorylation (or dephosphorylation failure), and thus relative increased activity, of ERK is not clear.

Moreover, the decreased lipid accumulation and adipocyte size in the HFD-fed KO mice were postulated to arise from attenuated modulation of SNARE assembly. In adipocytes, lipid droplet formation and growth occurs through fusion of neutral TAG packaged-amphipathic lipoproteins with the phospholipid monolayer surrounding the lipid droplet. This fusion is believed to be mediated by the adipocyte vSNARE protein VAMP-4 and the tSNARE proteins syntaxin-5 and SNAP-23 (Bostrom et al., 2007). Analysis of epididymal WAT showed that the amount of co-immunoprecipitated VAMP-4 and syntaxin-5 in the HFD-fed KO mice was significantly less (by ~35%) than that in the HFD-fed Wt mice. This suggested that in adipocytes γ-synuclein modulates SNARE complex-mediated fusion between the amphipathic lipoprotein-packaged neutral TAG and the phospholipid monolayer surrounding the lipid droplet, thus contributing towards lipid accumulation in WAT.

1.4. The role of γ-synuclein in mammary gland tumourigenesis

γ-synuclein was named breast cancer-specific gene1 (BCSG1) because it was found to be aberrantly expressed in a large percentage of advanced infiltrating breast carcinomas, compared to normal tissue and benign tumours where its levels were absent or hardly detectable (Ji et al., 1997). Investigations of γ-synuclein, whose physiological function is not clearly known yet, have since revealed some properties that support its role in breast cancer: it was found to stimulate the growth and proliferation of cancer cells, promote the survival of cancer cells and inhibit apoptosis, inhibit the mitotic check point function and thereby increase chromosomal instability, and enhance breast cancer cell motility and metastasis. These findings were largely based on cell culture system studies utilizing breast cancer cell lines and raise questions about the *in vivo* role of γ-synuclein in the development and progression of breast cancer. The studies that led to these findings are discussed below.

1.4.1. Aberrant expression of γ-synuclein in tumours of different tissues occurs in a stage-specific manner

To identify genes differentially expressed in breast cancer tissue compared to normal tissue, a high-throughput differential cDNA sequencing approach was utilized. A gene that was expressed abundantly in a breast cancer cDNA library but scarcely in a normal breast cDNA library was isolated and named BCSG1 (Ji et al., 1997). Furthermore, *in situ* hybridization analysis found BCSG1 to be expressed in a tumour stage-specific manner: it was undetected in normal or benign lesions, partially expressed in ductal carcinoma *in situ* and abundantly expressed in advanced infiltrating carcinoma. This raised the possibility of using it as a marker of breast

cancer progression. No tumour-specific mutations were found when sequence information from breast tumour and normal mRNA and gene were compared, suggesting that the development of breast tumour correlates with overexpression of the wild type gene (Ninkina et al., 1998).

In addition to breast carcinomas, the aberrant expression of γ-synuclein was also confirmed in preneoplastic lesions of the ovary and in a high percentage of ovarian carcinomas where it was also mostly restricted to late stages III and IV. Consistent with previous findings, when the tumours were analysed for gene mutations neither DNA abnormalities like rearrangements and amplifications nor sequence changes were detected (Bruening et al., 2000). This, again, suggested that the aberrant expression was mediated at the transcriptional or post-transcriptional levels. Moreover, the abnormal expression of γ-synuclein was also detected in a high percentage (67.5%) of tumours covering a wide range of cancer types, including liver, gastric, lung, colon, oesophagus, prostate, cervical and breast, but rarely in normal adjacent tissue (0.6%). This expression was also stage-specific where little expression was detected in the early stage I and abundant expression was detected in the later stages II-IV (Liu et al., 2005). Another important finding was the strong correlation between the aberrant expression in the primary tumours and the progression to distant metastases in patients irrespective of the cancer type. Further studies, particularly in breast cancer (Guo et al., 2007; Wu et al., 2007; Wu et al., 2003), and in liver cancer (Zhao et al., 2006), confirmed the above findings of late stage-specific aberrant expression of γ-synuclein in tumours and its correlation to metastasis. The above studies lend support to the potential use of γ-synuclein as a marker of cancer progression and as a possible target for cancer treatment.

1.4.2. Mechanisms of γ-synuclein gene aberrant expression

The loss of epigenetic control of γ-synuclein expression through CpG island demethylation was first revealed in a study utilizing human cancer cell lines (Lu et al., 2001). The CpG island of exon 1 of γ-synuclein-positive SKBR-3 and T47D breast cancer cells were found unmethylated, but the CpG island of exon 1 of γ-synuclein-negative MCF-7 cells was densely methylated. When the demethylating agent 5-Aza-2'-deoxycytidine was added to the MCF-7 cells γ-synuclein transcription was activated. Moreover, the 5' promoter region was found to be important for the basal transcriptional activity of γ-synuclein gene through a GC-rich sequence upstream of the transcription initiation site. This sequence was bound specifically by the transcription factor SP1 in cancer cells that were either positive or negative for γ-synuclein expression.

In another study, methylation-specific PCR demonstrated the demethylated status of the CpG island of γ-synuclein gene in all hepatocellular carcinomas examined (Zhao et al., 2006). Gupta and co-workers also demonstrated that demethylation of the CpG island of exon 1 is a common mechanism employed by both breast and ovarian tumour-derived cell lines in the aberrant expression of γ-synuclein gene (Gupta et al., 2003a). Also, cigarette smoke extract induced demethylation of γ-synuclein CpG island in the γ-synuclein-negative A549 lung cancer cells, leading to the expression of the gene. This was shown to be due to an effect of down-regulating DNA methyl transferase3B (DNMT3B) that keeps γ-synuclein CpG island in a methylated state to silence its expression. Cigarette smoke extract also stimulated *in vitro* cell invasion of these cells in a γ-synuclein-dependent manner, as the number of invading cells

decreased to the control levels when siRNA was used to knockdown γ-synuclein (Liu et al., 2007a).

The aberrant expression of γ-synuclein may be further aggravated by the presence of high levels of the transcription factor activator protein 1 (AP1) in cancer cells. Intron 1 of γ-synuclein gene was shown to contain two AP1 binding sites, the mutation of which resulted in the marked down-regulation of γ-synuclein expression and subsequent suppression of tumour phenotype (Lu et al., 2002). It was also shown that c-Jun, the major component of AP1, bound the two AP1 sites and that transfecting a dominant negative mutant of c-Jun into T47D breast cancer cell line significantly reduced transcription of γ-synuclein. This investigation also demonstrated a significant inhibition of anchorage-independent growth of T47D cells expressing either the dominant negative mutant of c-Jun or γ-synuclein antisense mRNA. It is thus feasible that in the aberrant expression demethylation of the CpG island occurs first (to allow the basal transcription to proceed) followed by increased expression of γ-synuclein through elevated levels of AP1 in cancer cells. Indeed, many signalling pathways including c-Jun N-terminal kinase (JNK), protein kinase C (PKC) and MAPK/ERK were shown to converge on AP1 sites (Grundker et al., 2001; Song et al., 2001). The role of γ-synuclein in the proliferation and growth, survival and resistance to apoptosis, and in invasion and metastasis of cancer cells was shown in several studies using mostly cell culture systems, but also using *in vivo* systems.

1.4.3. γ-synuclein in breast cancer cell growth and proliferation

To investigate the role of γ-synuclein in cancer cell proliferation, γ-synuclein cDNA was stably transfected into γ-synuclein-negative MCF-7 breast cancer cells. This

expression resulted in a significant increase in the growth of these cells under both anchorage-dependent and anchorage–independent conditions, suggesting a role for γ-synuclein in cell growth and proliferation (Liu et al., 2000). Also, and as already mentioned above, knocking down of γ-synuclein using antisense mRNA in the γ-synuclein-positive T47D breast cancer cell line produced a significant inhibition of anchorage-independent growth of the cells (Lu et al., 2002). These findings were confirmed by a recent study utilizing short hairpin RNA (shRNA) to knockdown γ-synuclein in γ-synuclein-transfected MCF-7 cells and xenografting them in nude mice (Shen et al., 2011). The γ-synuclein-knockdown xenografts yielded significantly smaller tumour masses than the control ones, suggesting a role for γ-synuclein in tumour growth and a possible use as a therapeutic target.

To find a role for γ-synuclein in steroid-responsive mammary tumourigenesis, the effect of γ-synuclein on the transcriptional activity of estrogen receptor-alpha (ER-α) was investigated (Jiang et al., 2003). Estradiol (E2)-stimulated ER-α transcriptional activity was significantly increased when MCF-7 cancer cells overexpressing γ-synuclein were treated with estrogen, compared to estrogen-treated, γ-synuclein-negative MCF-7 cells. This effect of γ-synuclein was ligand-dependent as γ-synuclein had no effect in the absence of E2. Moreover, it was shown that overexpression of γ-synuclein stimulated ligand-dependent cell proliferation whereas suppression of endogenous γ-synuclein expression by antisense γ-synuclein mRNA-expressing plasmid constructs significantly inhibited it. Treatment with antiestrogens inhibited this ligand-dependent effect. Taken together, these results suggest that γ-synuclein is required for efficient ER-α signalling.

Building on this study, the same group showed that γ-synuclein was a component of the heat shock protein (Hsp)-ER-α complex, and that it enhanced the affinity of ER-α to estrogen as it activated the ligand-dependent ER-α transcriptional activity (Jiang et al., 2004). It is noteworthy to emphasise here once again that all three members of the synuclein family have been shown to possess chaperone-like activity: they suppressed the aggregation of thermally denatured alcohol dehydrogenase and chemically denatured insulin (Souza et al., 2000). Taken together, these data support a role for γ-synuclein in hormone-responsive mammary gland tumourigenesis.

Contrary to the above findings of enhancing breast cancer cell growth by aberrant expression of γ-synuclein, growth of human esophageal squamous cell carcinoma (ESCC) was negatively affected by upregulation of γ-synuclein (Zhou et al., 2003). In this investigation, semiquantitative RT-PCR on 27 pairs of ESCC samples and corresponding normal tissue was performed to assess the expression pattern of γ-synuclein. All normal samples were found to express γ-synuclein. However, γ-synuclein was downregulated in approximately 60% (16/27) of the ESCC samples while it was upregulated in only 22% (6/27) of the samples and was not changed in 5 samples. In a functional assay, γ-synuclein was ectopically overexpressed in ESCC 9706 cell line. This retarded the growth rate in either low or high serum medium and inhibited the transformation ability of the cells growing in soft agar. These findings led to the conclusion that γ-synuclein may act as a negative regulator in human ESCC development.

1.4.4. γ-synuclein may promote survival and inhibit apoptosis of cancer cells

One of the properties that tumours acquire in their defiance of the normal cell physiology is the ability to promote survival and inhibit apoptosis. A role for γ-synuclein in promoting this property was revealed in a cell culture study utilizing ovarian cancer cell lines ectopically overexpressing γ-synuclein (Pan et al., 2002). In these cells, co-immunoprecipitation of γ-synuclein and two major mitogen-activated protein kinases (MAPKs), extracellular-regulated protein kinases (ERK1/2) and c-Jun N-terminal kinase 1 (JNK1), was shown, thus demonstrating the ability of this protein to associate with kinases involved in cell proliferation and apoptosis. Overexpression of γ-synuclein induced activation of the survival factor ERK1/2 and attenuated activation of the pro-apoptotic factor JNK1 when the cells were subjected to heat shock, arsenate or UV radiation stress. In addition, the γ-synuclein overexpressing cells exhibited resistance to the chemotherapeutic drugs vinblastine and paclitaxel. However, when cells were treated with the mitogen-activated protein kinase kinase (MEK1/2) U0126 inhibitor, ERK1/2 activation was suppressed and resistance to paclitaxel was partially overcome. Also, γ-synuclein overexpression significantly down-regulated JNK1 and its downstream caspase-3 activity in response to vinblastine or paclitaxel application, suggesting that γ-synuclein blocks the JNK1-regulated apoptotic response induced by these chemotherapeutics. Taken together, these results support a role for γ-synuclein in promoting survival of cancer cells through activation of ERK1/2 and inhibiting apoptosis through downregulation of JNK1 activity (Pan et al., 2002).

γ-synuclein was also found to associate with the mitotic checkpoint kinase BubR1 in breast cancer cells (Gupta et al., 2003b). This association resulted in the reduction of

BubR1 protein levels without affecting its mRNA levels. This was evidenced by blocking of this effect through treatment of γ-synuclein transfected cells with the selective 26S proteasome inhibitor MG-132, suggesting the involvement of the proteasome machinery in γ-synuclein-mediated reduction of BubR1 levels. Inaba and colleagues treated γ-synuclein-positive breast cancer cells with the microtubule-destabilizing drug nocodazole and reported a 3-fold reduction in mitotic index (Inaba et al., 2005). This treatment also resulted in multinucleation in over one third of the cells compared to only 10% in the γ-synuclein-negative cancer cells. Moreover, apoptosis was induced in about 30% of the γ-synuclein-negative cells, whereas only 10% of the γ-synuclein-positive cells became apoptotic. Furthermore, nocodazole treatment of γ-synuclein-expressing breast cancer cells suppressed the activity of caspase 3. These effects were relieved by overexpressing BubR1. Taken together, these results suggest that γ-synuclein overexpression compromises the mitotic checkpoint control by interfering with the function of BubR1. This contributes to chromosomal instability of cancer cells and subsequently may accelerate the progression of cancer and speed up tumour metastasis, and may contribute to the resistance to anti-microtubule drug-induced apoptosis.

1.4.5. γ-synuclein and metastasis

The role of γ-synuclein overexpression in invasion and metastasis of breast cancer cells was first shown in a study using γ-synuclein-negative MDA-MB-435 cells (Jia et al., 1999). The cells were transfected with γ-synuclein and their properties were studied in cell culture as well as *in vivo*. In cell culture, γ-synuclein overexpression significantly stimulated the migration and invasion of the cells at least 3-fold and 4-fold, respectively, compared to γ-synuclein-negative cells. For *in vivo* studies, the

transfected and control cells were implanted in the mammary fat pads of athymic nude mice. Mice developed tumours with no difference in incidence. Axillary lymph nodes and lungs were examined at autopsy 40 days post implantation for general morphology and microscopically on H&E-stained sections. γ-synuclein-positive cells showed significantly higher average lymph node positivity (about 70%) than γ-synuclein-negative cells (27%). Lung metastases were also significantly higher in γ-synuclein-positive cells. These results emphasize the correlation between the abundant levels of γ-synuclein in primary tumours and the progression to metastasis.

The effect of γ-synuclein overexpression on cell motility was further demonstrated in breast and ovarian cancer cell lines (Pan et al., 2006). In the ovarian cancer line OVCAR5 that expresses high levels of γ-synuclein, *in vitro* cell motility was significantly decreased when γ-synuclein was knocked down using siRNA compared to untreated or mock-treated cells. The levels of the active forms of GTPases Ras-related C3 botulinum toxin substrate (RAC) and cell division control protein 42 (CDC42) were also increased in OVCAR5 cells by overexpressing γ-synuclein. In addition, γ-synuclein overexpression increased the levels of activated RHO GTPase 2-3 fold in MDA-435 breast cancer line. Also, ERK increased cell motility and was associated with and activated by γ-synuclein in A2780 and OVCAR5 ovarian cancer lines overexpressing γ-synuclein. The involvement of ERK and RHO pathways in γ-synuclein–enhanced cell motility was further evidenced by a significant reduction in cell motility when the cells were treated with known inhibitors of GTPase (C. difficile Toxin B) and ERK (MEK1 inhibitor UO126). These data suggest a role for γ-synuclein in breast and ovarian cancer metastasis by enhancing cell motility through activation of the RHO family GTPases and ERK.

1.4.6. γ-synuclein transgenic mammary glands exhibit increased epithelial proliferation

Further support to the role of γ-synuclein in mammary gland tumourigenesis came from a study using transgenic mice overexpressing γ-synuclein under the control of mouse mammary tumour virus (MMTV) promoter (Liu et al., 2007b). Whole mount histological analysis showed that the transgenic mammary gland exhibited a significant increase in the ductal branching morphology and terminal end bud density starting at 10 weeks of age. This indicates a highly proliferative capacity of epithelial cells at the terminal end buds. This pregnancy-like phenotype was confirmed by H&E-stained sections which also revealed hyperplasia-like structures in the transgenic mammary glands characterized by areas of multilayered epithelium. A one year-follow up revealed no development of carcinoma.

To determine whether γ-synuclein-enhanced ER-α signalling was responsible for this phenotype, ER-mediated transcriptional activities of the E2-regulated Trefoil factor 1 (TFF1/PS2) and Cathepsin D (Cat-D) genes were measured. Compared to control mice, the levels of PS2 and Cat-D in the transgenic mammary glands were 3.4-fold and 4.8-fold higher, respectively. No significant difference in ER-α levels was observed between the control and transgenic mice, indicating that the upregulation of PS2 and Cat-D was not due to ER-α levels but due to increased ER-α signalling. This conclusion was further supported by the fact that inhibiting ER-α signalling, through the use of tamoxifen (an estrogen antagonist) and ovarectomized mice, blocked γ-synuclein-induced proliferation. These γ-synuclein-induced ER-α effects are likely to be mediated by the chaperone activity of γ-synuclein as it participates in the Hsp-based ER-α-multiprotein chaperone complex.

1.4.7. γ-synuclein as a potential biomarker for breast cancer progression and therapeutic target

To determine whether γ-synuclein may be used as a biomarker of breast cancer prognosis and progression, 438 clinical breast specimens, of which 358 were cancerous, were screened for γ-synuclein expression by immunohistochemistry (Guo et al., 2007). The expression was strongly correlated with the stage of breast cancer, tumour size, lymph node involvement, metastasis and Her-2 (ErbB2) status, but not with estrogen receptor and progesterone receptor expression status. After a 64-month follow up patients whose tumours expressed γ-synuclein had a significantly shorter disease-free survival (DFS) and overall survival (OS) and a high probability of death compared to those with γ-synuclein-negative tumours. Multivariate analysis concluded γ-synuclein to be a strong independent prognostic variable. This can be very helpful when taking decisions of breast mastectomy.

γ-synuclein may also be a potential target for treatment. In fact, an ANK peptide was designed and shown by co-immunoprecipitation and colocalization techniques to associate with γ-synuclein (Singh et al., 2007). When this peptide was microinjected into γ-synuclein-positive MCF-7 cells a nocodazole-induced cell killing response similar to that of γ-synuclein-negative cells was produced. Moreover, overexpression of eGFP-ANK fusion protein resulted in about 3.5-fold reduction in γ-synuclein-induced resistance to paclitaxel. This effect of ANK peptide is thought to be through its association with γ-synuclein, thus allowing BubR1 to function in the mitotic checkpoint control and trigger apoptosis. Additional support to this finding can be found in a previous investigation by Zhou and co-workers (Zhou et al., 2006). They showed a significant correlation between γ-synuclein positivity and resistance to the

antimicrotubule drug paclitaxel in 12 breast cancer cell lines. They further demonstrated that downregulating γ-synuclein expression in these cells sensitized them to paclitaxel-induced cytotoxicity.

The highlighted above studies indicate that γ-synuclein plays a role in the tumourigenesis of the mammary gland. It stimulates the growth and proliferation of cancer cells, promotes the survival of cancer cells and inhibits apoptosis, inhibits the mitotic check point function and thereby increases chromosomal instability, and enhances breast cancer cell motility and metastasis. The above effects were obtained as a consequence of aberrant expression/overexpression of γ-synuclein largely in cell culture systems utilizing breast cancer cell lines. In transgenic mice, its aberrant expression seemed to stimulate ligand-dependent ER-α signalling, leading to a highly proliferative pregnancy-like phenotype of mammary epithelial cells and branching morphology. Therefore, if γ-synuclein had an influential role in enhancing the progression, and perhaps contributing to the development of mammary gland tumourigenesis, then abrogation of its expression would be expected to prevent the formation or retard the progression of mammary tumours. If such a result was achieved, more serious efforts would be directed towards exploring the use of γ-synuclein as a biomarker of breast cancer progression and prognosis, and certainly as a target for treatment. However, the role of endogenous γ-synuclein in mammary gland tumourigenesis has not been studied in an appropriate *in vivo* model and our research programme is the first attempt to demonstrate directly whether γ-synuclein is required for the development and/or progression of ErbB2-induced mammary tumours.

1.5 Aims

The main goal of this research project was to study the possible role of endogenous γ-synuclein in mammary gland tumourigenesis in an appropriate *in vivo* system. For this purpose, a breast cancer transgenic, ErbB2 mutant mouse model was chosen from which γ-synuclein gene was later deleted. This mutant ErbB2 model was chosen due to a previous observation in our lab correlating the expression of ErbB2 with that of γ-synuclein in the murine mammary tumour cell line MG1361 , a cell line that was originally established from a mammary adenocarcinoma isolated from the chosen model. To assess the effect of γ-synuclein gene ablation on ErbB2-induced mammary gland tumourigenesis the following objectives were set:

1. To investigate expression of γ-synuclein in normal mammary gland tissue and mammary tumours in mouse cancer models.

2. To study expression of γ-synuclein in mouse and human cancer cell lines and the subcellular localization of expression in the MG1361 mouse mammary tumour cell line.

3. To reveal the effect of γ-synuclein gene ablation on the normal development of the mouse mammary gland.

4. To investigate the effect of γ-synuclein gene ablation on mammary gland tumourigenesis in the constitutively activated ErbB2 transgenic model.

Chapter 2. Materials and Methods

2.1. Mouse lines used

2.1.1. Generation of experimental and control cohorts

Figure 2.1 below shows a diagram summarizing the breeding scheme used to produce the control and experimental groups.

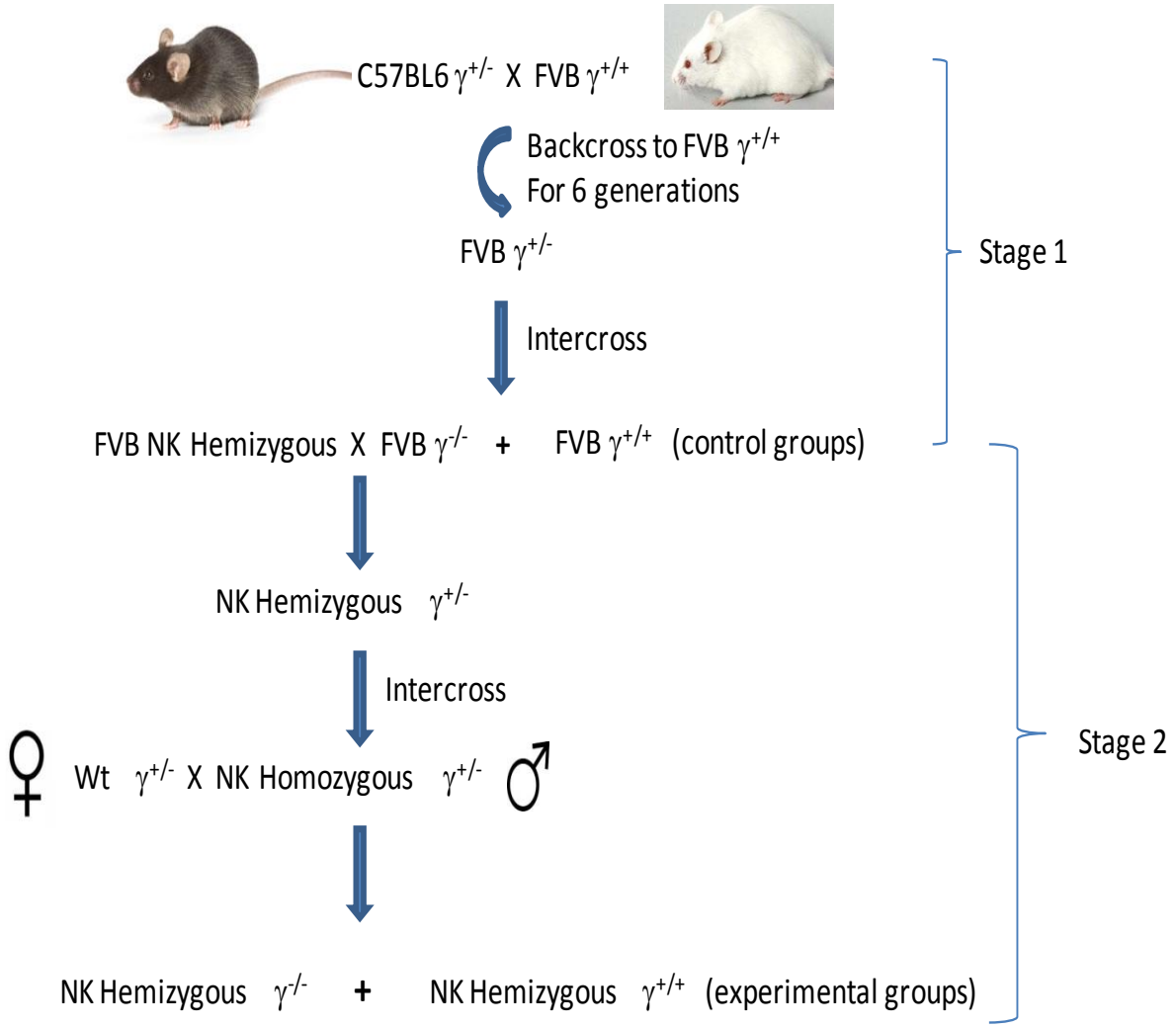

Figure 2.1. Breeding scheme. Stage I produces the control groups: FVB $\gamma^{-/-}$ and FVB $\gamma^{+/+}$. Stage II yields the experimental groups carrying the constitutively activated NK transgene in a Hemizygous form: one group homozygous for the γ-synuclein KO allele (NK Hemizygous / $\gamma^{-/-}$) while the other homozygous for the γ-synuclein Wt allele (NK Hemizygous / $\gamma^{+/+}$).

The experimental cohorts used in the main *in vivo* experiment were generated by breeding FVB γ-synuclein KO line with a breast cancer model harbouring a constitutively activated ErbB2 transgene under the control of MMTV promoter (NK line). The γ-synuclein KO line was generated in the laboratory of Prof. Vladimir Buchman as described previously by Ninkina and co-workers (Ninkina et al., 2003), while the establishment of the NK mutant line was described earlier by Muller and co-workers (Muller et al., 1988). The pregnancy passage control and experimental females were mated at about 7 weeks of age and pups weaned at 18-20 days of age.

2.1.2. Husbandry information

All work on animals was carried out in accordance with the United Kingdom Animals (Scientific Procedures) Act (1986) and European Directive EC 86/609. The animals were bred and maintained in cages with unlimited supply of food (Rodent pellets from Special Diets Services) and drinking water, with beddings changed 1-2 times per week. A light cycle of 12 hrs light:12 hrs darkness was used.

2.2. Genotyping

2.2.1. Standard PCR technique.

This was used to genotype the γ-synuclein Wt and KO alleles throughout the breeding process, as well as the NK transgene in the experimental groups. Genomic DNA (gDNA) was extracted using a phenol-based method as outlined below.

Phenol-based gDNA Extraction

Ear/tail biopsy of about 20-50 mg was obtained from the animal into a 1.5 ml eppendorf tube and stored at -20^{o} C until DNA extraction. 300 µl of *DNA extraction buffer solution was added and the tube incubated in a water bath at 55^{o} C for a minimum of 4 hours or overnight. After pulse vortexing, 300 µl of basic phenol (pH 8.0) (Sigma) was added and the tube vortexed and centrifuged for 10 minutes at 13000 rpm. The supernatant was transferred to a new tube for another round of phenol extraction and the supernatant transferred to a new eppendorf tube. An equal volume mixture of phenol/chloroform (Fisher Chemical) was added and same centrifugation repeated. The supernatant was transferred to a new tube and 10 µl of 3M NaOAc (sodium acetate, Sigma) plus 600 µl of absolute analytical grade ethanol (Fisher Chemical) was added. The tube was inverted few times for mixing, centrifuged for 2 minutes at maximum speed and the supernatant was discarded. The formed pellet was washed 3 times with 70% cold ethanol, speed-vacuum dried at 37^{o} C for 5-10 minutes and resuspended in 50 µl of nuclease-free, double distilled water.

***DNA extraction buffer**

1 % SDS (Sodium Dodecyl Sulfate) (Sigma-Aldrich)

100 mM NaCl (Sigma-Aldrich)

50 mM Tris pH 8.0 (Hydroxymethylaminoethane) (Sigma-Aldrich)

2 mM EDTA (Ethylenediaminetetraacetic acid) (Sigma-Aldrich)

2 mg/ml Proteinase K (Sigma-Aldrich), added fresh.

PCR protocol

5 µl of DNA suspension was added to a thin-walled PCR reaction tube and 45 µl of the following PCR Mastermix (prepared for 10 samples) was added:

PCR-grade water	440 µl
10x PCR Reaction Buffer (Fermentas)	50 µl
dNTPs (25 mM) (Fermentas)	4 µl
*Primers (100 µM (Sigma): forward	2.5 µl
Reverse	2.5 µl
Taq DNA Polymerase (5 U/µl) (Fermentas)	2.5 µl

The samples were then placed in a thermal cycler machine (PCR Express from Hybaid) and subjected to the following program:

2 mins	Initial denaturation	94 ^{o}C
Then 45 cycles of 15 sec	Denaturation	94 ^{o}C
30 sec	Primer annealing	60 ^{o}C
40 sec	Template extension	72 ^{o}C

The samples were then loaded and electrophoresed on a *2.5% agarose gel to separate the amplified fragments for genotype identification/confirmation. The bands were visualized and photodocumented using Gel Doc 2000 Transilluminator and Quantity One 4.2.1 software (Bio-Rad).

***2.5% agarose gel**

*TAE Buffer	100 ml
Agarose powder (Eurogentec)	2.5 g
Ethidium bromide (10 mg/ml) (Sigma)	5.0 µl

***TAE electrophoresis buffer (50x stock solution)**

Tris-base (Sigma)	242 g
0.5 M EDTA (pH 8.0) (Sigma)	100 ml
Glacial acetic acid (Fisher Scientific)	57.1 ml
Deionized water	adjust to 1 litre

***Primer sequences used for standard PCR genotyping**

For γ-synuclein genotyping three primers, with a common upstream primer for both Wt and KO alleles and a specific downstream primer for each, were used to potentially produce two amplified fragments: a wild-type fragment of 480 bp and a knock-out one of 397 bp:

Common upstream	5’-AGTCCTGGCACCTCTAAGCA-3’

Wild type downstream	5’-GGGCTGATGTGTGGCTATCT-3’
Knock-out downstream	5’-GAAGAACGAGATCAGCAGCC-3’

For NK transgene genotyping, a forward and a reverse primer produced a 622 bp fragment:

Forward	5’-TTTCCTGCAGCAGCCTAC-3’
Reverse	5’-CGGAACCCACATCAGGCC-3’

2.2.2. Quantitative real-time PCR (q-PCR)

This was used for genotyping the NK homozygous male parent used to produce the experimental NK hemizygous female cohorts, as it was necessary to differentiate between the homozygous and hemizygous genotypes. The technique was also used, with a preceding reverse transcription reaction step (qRT-PCR), to assess the level of mRNA expression in some mouse mammary cancer cell lines, as will be indicated later. For the purpose of genotyping, genomic DNA was purified from ear biopsies using a commercial kit (Promega Wizard SV Genomic DNA purification kit) in accordance with the manufacturer’s protocol. The real-time qPCR reaction was performed in an Applied Biosystems StepOne Real-Time PCR System (Applied Biosystems). Two *mastermixes were prepared, one included specific forward and reverse *primers to amplify a 69 bp fragment from the NK transgene, while the other utilized specific *primers for the housekeeping gene GAPDH for use as an internal control. The passive reference dye ROX (Finnzymes) was used to calibrate the thermal cycler machine for background fluorescence (non-PCR related fluorescence signal variation).

***Mastermix solution (sufficient for 24 wells/reactions)**

PCR grade water	376 µl
10x TrueStart^{TM} PCR buffer (Fermentas)	58 µl
25 mM $MgCl_2$ (Fermentas)	58 µl
dNTPs (25 mM) (Fermentas)	6 µl
CYBR Green (100 x) (Finnzymes)	6 µl
Rox (50x) (Finnzymes)	6 µl
Primers (100 µM) (Sigma): forward	3 µl
reverse	3 µl
TrueStart^{TM} HotstartTaq Polymerase (5U/µl) (Fermentas)	4 µl

***Primers to amplify a 69 bp fragment from the NK transgene**

Forward	5'-CCCCGGGAGTATGTGAGTGA-3'
Reverse	5'-TGAGCTGTTTTGAGGCTGACA-3'

***Primers for γ-synuclein expression**

Forward	5'-CCATGGACGTCTTCAAGAAAGG-3'
Reverse	5'-CGTTCTCCTTGGTTTTGGTG-3'

***Primers for the housekeeping gene GAPDH**

Forward	5'-CACTGAGCATCTCCCTCACA-3'
Reverse	5'-GTGGGTGCAGCGAACTTTAT-3'

18 µl of the relevant mastermix was added to a well containing 2 µl of gDNA template. Each sample was run in triplicates to ensure accuracy. The 48 well plate was then spun for a minute at 1200 rpm/min and loaded onto the StepOne real-time thermocycler. The samples underwent the following program:

10 mins		Hot start/Initial denaturation	94 ^{o}C
Then 40 cycles of	15 sec	Denaturation	94 ^{o}C
	60 sec	Primer annealing and extension	60 ^{o}C

A step-wise melting curve at increments of 0.3 ^{o}C was performed at the end of the thermocycling to determine the melting point of the amplicon and ensure specificity. StepOne Software v 2.0 (Applied Biosystems) was used to run and analyse the products. Fold change was calculated using the $2^{-\Delta\Delta Ct}$ comparative method.

2.3. Tumour monitoring

The mammary glands of the control and experimental female groups were monitored for tumour development. This was done by regular palpation (once or twice a week) of the mammary glands and recording the time and size of any tumours detected. Tumour size/volume was measured manually using an external calliper (Camlab) to determine width (greatest transverse diameter) and length (greatest longitudinal diameter) linear dimensions. Tumour size was calculated by use of the modified ellipsoid formula:

$$\text{Tumour volume} = \tfrac{1}{2} \times \text{Length} \times \text{Width}^2.$$

The following parameters were recorded and tabulated: age of animal (days) at parity, age at tumour detection, number of palpable tumours/animal, age at sacrifice, days from parity to sacrifice, days from tumour detection to sacrifice, age tumours reached a size of ~250 mm^3. To assess tumour kinetics, days for tumours to progress from a size of 250 mm^3 to a size of 750 mm^3 and 1500 mm^3 was noted. Eventually, the animals were sacrificed when the length of a tumour reached 20 mm, as required by the Home Office regulations. Animal sacrifice was carried out by cervical displacement in a designated procedure room in the animal house. At sacrifice, formed tumours and normal mammary gland tissue were harvested. Each harvested tissue was divided into 2 halves, one placed directly into liquid Nitrogen for subsequent storage at -80 ^oC while the other half was placed into a 20 ml tube containing fresh 4% formaldehyde fixative solution for histological sectioning. Furthermore, metastasis was investigated by post-mortem visual inspection and histological analysis of lung and kidney tissues.

2.4. Mammary gland whole mounts

Upon sacrificing the animal, either of the fourth pair of mammary glands (L4 or R4) was dissected out and spread on a microscope slide taking care to preserve the shape and structure of the gland. The gland was then fixed in *Carnoy's solution for about 3 hours and transferred to 70% ethanol for 15 minutes. It was then washed with running tap water for about a minute and transferred to *Carmine solution for overnight staining in the dark at room temperature. The gland was later washed with tap water until the water ran clear. It was then dehydrated in a series of increasing alcohol concentration (50%, 70%, 90% and 100%) for 10 minutes/step and then immersed in xylene overnight for defatting the gland tissue to obtain clear ductal morphology. The gland was then mounted in DPX for visualization under a dissecting microscope and photodocumented.

***Carnoy's solution**

60% ethanol, 30% chloroform and 10% acetic acid.

***Carmine Alum staining solution**

To 500 ml distilled water, 1 g of carmine And 2.5 g of aluminum potassium sulfate were added and mixed well. The solution was then boiled for 20 minutes and the final volume was adjusted to 500 ml with distilled water. The solution was filter sterilized and a crystal of thymol was added as a preservative. The staining solution was stored at 4°C.

2.5. Conventional histology

(All reagents were purchased from Fisher Scientific unless otherwise stated).

2.5.1. Fixation

Harvested tissue samples were immediately fixed in a freshly prepared *4% formaldehyde (Sigma-Aldrich) solution overnight at 4 °C and then transferred to 70% alcohol before processing.

***4% formaldehyde solution in PBS**

For preparation of a 100 ml volume, 4 g of paraformaldehyde powder (Sigma) was weighed in a fume cupboard and transferred into a bottle containing about 80 ml of ddH_20 already placed on a hotplate magnetic stirrer (about 60^oC).The bottle was heated up for few minutes and about 100 µl of 10 N NaOH was added to adjust the pH to between 7 and 8 for paraformaldehyde to dissolve and form a clear solution of formaldehyde. The solution was allowed to cool and then filtered through a filter paper. 10 ml of *10x PBS was added and the volume adjusted to 100 ml. The pH was rechecked and, if necessary, adjusted to 7.2-7.8.

***10x PBS solution**

This was prepared by dissolving PBS tablets (Sigma-Aldrich) in the appropriate volume of ddH_20 according to the manufacturer's instructions.

2.5.2. Histological sectioning

The samples were embedded with paraffin wax at 60°C by a Leica TP1050 fully enclosed automatic tissue processor (Leica) using the following schedule:

70% alcohol	1:00 hr

90% alcohol	1:30 hr
100% alcohol	1:30 hr
100% alcohol	2:00 hr (x2)
Xylene	1:00 hr (x2)
Paraffin wax	1:30 hr
Paraffin wax	2:00 hr (under vacuum) (x2)

After processing, samples were embedded in paraffin wax blocks using a Leica EG1150H Embedding Centre. The paraffin wax was then allowed to harden rapidly by placing the blocks on a Leica EG1140C cold plate. 5µm-thick sections were then cut using a Leica RM2235 rotary microtome, floated on warm water and mounted on Polysine microscope slides. The sections were allowed to dry overnight at 45 ^{o}C.

2.5.3. Hematoxylin and Eosin (H&E) staining

Slides were stained for H&E using an R.A. Lamb Histomate staining machine (R.A. Lamb) programmed to carry out the following protocol:

Xylene	2 Mins (x3)
100% Alcohol	2 Mins (x3)
95% Alcohol	1 Mins
70% Alcohol	1 Mins
Water	3 Mins
Gills II Haematoxylin	5 Mins
Water	3 Mins
1% Acid Alcohol	10 Secs
Water	5 Mins

1% Eosin	5 Mins
Water	30 Secs
70% Alcohol	30 Secs
95% Alcohol	1 Mins
100% Alcohol	1 Mins
100% Alcohol	2 Mins (x2)
Xylene	1 Mins
Xylene	2 Mins (x2)

DPX mountant (BDH) was then used to mount the sections under a cover glass (VWR international).

2.6. Immunohistochemistry (IHC)

Normal and tumour mammary gland samples were fixed in either 4% formaldehyde overnight at 4 °C or in Carnoy's solution for 4 hours at room temperature. 5 μm-thick sections were then obtained onto microscope slides as outlined above in the conventional histology section. Immunostaining for mouse γ-synuclein in the mammary tissue sections utilized an affinity-purified polyclonal antibody (SK23), which was produced in the laboratory of Prof. Vladimir Buchman (Buchman et al., 1998b). The sections were first deparaffinized by rocking in xylene for 5 minutes and then rehydrated using a decreasing concentration of alcohol solution as follows:

100% Ethanol	Rock for 5 Mins
95% Ethanol	Rock for 5 Mins
50% Ethanol	Rock for 5 Mins
ddH_20	Rock for 5 Mins (x2)

The sections were quenched for endogenous peroxidase activity in a solution of 3% H_2O_2 (Sigma) in Methanol (Fisher Scientific) for 20 minutes and then washed 3 times with ddH_20 for 5 minutes each time. They were next blocked for 90 minutes in *10% horse serum (Invitrogen) made in T-PBS solution (1x PBS containing 0.4% Triton X-100). This was followed by an overnight incubation at 4 °C in a 1:500 dilution of rabbit polyclonal SK23 anti-mouse γ-synuclein (primary antibody) in blocking solution. The sections were washed in 1x PBS 3 times of 5 minutes each and subsequently incubated in a 1:500 dilution of secondary antibody (biotinylated goat anti-rabbit IgG) (Vector Laboratories) in T-PBS solution. Vectastain containing Avidin-Biotin-Horseradish Peroxidase enzyme Complex (ABC complex) (Vector

Laboratories) was later added according to the manufacturer's protocol. The samples were then washed with 1x PBS. Immunoreactivity was detected by addition of the horseradish peroxidase (HRP) substrate Diaminobenzidine (DAB) (Sigma) until visualization of the characteristic brown colour product was possible (about 5 minutes). The samples were instantly washed with 1x PBS to prevent excess colouration. They were next washed 3 times in ddH_2O and dehydrated by passing through a series of increasing alcohol concentration as follows:

50% Ethanol	Rock for 5 Mins
95% Ethanol	Rock for 5 Mins
100% Ethanol	Rock for 5 Mins
Xylene	Rock for 5 Mins

The sections were finally mounted in DPX for visualization under light microscopy.

2.7. Cell culture of human and mouse cancer cell lines.

2.7.1. Mouse cancer cell lines

Cell line	Brief description	Culture conditions
MG 1361 (ICLC)	Transgenic mammary gland adenocarcinoma; Transformed by Rat activated Neu oncogene.	William's medium E (Gibco) + 15% FBS (Fetal Bovine Serum) (Gibco) + 2 mM L-Glutamine (Gibco) + 1% non-essential amino acids (Sigma-Aldrich) + Penicillin (50 IU/ml) and Streptomycin (50 µg/ml) (Sigma-Aldrich). Incubation at 37 °C and 5% CO_2. Cultures split at 1:4.
4T1 (ATCC)	Tumourigenic mammary adenocarcinoma	RPMI-1640 medium (Sigma-Aldrich) + 10% FBS + 2 mM L-Glutamine + Penicillin (50 IU/ml) and Streptomycin (50 µg/ml). Incubation at 37 °C and 5% CO_2. Cultures split at 1:4.
EpH4	Non-tumourigenic mammary carcinoma	Dulbecco's Modified Eagle Medium (DMEM) (Gibco) + 10% FBS + 2 mM L-Glutamine + Penicillin (50 IU/ml) and Streptomycin (50 µg/ml). Incubation at 37 °C and 5% CO_2. Cultures split at 1:4.
N202-A	Derived from the Rat-Neu overexpressing line N202 which is a mouse mammary cancer cell line.	Dulbecco's Modified Eagle Medium (DMEM) + 20% FBS + 2 mM L-Glutamine + Penicillin (50 IU/ml) and Streptomycin (50 µg/ml). Incubation at 37 °C and 5% CO_2. Cultures split at 1:4.
N202-B	Derived from N202-A with downregulation of Neu expression.	Dulbecco's Modified Eagle Medium (DMEM) + 20% FBS + 2 mM L-Glutamine + Penicillin (50 IU/ml) and Streptomycin (50 µg/ml). 37 °C and 5% CO_2. Cultures split at 1:4.

Table 2.1. Brief description and culture conditions of mouse cancer cell lines.

Table 2.1 above and table 2.2 below show brief descriptions and culture conditions of mouse and human cancer cell lines used in this study, respectively.

2.7.2. Human cancer cell lines

These included the 9 breast cancer cell lines MDA-MB-468, MDA-MB-231, MCF-7, GI101, Hs578T, BT20, BT474, SKBR3 and T47D, and the ovarian cancer cell line SKOV3.

Cell line	Brief description	Culture conditions
MCF-7, MDA-MB-231, SKBR3, BT20, MDA-MB-468, Hs578T	Mammary adenocarcinoma	Dulbecco's Modified Eagle Medium (DMEM) + 10% FBS + 2 mM L-Glutamine, [+ 10 µg/ml Bovine Insulin for Hs578T] + Penicillin (50 IU/ml) and Streptomycin (50 µg/ml). Incubation at 37 °C and 5% $CO_{2.}$ Cultures split at 1:4. (Hs5787 culture split at 1:3; MDA-MB-231 culture split at 1:6).
T47D	Mammary ductal carcinoma	Dulbecco's Modified Eagle Medium (DMEM) + 10% FBS + 2 mM L-Glutamine + Penicillin (50 IU/ml) and Streptomycin (50 µg/ml). Incubation at 37 °C and 5% $CO_{2.}$ Cultures split at 1:4.
SKOV-3	Ovarian adenocarcinoma	Dulbecco's Modified Eagle Medium (DMEM) + 10% FBS + 2 mM L-Glutamine + Penicillin (50 IU/ml and Streptomycin (50 µg/ml). Incubation at 37 °C and 5% $CO_{2.}$ Cultures split at 1:4.
BT474	Mammary ductal carcinoma	RPMI-1640 medium + 10% FBS + 2 mM L-Glutamine + 1mM Na Pyruvate (Sigma-Aldrich) + 0.01 mg/ml Bovine Insulin (Sigma-Aldrich) + Penicillin (50 IU/ml and Streptomycin (50 µg/ml). 37 °C and 5% $CO_{2.}$ Cultures split at 1:2.

Table 2.2. Brief description and culture conditions of human cancer cell lines. Standard microbiological procedures and aseptic conditions were followed at all stages of handling and growing of cell lines.

2.7.3. Defrosting cell stocks

Cells stored in Cryotubes (Thermoscientific) in liquid N_2 were brought up by putting tubes directly into dry ice and thawing in water bath at 37 °C as soon as possible. Under sterile conditions in the laminar flow cabinet, 1 ml of prewarmed (37 °C for at least 20 minutes) appropriate media was added and the cells transferred to a 15 ml falcon tube (Thermoscientific). The cells were centrifuged at 1100 rpm for 5 minutes and the supernatant media discarded into 3% Virkon solution (Du Pont). The cells were then resuspended in 7 ml of complete media by gentle pipetting up and down, transferred to a T25 culture flask (Corning) and incubated at 37 °C and 5% CO_2 in a humidified atmosphere.

2.7.4. Cell culture

After defrosting, cells were split as shown in tables above when they reached 80% confluency. 1-2 passages were allowed before cells were harvested for protein extraction. For passaging, T25 culture flask containing growing cells was placed in the laminar flow hood and the media was aspirated and discarded into Virkon solution. 1 ml of prewarmed 0.05% Trypsin with EDTA (Invitrogen) was added to remove the remaining media, as it might inhibit Trypsin activity, and then aspirated. 1-2 ml of Trypsin was added onto the monolayer of growing cells and the flask was incubated at 37 °C and 5% CO_2 for 2-5 minutes. The flask was then banged gently on the side to help detach the cells and placed under an inverted microscope to make certain of cell detachment. Trypsin was then inactivated by adding 10 ml of full medium with serum, and after gentle trituration using 10 ml pipette the cell suspension was transferred into a 15 ml falcon tube and centrifuged at 1100 rpm for 5 minutes. The supernatant containing trypsin was discarded and the cell pellet was resuspended in 4 ml of prewarmed complete media. The cell suspension was split as

recommended into a new T25 flask and media added up to 7 ml. The flasks were incubated as before and the media was changed every 2-3 days until 80% confluency.

2.7.5. Cell harvesting

When cells reached 80% confluency and were ready for harvesting, the media was aspirated and 10 ml of 1x PBS was added for washing. Upon aspiration, 2-3 ml of 1x PBS was added and the layer of attached cells was scrapped with a rubber cell scraper (BD Biosciences). The cells were collected in a 15 ml falcon tube and centrifuged at 1100 rpm for 5 minutes. The supernatant was discarded and cells were either lysed immediately or the cell pellet was placed on dry ice and transferred to a deep freeze (-80 °C) for storage until time for protein/RNA extraction.

2.8. Immunocytochemistry

2.8.1. Growing MG1361 cells on coverslips

Round 16 mm coverslips (VWR International) were used to culture the mouse MG1361 mammary tumour cell line. The coverslips were first placed in a 12-well plate (Thermoscientific) and submerged in absolute ethanol for sterilization. Ethanol was aspirated and the coverslips were allowed to air-dry in the laminar flow cabinet. They were then rinsed 3 times with sterile ddH_2O and allowed to dry. For enhanced cell adhesion, the coverslips were coated with a solution of Poly-L-Lysine (PLL) (Sigma-Aldrich). About 80 µl of an equal volume mixture of 0.01% PLL and sterile ddH_2O was applied evenly across the surface of the coverslips. They were then incubated at 37 °C and 5% CO_2, followed by PLL aspiration and air-drying in the laminar flow hood. The coverslips were then seeded with the mouse mammary cancer cell line MG1361. This was done by taking 80% confluent cells growing in a T25 flask and trypsinizing and washing the cells with 1x PBS as above. They were then washed with 10 ml of William's medium E and resuspended in 10 ml of media. 5 ml of the cell suspension was then added to 15 ml of media and 2 ml of this was plated in each of 10 wells that contain the PLL-coated coverslips. Cells were allowed to adhere and grow until they reached 80% confluency, at which time they were ready for immunostaining.

2.8.2. Immunostaining of MG1361 cancer cells

The 80% confluent cells growing on coverslips were transferred into a new 12-well plate with about 500 µl of media they were growing in added to prevent drying. They were then washed with 1 ml of cold 1x PBS. The PBS was aspirated and cells were fixed by adding 4% formaldehyde solution in PBS. The plate was incubated at 4 °C

for 20 minutes. The fixative was aspirated and the cells were washed with cold 1x PBS. The cells were incubated with 1 ml of cold methanol for 5 minutes at room temperature. After, the cells were washed 3 times with cold 1x PBS. 10% goat serum was applied as blocking buffer with 1 hour incubation at room temperature. After the incubation time was up, 100 µl of each of five *primary antibody solutions in 1% blocking buffer was pipetted onto a parafilm strip to form a bubble. The blocking buffer was then aspirated from the wells and coverslips carefully placed with the cells down onto the bubble and incubated at room temperature for 2 hours. Upon completion of the 2 hour incubation with primary antibody, the cells were placed back in the 12-well plate and washed 3 times with cold 1x PBS. 500 µl of secondary antibody solution, containing 1:3000 dilution of each of goat anti-rabbit IgG-Alexa fluor 546 (Invitrogen) and goat anti-mouse IgG-Alexa fluor 488 (Invitrogen), was added to the cells and incubated for 1 hour in the dark at room temperature. The cells were then washed 3 times with cold 1x PBS. 0.1 µg/ml of DAPI solution in 1% PBS was applied for 5 minutes at room temperature protected from light. Finally, the cells were washed 3 times with cold 1x PBS and mounted on slides using Immuno-mounts for observation under confocal fluorescent microscopy.

***Primary antibody solutions**

- Affinity purified rabbit anti-mouse γ-synuclein (SK23) diluted 1:250 in 1% blocking buffer.
- Affinity purified rabbit anti-mouse γ-synuclein (SK23) + mouse anti-vimentin (BD Pharmigen) both diluted 1:250 in 1% blocking buffer.
- Affinity purified rabbit anti-mouse γ-synuclein (SK23) + mouse anti- γ-tubulin (Sigma-Aldrich) both diluted 1:250 in 1% blocking buffer.

- Affinity purified rabbit anti-mouse γ-synuclein (SK23) diluted 1:250 + mouse anti-α-tubulin (Sigma-Aldrich) diluted 1:5000 in 1% blocking buffer.
- Affinity purified rabbit anti-mouse γ-synuclein (SK23) diluted 1:250 + mouse anti-β-Actin (Sigma-Aldrich) diluted 1:5000 in 1% blocking buffer.

2.9. γ-synuclein mRNA expression in mouse mammary cancer cell lines

qRT-PCR utilizing Cyber-green chemistry was used to compare the level of γ-synuclein mRNA expression in ErbB2-positive mouse cancer cell line MG1361 to that of ErbB2-negative 4T1 and EpH4 mouse cancer cell lines, as well as to Wt-SpC (spinal cord) that highly expresses γ-synuclein. In a separate run, the levels of γ-synuclein mRNA expression in N202A, N202E and 4T1 cell lines were compared. To this end, total RNA was first isolated from cell pellets and spinal cord tissue using Qiagen RNeasy mini kit according to the manufacturer's protocol (Qiagen). The quantity and purity of extracted RNA was assayed by measuring A_{260} and A_{280} using NanoDrop spectrophotometer (Labtech International). Subsequently, first strand synthesis on normalized RNA samples was carried out using random hexadeoxynucleotide primers (HP) (Promega). 1 µl of HP (from 0.5 mg/ml stock) was added to an eppendorf tube containing 1 µg of RNA in 12 µl of nuclease-free MQ H_2O. The solution was then incubated at 68 °C for 10 minutes to denature the secondary structure of RNA. The tubes were spun briefly and 7 µl of premix solution was added (4µl of 5x first strand buffer + 2µl of 0.1 M DTT + 1 µl of 10mM dNTPs). They were then incubated at room temperature for 10 minutes to allow binding of random primers to template RNA. The tubes were prewarmed in a 39 °C water bath for 2 minutes and 1 µl of superscript reverse transcriptase I was added. First strand cDNA synthesis was allowed to proceed at 39 °C for 1 hour. Finally, the tubes were transferred to ice, 30 µl of nuclease-free MQ H_2O added and the samples aliquoted into 15 µl and kept at -80 °C until qPCR was performed.

2.10. Western blotting

2.10.1. Isolation of total protein from cell pellets

The cell pellet (about 200 µl volume) was used fresh or taken out of the -80 °C and placed directly on ice. 400 µl of *2x Laemmli buffer without 2-mercaptoethanol was added with gentle mixing by pipetting up and down. A homogenizer (or a small syringe with a 23G needle) was used to aid lysing the cells. When the lysate was too viscous more buffer was added and/or boiling was performed for about 10 mins. A portion of the cell lysate (without 2-mercaptoethanol) was used to determine the protein concentration using the Bradford assay according to the manufacturer's protocol (Bio-Rad Protein Dc Assay). 100 µl of the cell lysate was transferred to a new eppendorf tube and 1.0 µl of 2-mercaptoethanol was added and mixed well. The lysate was then boiled at 100 °C for about 10 minutes to help denature the total proteins, placed on ice for about 5 minutes and kept at -20 °C until loading into an SDS-PAGE gel for Western blotting.

***2x Laemmli buffer without 2-mercaptoethanol**

Tris-HCl pH 6.8	100 mM
Glycerol	20%
SDS	4%
Bromophenol blue	0.02%

To prepare 2x Laemmli buffer with 2-mercaptoethanol it was added to a final concentration of 0.2 M.

2.10.2. Extraction of cytoplasmic protein from mammary tissues

About 30 mg of frozen tissue was weighed into an eppendorf tube containing 300 µl of ice-cold lysis buffer with protease inhibitors added. The tissue was homogenized using motorised pestle and resulting homogenate was centrifuged for 10 mins at 6500 rpm at 4 C°. 100 µl of the supernatant was transferred to a new eppendorf tube containing 100 µl of 2x Laemmli buffer without 2-mercaptoethanol and mixed well. A portion was used to determine the protein concentration using the Bradford assay according to the manufacturer's protocol (Bio-Rad Protein Dc Assay). 100 µl of the sample was transferred to a new eppendorf tube and 1.0 µl of 2-mercaptoethanol was added and mixed well. The tissue sample was then boiled at 100 °C for 10 minutes, placed on ice for about 5 minutes and kept at -20 °C until loading onto an SDS-PAGE gel for Western blotting.

***Lysis buffer with no protease inhibitors**

Tris-HCl pH 7.5	50 mM
NaCl	150 mM
Triton X-100	1%

For lysis buffer with protease inhibitors, 1 tablet of Complete Mini (Roche) was added per 10 ml of buffer just before use, in accordance with the manufacturer's instructions.

2.10.3. Sodium Dodecyl Sulfate-PolyAcrylamide Gel Electrophoresis (SDS-PAGE)

Having prepared proteins from cell pellets/mammary gland tissue in SDS loading buffer (Laemmli buffer), the samples were loaded into an SDS-PAGE gel for separation of proteins according to their molecular weight. For this, a mini-gel

apparatus (Bio-Rad) was assembled, and after the gel was set the *electrophoresis running buffer was added. Normalized levels of protein samples (15 µg) were loaded, with one well loaded with 3 µl of a molecular weight size marker (Fermentas PageRuler Plus). The gel was composed of two layers: an upper *stacking layer with 6% polyacrylamide concentration and a lower *resolving layer with 16% polyacrylamide. The gel was run at 200 volts for 50-60 minutes, giving the SDS-rendered negatively charged polypeptide chains enough time to separate.

***Stacking gel**

Acrylamide/Bisacrylamide (Sigma-Aldrich)	6%
Tris-base pH 6.8	155 mM
SDS	100 mM
APS (Ammonium Persulfate) (Sigma)	100 mM
TEMED (Tetramethylethylenediamine) (Fluka)	3 µl /3 ml of gel solution

***Resolving gel**

Acrylamide/Bisacrylamide	16%
Tris-base pH 8.8	312 mM
SDS	100 mM
APS	100 mM
TEMED	5 µl/5 ml of gel solution

***Electrophoresis buffer**

Tris-base	25 mM
Glycine (Sigma)	192 mM
SDS	0.1%

2.10.4. Transfer of proteins from the gel onto a PVDF membrane.

A semi-dry blotting apparatus (Sigma) was used to transfer the separated proteins from the mini-gel onto a Hybond-P (Amersham), hydrophobic polyvinylidene difluoride (PVDF) membrane. The membrane was cut to the size of the resolving gel (5 cm x 8 cm), washed with methanol, rinsed with MQ water and soaked in transfer buffer. Two pieces of thick blotting paper were cut to the size of the membrane/gel and soaked in *transfer buffer. The semi-dry blotting unit was placed on a level bench and a small amount of transfer buffer was applied to the center. A sandwich of blotting paper/gel/membrane/blotting paper was assembled and placed in the center. Transfer was allowed to run at 100 mA for 90 minutes. At the end of the run, the membrane was washed 3x 5 minutes in *TBS-T (Tris Buffered Saline with 0.1% Tween 20) to remove methanol and proceed to blocking. The gel was washed with water and rocked in few millilitres of Gelcode Blue stain reagent solution (Thermoscientific) to confirm protein separation.

***10x Transfer buffer**

Tris-base	250 mM
Glycine	1.5 M

To prepare fresh 1x transfer buffer, 10 ml of 10x transfer buffer was added to 20 ml of methanol and 70 ml of ddH_2O.

***TBS-T**

One pouch of Tris Buffered Saline powder pH 8.8 (Sigma) and 10 ml of 10% Tween 20 were dissolved in a total of 1 L MQ H_2O by stirring on a magnetic stirrer for 10 minutes.

2.10.5. Immunodetection

Before adding the primary antibody, the membrane was blocked with 4% dried skimmed milk (Marvel) in TBS-T for 60-90 minutes at room temperature to prevent non-specific background binding of the primary and/or secondary antibodies to the membrane. The blocked membrane was then incubated with *primary antibody solution overnight at 4 °C. The membrane was then washed 3x 10 minutes to remove the primary antibody and incubated with *HRP-conjugated secondary antibody for 60-90 minutes at room temperature. It was later washed 3x 10 minutes to remove the secondary antibody. To detect protein bands, ECL+ Enhanced ChemiLuminescence detection system (Amersham) was used according to the manufacturer's protocol. To ensure equal loading of samples, the membrane was reprobed with antibody against housekeeping proteins GAPDH or beta-actin. This was done by first washing it 3x 5 minutes with TBS-T to remove ECL+ and then stripping off antibodies using an *antibody stripping buffer. The membrane was incubated in the stripping buffer for 30 minutes at 55 °C and later washed 3x 5 minutes with TBS-T solution. It was then re-blocked with 4% milk and proceeded as above to reveal GAPDH or beta-actin bands.

***Primary antibody solutions**

- Affinity purified rabbit polyclonal anti-mouse γ-synuclein (SK23) diluted 1:1000.
- Mouse monoclonal anti- GAPDH, clone 6C5, (Santa Cruz Biotechnology) diluted 1:5000.
- Affinity purified rabbit polyclonal anti-human γ-synuclein (SK109) diluted 1:500.

- Rabbit polyclonal beta-actin – loading control (ab8227, Abcam) diluted 1:1000.

***HRP-conjugated Secondary antibodies (Amersham)**

- Peroxidase conjugated anti-mouse immunoglobulin antibody
- Peroxidase conjugated anti-rabbit immunoglobulin antibody

***Antibody stripping buffer**

Tris-HCl pH 6.8	62.5 mM
SDS	2%
2-mercaptoethanol (added just before use)	100 mM

2.11. Extraction and purification of γ-synuclein protein from human breast cancer cell line SKBR3.

2.11.1. Protein precipitation with Ammonium Sulfate

All of the extraction steps were carried out on ice to prevent protein degradation. SKBR3 cells were cultured and harvested as above, with about 1.9 grams of cell pellet was produced and kept at -80 °C until lysis. The pellet was homogenized in 10ml of lysis buffer containing Complete Mini Protease Inhibitors (Roche) using glass/Teflon homogenizer. The homogenate was centrifuged at 4° C for 20 minutes at 13,000 rpm and the supernatant was transferred to a new tube. Enough buffer (50 mM Tris-HCl pH 7.5) was added to resuspend the pellet and a 30 µl aliquot was taken from both the supernatant (Lysate fraction) and the pellet (Nuclear fraction) for Western blot analysis of γ-synuclein content. Proteins were precipitated from the supernatant by gradual addition of 0.6 volume of saturated (4M) $(NH_4)_2SO_4$ with gentle mixing. The solution was incubated on ice for 10 minutes. It was then centrifuged at 4° C for 20 minutes at 13000 rpm and the supernatant was transferred to a new tube. Enough buffer (50 mM Tris-HCl pH 7.5) was added to resuspend the pellet and a 30 µl aliquot was taken from both the supernatant (1.5 M supernatant fraction) and the pellet (1.5 M pellet fraction) for Western blot analysis. A calculated amount of $(NH_4)_2SO_4$ crystals was added with gentle swirling to increase the concentration to 2 M and the solution was incubated on ice for 10 minutes. It was then centrifuged at 4° C for 20 minutes at 13000 rpm and the supernatant was transferred to a new tube. Enough buffer (50 mM Tris-HCl pH 7.5) was added to resuspend the pellet and a 30 µl aliquot was taken from both the supernatant (2 M supernatant fraction) and the pellet (2 M pellet fraction) for Western blot analysis.

This process of gradual increase in $(NH_4)_2SO_4$ concentration to precipitate proteins was repeated twice to obtain 2.5 M and 3 M fractions of both supernatant and pellet, with aliquots taken for Western blot monitoring of γ-synuclein content. All fractions were kept at -80° C until further purification.

2.11.2. Gel Filtration Chromatography

The 2 M pellet fraction containing γ-synuclein, resuspended in 4.5 ml of 50 mM Tris-HCl pH7.5 buffer, was defrosted on ice and centrifuged at 4° C for 20 minutes at 13000 rpm to eliminate any particulate matter. The supernatant was transferred to a new tube and a 30 µl aliquot was taken for Western blot analysis of γ-synuclein content. A Superdex 75 10/600 GL column (GE Healthcare) was used to fractionate the protein sample as a first step of purification. The column was mounted on an AKTA prime plus system (GE Healthcare), a fully automated liquid chromatography system. A PrimeView software was used to acquire and evaluate data communicated from the AKTA purifier. Prior to applying the sample, the column was washed with 5 column volumes of MQ water to remove the 20% ethanol it was stored in. It was then equilibrated with 5 column volumes of gel filtration buffer (50 mM Tris-HCl pH 7.5/100 mM NaCl). Both MQ water and buffer were degassed and filtered before use. The 4.5 ml sample was applied at 3 runs of 1.5 ml each. The column was run at a flow rate of 1 ml/min and over fifty 2 ml-fractions were collected for each run. The fractions were kept in the cold room as they were collected and aliquots were taken for Western blot analysis of γ-synuclein content.

2.11.3. Ion Exchange Chromatography

6 fractions from the gel filtration run above that were positive for γ-synuclein were combined (for a total of 12 ml sample) for further purification using an anion

exchange matrix (Resource-Q column from GE Healthcare). The same fully automated AKTA purifier system was used along with the complementary PrimeView software. The column was first washed with 5 column volumes of MQ water, applied at 4 ml/min, to remove the 20% ethanol it was stored in. It was then washed with 5 column volumes of binding buffer (50 mM Tris-HCl pH 7.5/100 mM NaCl). MQ water, binding buffer and elution buffer (50 mM Tris-HCl pH 7.5/1 M NaCl) were degassed and filtered before use. The column was then washed with 5 column volumes of elution buffer followed by equilibration with 5 column volumes of binding buffer. The sample was loaded at a flow rate of 4 ml/min and 12 ml of flow through was collected. The column was washed with binding buffer and 40 ml of wash was collected. A linear gradient elution was then performed with an increasing ionic strength of up to 0.5 M NaCl, with fifty five 3 ml-fractions collected. This was followed by a step elution to 1 M NaCl ionic strength to elute remaining bound protein, with fifteen 3 ml-fractions collected. The column was finally washed with 5 volumes of binding buffer, then 10 volumes of MQ water and last washed with 5 volumes of 20% ethanol for storage. Aliquots were taken from flow through, wash and eluted fractions for Western blot analysis of γ-synuclein content.

2.11.4. Dialysis

Dialysis tubing, high retention seamless cellulose tubing (Sigma), with a molecular weight exclusion of 12 kDa was used to remove smaller molecules and salts. The tubing was cut into 15 cm segments which were then washed by boiling submerged for 10 minutes in a solution of 100 mM EDTA pH 8.0 (Sigma). The tubing segment was clipped at one end, the sample pipetted in and clipped at the other end. It was then placed in a large beaker containing 2 l of 5 mM Ammonium Carbonate (Sigma) to be dialysed overnight at 4°C with constant stirring. The dialysis solution was

decanted and a fresh one added for a further 3-hour dialysis. The sample was then transferred to a 50 ml falcon tube, placed on dry ice and was freeze-dried overnight. The lyophilized sample was resuspended in 200 µl of 10 mM Tris-HCl pH 7.5. 30 µl aliquots were taken before and after dialysis as well as after lyophilisation for Western blot analysis of γ-synuclein content.

2.12. Enzymatic testing of purified γ-synuclein for glycosylation and phosphorylation.

2.12.1. Enzymatic glycosylation test.

N-Glycosidase F (PNGase F) (BioLabs), an amidase that cleaves between the innermost *N*-Acetylglucosamine (GlcNAc) and Asparagine, was used according to the manufacturer's protocol to investigate whether γ-synuclein was post-translationally modified by N-linked glycosylation. 9 µl of purified γ-synuclein (about 1 µg) was added to an eppendorf tube containing 1 µl of 10x glycoprotein denaturing buffer and incubated at 100 °C for 10 minutes. Upon denaturation, 2 µl of 10x G7 reaction buffer, 2 µl of 10% NP40, 6 µl of MQ water and 1 µl of PNGase F enzyme (500 U) were added. The reaction was then incubated at 37 °C for 1 hr. After, 7 µl of 4x Laemmli buffer was added, tubes incubated at 100 °C for 5 minutes to deactivate the enzyme and 15 µl was loaded onto a 13% SDS-PAGE. Upon electrophoresis, the samples were immunoblotted and processed as outlined above (sections 2.10.4 for and 2.10.5) for detection of γ-synuclein.

2.12.2. Enzymatic phosphorylation test.

Shrimp alkaline phosphatase (SAP) (Promega) was used to remove any phosphate groups may have been added as post-translational modification to γ-synuclein. 9 µl of purified γ-synuclein (about 1 µg) was added to an eppendorf tube containing 2 µl of 10x SAP buffer, 2 µl of SAP enzyme (10 U) and 7 µl of MQ water, and incubated at 37 °C for 30 minutes. The reaction was then inactivated by incubation at 65 °C for 15 minutes. After, 7 µl of 4x Laemmli buffer was added and 15 µl was loaded onto a 13% SDS-PAGE. Upon electrophoresis, the samples were immunoblotted and

processed as outlined above (sections 2.10.4 for and 2.10.5) for detection of γ-synuclein.

2.13. Statistical analysis

As the sample sizes used for both γ-synuclein Wt and γ-synuclein KO experimental females were small (N=21 and N=22, respectively), non-parametric statistics was used. For this purpose, the Wilcoxon's rank sum test was performed using Minitab-16 software program. This was used to analyse the significance of differences between the γ-synuclein Wt and γ-synuclein KO experimental females in the different animal parameters collected: number of palpable tumours; age at parity; age at sacrifice; age at detection of the first palpable tumour; age at detection of all palpable tumours; age at which tumours reached a size of 250 mm^3; age required for tumours to grow from a size of 250 mm^3 to a size of 1500 mm^3. The level of significance used was α=0.05, i.e, if the calculated p-value was less than or equal to 0.05 then the null hypothesis of no significant difference between the two compared medians was rejected in favour of the alternative hypothesis that the difference was significant and thus due to the knocking out of γ-synuclein from the genome.

Results

Chapter 3. Expression of γ-synuclein in mouse and human mammary tumour cell lines and its subcellular localization in the murine mammary tumour cell line MG1361.

3.1. Expression of γ-synuclein in mouse and human mammary tumour cell lines

3.1.1. Introduction

Previously, an observation was made in our lab correlating the expression of γ-synuclein with that of ErbB2/Neu/Her2 receptor tyrosine kinase in the mouse mammary tumour cell line MG1361. This cell line was originally established from a mammary adenocarcinoma isolated from the transgenic breast cancer mouse model FVB-Tg(MMTV-ErbB2)NK1Mul/J which was developed by the Jackson laboratory and herein referred to shortly as “NK” (Sacco et al., 1998). This transgenic mouse strain expresses an activated form of the rat ErbB2 (c-neu) to yield a constitutively active receptor. To confirm this correlation, further mammary tumour cell lines that are known to be either positive or negative for ErbB2 were investigated for γ-synuclein expression. Quantitative RT-PCR was performed to compare the relative levels of γ-synuclein expression in two ErbB2-negative mouse mammary tumour cell lines (the tumourigenic 4T1 cell line and the nontumourigenic EpH4 cell line) and the ErbB2-positive tumourigenic MG1361 cell line. RNA extracted from the mouse spinal cord, a tissue with high levels of γ-synuclein expression, was used as a positive control.

In a separate set of experiments, γ-synuclein mRNA and protein expression were compared in two murine mammary tumour cell lines (N202A and N202E) using quantitative (q)RT-PCR and Western blotting, respectively. These two cell lines were established from a mammary tumour isolated from a transgenic breast cancer mouse model (FVB/N-Tg(MMTVneu)202Mul/J), which was developed by the Jackson laboratory and herein referred to shortly as “N202”. This transgenic strain

expresses the wild type rat ErbB2 gene. The N202A cell line expresses high levels of the ErbB2 receptor, while the N202E cell line, which was actually derived from N202A, has downregulated expression of the receptor. This study was also extended to a panel of 9 human breast cancer cell lines and 1 ovarian cancer cell line, SKOV3. Some of these cell lines are known to express very low levels or do not express at all ErbB2 (BT20, MDA-MB-468, MDA-MB-231, MCF-7, GI101 and HS578T), while other lines express relatively high levels of ErbB2 (BT474, SKBR3, T47D and SKOV3).

3.1.2. Results and discussion

Figure 3.1 below compares the expression of γ-synuclein in different murine mammary tumour cell lines and wild type spinal cord (WT-SpC), with the tumourigenic 4T1 cell line set as control. The graph clearly shows that the transformed, non-tumourigenic cell line EpH4 had the same relatively very low level of expression as that of the control tumourigenic 4T1 cell line. Both of these cell lines are known to be ErbB2-negative. However, expression in the ErbB2-positive MG1361 cell line was 83-fold greater than in the control 4T1, and about the same as in the spinal cord tissue from wild type C57BL6 mice that expresses high levels of γ-synuclein. The MG1361 cell line was originally established from the NK model that expresses a constitutively active mutant form of the receptor. This points to a correlation between ErbB2 positivity and γ-synuclein expression, suggesting a possible involvement of γ-synuclein in some aspect of ErbB2 function. This suggestion was strengthened when two closely related ErbB2-expressing mouse mammary tumour cell lines were investigated. N202A and N202E cell lines were established from a mammary adenocarcinoma isolated from a transgenic mouse line expressing rat ErbB2 (N202 model). N202A expresses relatively high level of the

ErbB2 proto-oncogene, while N202E, derived from N202A, has undergone downregulation of ErbB2 expression.

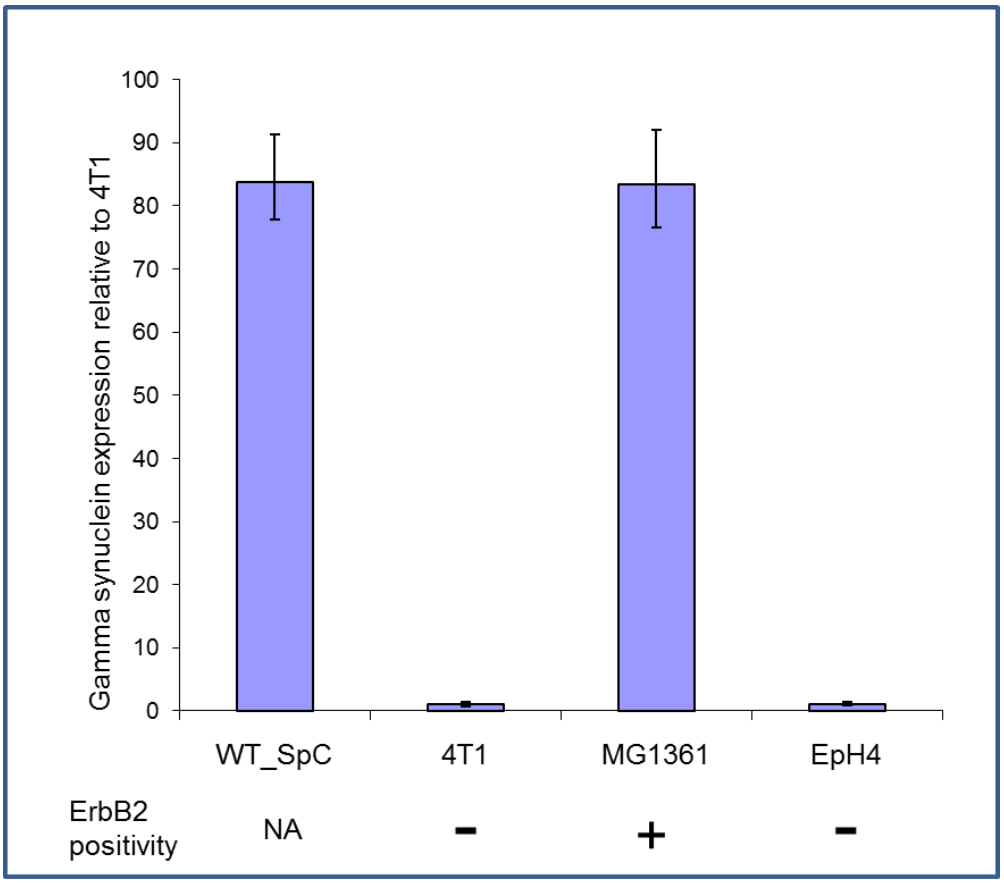

Figure 3.1. Quantitative RT-PCR comparison of γ-synuclein expression in murine mammary tumour cell lines positive or negative for ErbB2 receptor. qRT-PCR was used to determine the relative mRNA expression levels of γ-synuclein in the ErbB2-positive mouse mammary tumour cell line MG1361 and the ErbB2-negative mouse mammary tumour cell lines EpH4 and 4T1. The level of γ--synuclein mRNA expression in 4T1 was set as control and the spinal cord tissue from wild type C57BL6 mouse strain (WT-SpC) was used as a positive control for high levels of γ-synuclein expression. The run was made with three replicates (N = 3) and error bars in the figure correspond to standard error of mean. NA = non-applicaple.

Figure 3.2 below (right panel) shows that the expression level of γ-synuclein mRNA in N202A is approximately twice that in N202E, and that both cell lines had about 18- and 10-times higher expression than the control ErbB2-negative 4T1 cell line, respectively. This was confirmed at the protein level as shown in the left panel of the figure, where appreciably higher levels of the protein was detected by the mouse γ-synuclein specific antibody SK23 in N202A compared to in N202E cell line. Surprisingly, the detected γ-synuclein band in the western blot appeared at the approximately 30 kDa molecular weight position, which is roughly twice the size of the normal (monomer) band of ~18 kDa, a pattern also exhibited by the tumour tissues arising from the N202 mouse model that these cell lines were originally established from (as will be seen later in chapter 4).

Furthermore, to investigate whether this correlation between γ-synuclein and ErbB2 expression exists in human breast cancer cell lines, a panel of 9 human breast cancer cell lines and 1 ovarian cancer cell line, SKOV3, were investigated. As seen in figure 3.3, γ-synuclein protein was not detected in the cell lines that are known to express very low levels of ErbB2 or do not express it at all (MDA-MB-468, MDA-MB-231, MCF-7, GI101 and HS578T), with one exception being the cell line BT20 where γ-synuclein appeared mostly at the monomer position (~18 kDa) but also at the approximately 30 kDa position. The nature of this band is not known but based on molecular weight it may be a result of γ-synuclein protein dimerization, although post-translational modifications and splice variation could not be excluded. In the remaining breast cancer cell lines, γ-synuclein was detected mostly as a presumable dimer in BT474 and SKBR3, and mostly as a monomer in T47D and BT20. In the ovarian cancer cell line SKOV3 the protein appeared as both monomer and dimer.

Thus, the human cancer cell lines that are known to be ErbB2 positive expressed γ-synuclein at either or both forms. Higher molecular weight bands, mostly as trimers according to molecular weight, were also detected on the western blots.

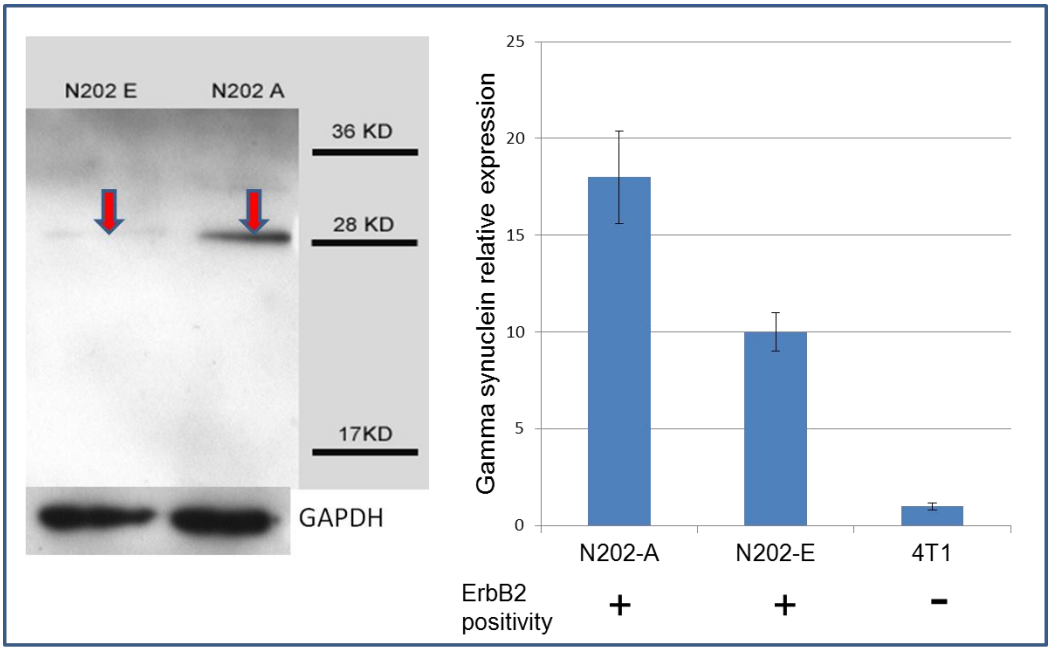

Figure 3.2. Immunodetection of γ-synuclein protein expression in N202 murine mammary tumour cell lines. Left panel: Western blot comparing γ-synuclein protein expression in mouse mammary cancer cell lines N202A, that overexpresses ErbB2, and N202E, that has downregulated ErbB2 expression. Red arrows point to γ-synuclein protein bands which are detected only at the presumable dimer position. Right panel: qRT-PCR revealing γ-synuclein mRNA expression levels of N202A and N202E cell lines relative to the ErbB2 negative breast cancer cell line 4T1. The run was made with three replicates (N = 3) and error bars in the figure correspond to standard error of mean.

This appearance of oligomers has been reported by Zhang and co-workers who also found endogenous γ-synuclein to exist in different ratios of dimers and monomers but mostly as a monomer in the cell lysate of A2780 human ovarian cancer cell line and mostly as a dimer in mouse brain tissue lysate. In the cell lysate of T47D breast cancer cell line, oligomers (mostly trimers) of γ-synuclein were only detected in the assay pellet that contained the cytoskeleton, but not in the supernatant which mainly represented the cytosolic cellular compartment where only monomers were detected (Zhang et al., 2010).

Thus, the correlation between γ-synuclein and ErbB2 positivity seems to hold in the human cancer cell lines as well. This lends further support to the possible involvement of γ-synuclein in some aspect of ErbB2 function, and thus supports the use of the transgenic ErbB2-overexpressing NK model to investigate the effect of γ-synuclein deletion on ErbB2-induced mammary gland tumourigenesis.

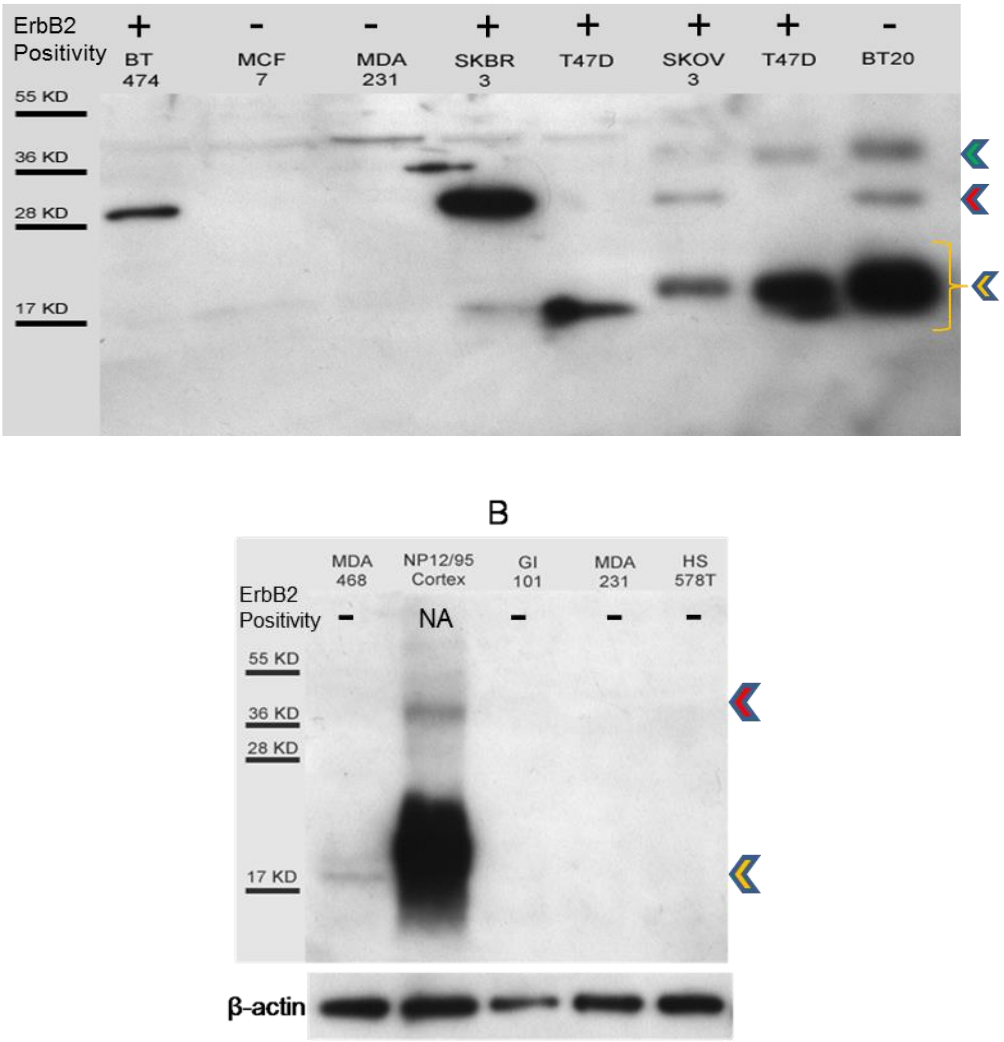

Figure 3.3. Immunodetection of γ-synuclein protein expression in 9 human breast cancer cell lines. Two Western blots (A & B) showing γ-synuclein protein expression in 9 human breast cancer cell lines (SKOV3 in blot A is an ovarian cancer cell line, and NP12/95 in blot B is a brain tissue loaded as a positive control for high γ-synuclein protein expression). The orange, red and green arrow heads point to the monomer, doublet and triplet forms of the protein, respectively. Cell lines that are ErbB2 positive, with the exception of BT20 that expresses very low levels of ErbB2, also express appreciable levels of γ-synuclein.

3.2. Subcellular localization of γ-synuclein in the murine mammary tumour cell line MG1361

3.2.1. Introduction

Most literature revealed that γ-synuclein is localized to the cytoplasm. However, few reports claimed that the protein may localize to various subcellular structures and that it may even translocate to the nucleus if the cell was subjected to stress conditions. To investigate the subcellular localization of γ-synuclein in mammary tumour cells, the line MG1361 was selected due to the fact that it was originally established from the same NK mouse model used for *in vivo* experiments in the current study. The cells were grown *in vitro* on coverslips and fluorescent immunocytochemistry technique was used to stain γ-synuclein protein as well as other cellular components constituting parts of some subcellular structures. These included γ-tubulin as a part of the centrosome, α-tubulin as a part of the midbody and spindle fibers, and β-actin as a part of the cytoskeleton. This would enable detection of any colocalization γ-synuclein may have with the above components and thus reveal possible involvement in relevant biological processes such as cell division and organization of the cytoskeleton.

3.2.2. Results and discussion

Figure 3.4 below shows cytoplasmic localization of γ-synuclein in dividing murine cancer cell line MG1361. γ-synuclein was fluorescently stained in red in the cytoplasm of non-dividing as well as dividing cells. It did not appear to colocalize with γ-tubulin, which stained in green and appeared at the centrosomal region of dividing cells. Moreover, figure 3.5 shows a dividing cell in the stage of cytokinesis with γ-

synuclein stained in red and localized to the cytoplasm. γ-synuclein did not appear to localize to the midbody where the constituent α-tubulin was stained in green.

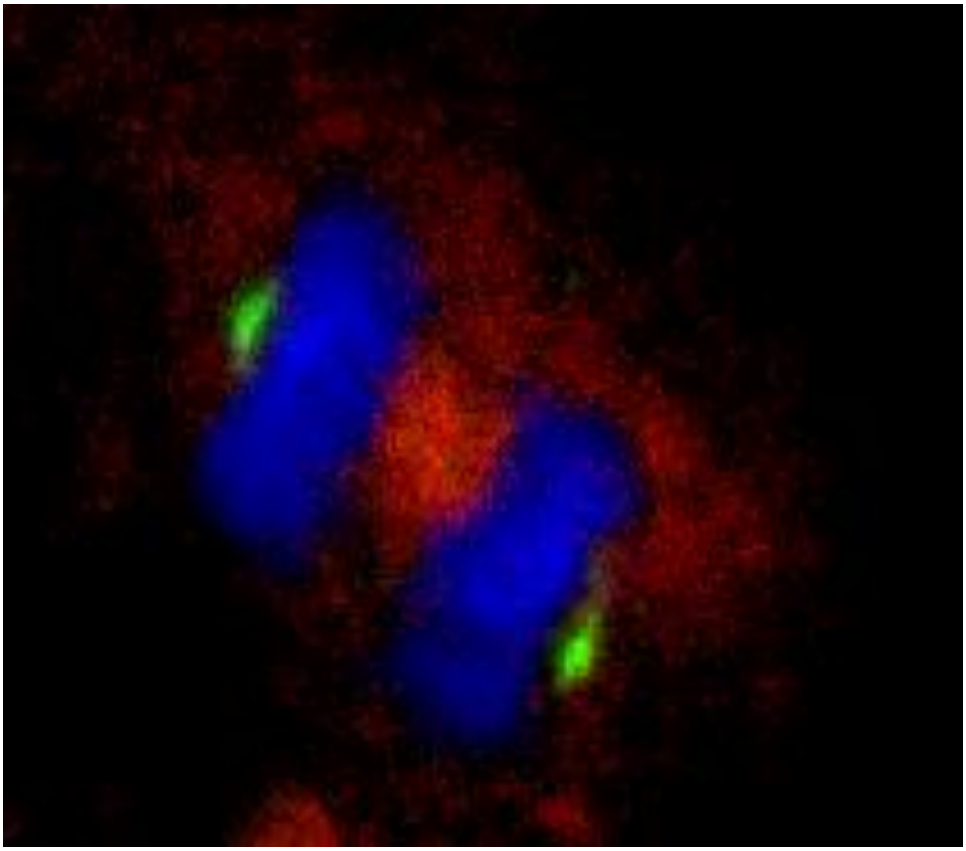

Figure 3.4. Immunofluorescent detection of γ-synuclein and γ-tubulin in dividing murine MG1361 cells. Immunofluorescent image (630x) of a cell in an anaphase of the cell cycle. γ-synuclein appears stained in red with cytoplasmic localization. It does not appear to colocalize with γ-tubulin, which appears stained in green as a part of the centrosomes. The chromosomes are counterstained with DAPI (blue).

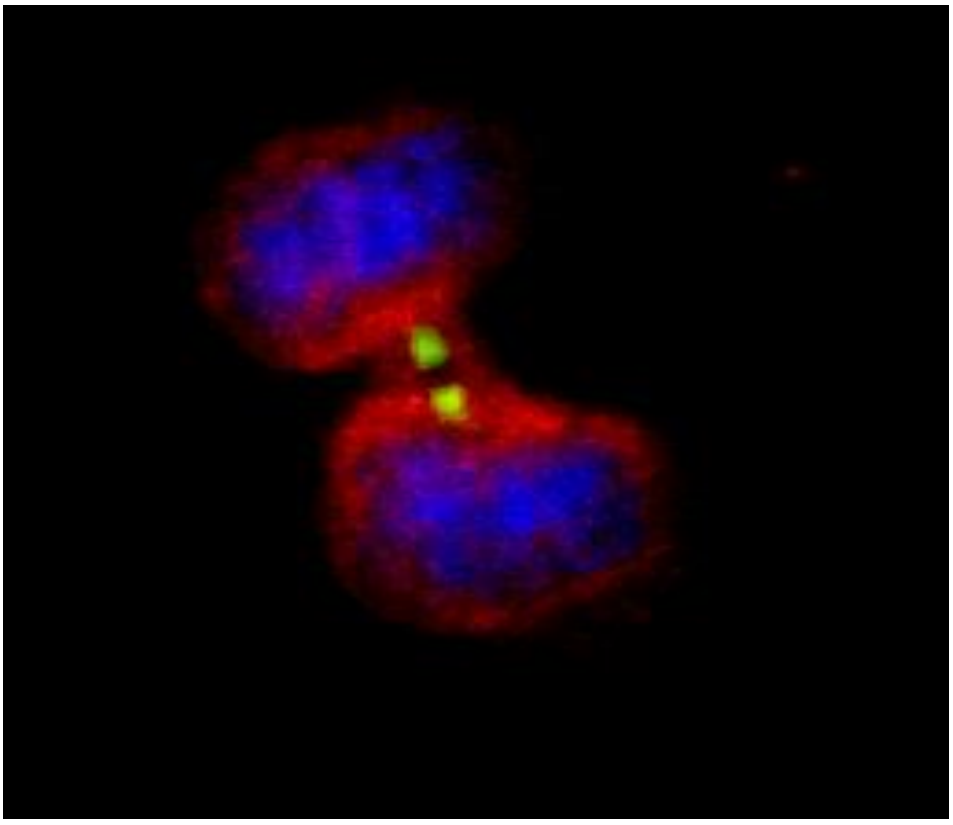

Figure 3.5. Immunofluorescent detection of γ-synuclein and α-tubulin in a dividing murine MG1361 cell. Immunofluorescent image (630x) of a cell at late cytokinesis stage of the cell cycle. γ-synuclein appears stained in red and localized to the cytoplasm. It does not appear to localize to the midbody region where α-tubulin appears stained in green. The chromosomes are counterstained with DAPI (blue).

These results are consistent with most other studies showing cytoplasmic localization of γ-synuclein. However, one group reported that, in the interphase of primary cultures of human optic nerve astrocytes, bovine retinal epithelial cells and human retinoblastoma Y79 cell line, γ-synuclein could be present in the perinuclear space and bound to centrosomes. They also reported that, in late mitosis of human astrocytoma cell line U373 and melanoma cells OM431 and C8161, γ-synuclein protein was observed to lose the association with centrosomes and redistribute to the midbody in telophase (Surgucheva et al., 2006; Surguchov et al., 2001). The different results could be due to different behaviours of γ-synuclein in different cell types and/or to different conditions of *in vitro* cell growth.

Figure 3.6 depicts α-tubulin fluorescently stained in green as a part of the mitotic spindle in a dividing cell at metaphase stage. γ-synuclein, stained in red, appears to have cytoplasmic cellular localization but does not seem to colocalize with α-tubulin in the microtubule spindle fibers. The Surguchov group claimed that γ-synuclein protein bound to the spindle poles in the mitotic phase of human retinoblastoma Y79 cells. Results of our study, however, clearly demonstrate that at least in MG1361 cells γ-synuclein is not associated with the spindle poles. In figure 3.7, an immunofluorescent image shows β-actin stained in green as a part of the cytoskeleton at the cell periphery. No colocalization was observed for γ-synuclein and β-actin, indicating that the former does not interact with β-actin in both dividing and nondividing MG1361 cells grown under such *in vitro* conditions.

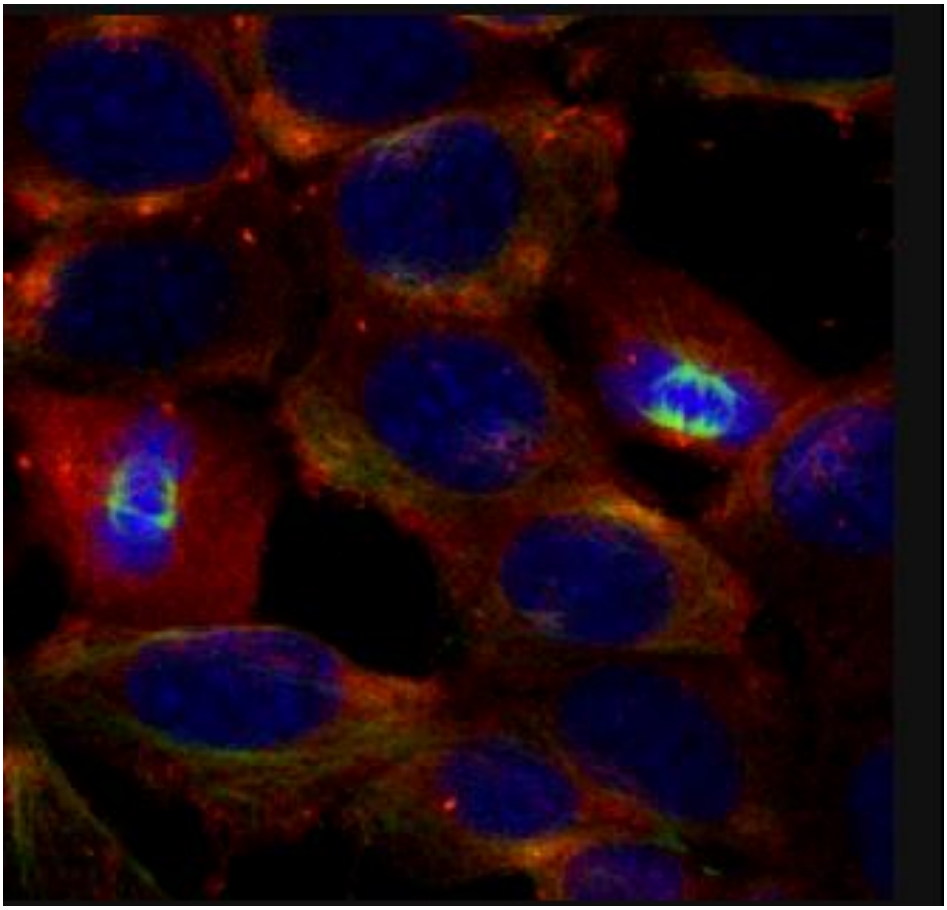

Figure 3.6. Immunofluorescent detection of γ-synuclein and α-tubulin in dividing murine MG1361 cells. Immunofluorescent image (630x) showing cytoplasmic localization of γ-synuclein that appears stained in red. γ-synuclein is not seen associated with α-tubulin which appears stained in green as a part of the mitotic spindle. The chromosomes are counterstained with DAPI (blue).

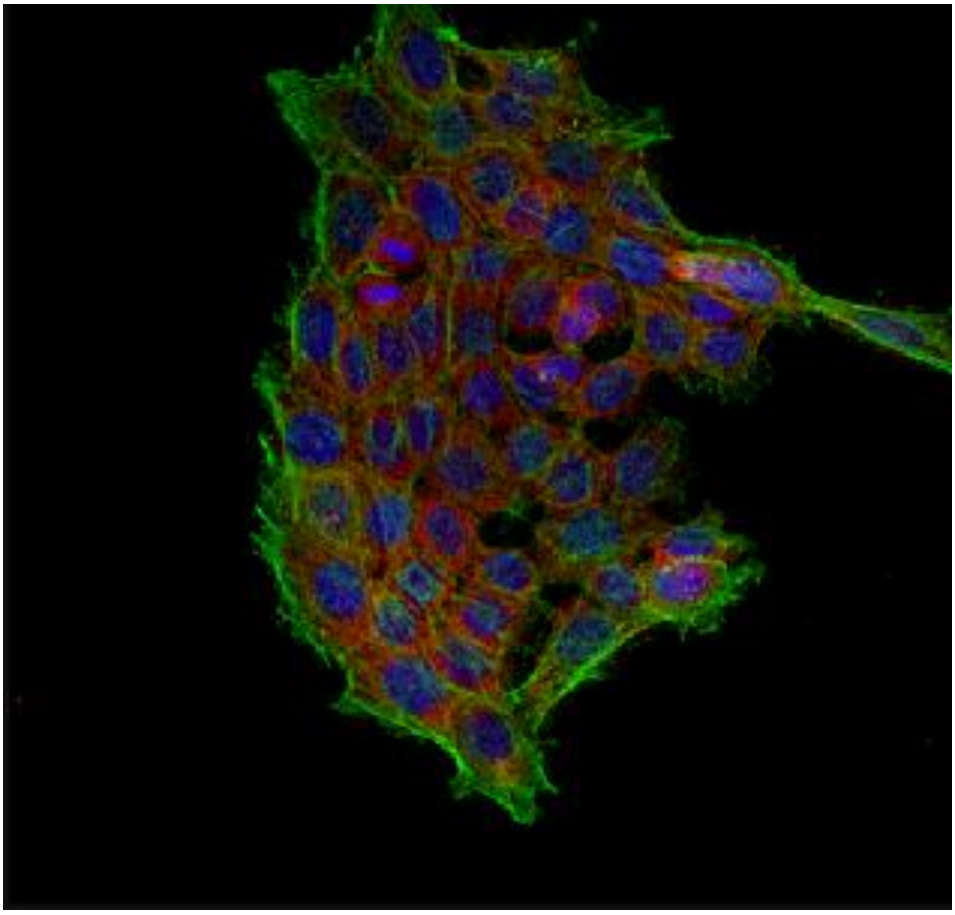

Figure 3.7. Immunofluorescent detection of γ-synuclein and β-actin in murine MG1361 cells. Immunofluorescent image (400x) showing β-actin stained in green as a part of the cytoskeleton at the cell periphery. γ-synuclein is stained in red and appears to have cytoplasmic localization with no association with β-actin. The chromosomes are counterstained with DAPI (blue).

Chapter 4. Expression of γ-synuclein in normal and tumourous mammary gland tissue in mouse breast cancer models

4.1. Introduction

γ-synuclein was reported to be aberrantly expressed in a large percentage of advanced infiltrating breast carcinomas, compared to normal tissue and benign tumours where its levels were absent or hardly detectable, and was thus named breast cancer-specific gene1 (BCSG1) (Ji et al., 1997). Since then, the possible role of γ-synuclein in mammary gland tumourigenesis has been investigated mostly using *in vitro* culture systems. For the most part, these systems utilized human breast cancer cell lines and mouse mammary tumour cell lines in which γ-synuclein expression was either upregulated or downregulated in order to reveal any effects on the growth, proliferation, survival and metastasis of the cancerous cells. The expression of γ-synuclein in mouse mammary tumours developed in mice modelling human breast cancer was not however investigated directly.

In this study, immunohistochemistry and western blotting techniques were used to investigate γ-synuclein expression in tumours isolated from three mouse models of breast cancer, the two ErbB2-positive transgenic NK and N202 models, and the Blg-Cre^{+} BRCA2$^{fl/fl}$ p53$^{fl/fl}$ double mutant model. The transgenic NK model expresses the activated form of rat ErbB2 (c-neu) receptor tyrosine kinase oncogene, while the transgenic N202 model expresses the wild-type rat ErbB2 proto-oncogene, both under the control of the mouse mammary tumour virus (MMTV) promoter that targets the expression to the mammary gland epithelium. The Blg-Cre^{+} BRCA2$^{fl/fl}$ p53$^{fl/fl}$ model houses conditional double deletions of BRCA2 and P53 genes in the mammary epithelium, triggered by the Cre-recombinase expressed under control of the mammary gland specific β-lactoglobulin (Blg) promoter. γ-synuclein expression was also investigated in normal mammary gland tissue from FVB mouse strain by

immunohistochemistry to determine which cell types do express the protein. This strain constitutes the genetic background of the NK model used in the *in vivo* experiments and into which the KO γ-synuclein allele was bred.

4.2. Results and discussion

Figure 4.1 below shows immunohistochemical staining for γ-synuclein protein in a normal FVB mouse mammary gland.

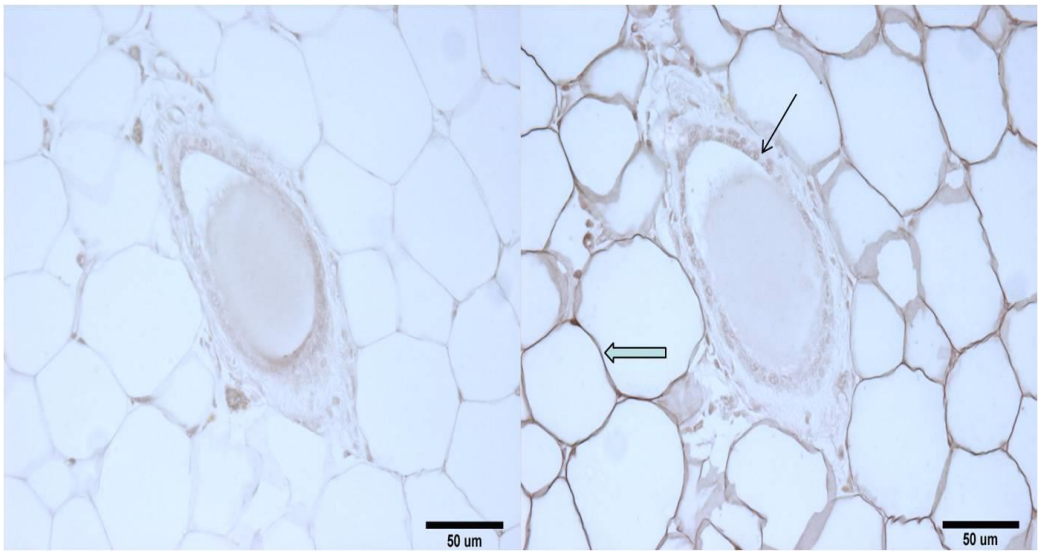

Figure 4.1. Immunohistochemical staining for γ-synuclein in mouse normal mammary gland. Two adjacent sections of a normal mammary gland from FVB mouse strain were counterstained with H&E. Right panel: staining with antibodies against mouse γ-synuclein (SK23) revealed expression in the thin cytoplasmic layer of adipocytes (block arrow) but not in the ductal epithelial cells (thin arrow). Left panel: as a negative control for staining specificity, the adjacent section was incubated only with secondary antibody. Both microscope images were taken at 400x of magnification.

It can be seen that γ-synuclein is not detected in the epithelium lining the mammary ducts, indicating that it is not expressed in the normal epithelium of the mammary gland (or if expressed then at undetectable levels). The white adipocytes making up most of the gland stroma, however, show very clear specific staining of γ-synuclein in the narrow cytoplasmic strip. γ-synuclein has been reported to be expressed in subcutaneous and visceral adipose tissue and to be increased with obesity, and postulated to have a role in the differentiation and physiology of adipocytes (Oort et al., 2008). In the current study, γ-synuclein staining was also observed in the endothelial cells lining some of the vasculature and in nerve fibers innervating the mammary glands investigated.

Figure 4.2 below shows immunohistochemical detection of γ-synuclein protein in epithelia-derived cells in a mammary gland tumour obtained from the NK model mouse. This abnormal expression was found in about 18% (5/27) of tumours investigated in both ErbB2-overexpressing models, 2/14 tumours of N202 model and 3/13 tumours of NK model. This percentage of γ-synuclein-positive tumours is comparable to a published study on human tumour tissue by Guo and co-workers (Guo et al., 2007). They reported a significant correlation between γ-synuclein aberrant expression and ErbB2 status ($P<0.001$): about 24% (37/151) of ErbB2-positive tumour samples expressed γ-synuclein, whereas only about 10% (21/207) of ErbB2-negative tumour samples expressed γ-synuclein. This correlation might point to an involvement of γ-synuclein in some aspect of ErbB2 activity, as already noted in the previous chapter presenting the results from human and mouse mammary tumour cell lines. In another study, however, no correlation was found between ErbB2 positivity and γ-synuclein expression in breast tumour samples ($P=0.46$):

about 32% (8/25) of ErbB2-positive tumour samples aberrantly expressed γ-synuclein, compared to about 37% (21/56) of ErbB2-negative tumour samples expressing γ-synuclein (Wu et al., 2007).

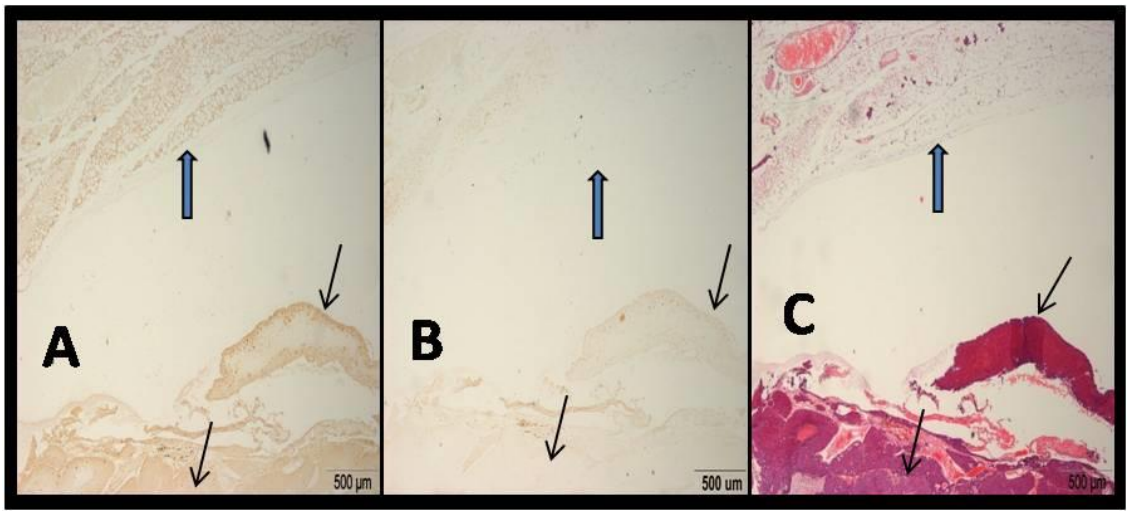

Figure 4.2. Immunohistochemical staining for γ-synuclein in tumour and adjacent normal mammary gland from NK mouse model. Immunohistochemical staining for γ-synuclein (A and B) and H&E staining (C) of three adjacent sections of tumour (thin arrows) and adjacent normal mammary gland tissue (block arrows). A: epithelia-derived tumour cells (thin arrows) and adipocytes of adjacent normal tissue (block arrow) are positively stained with antibodies against mouse γ-synuclein (SK23). B: as a negative control for staining specificity, the section was incubated only with secondary antibody. C: H&E stained section showing epithelia-derived tumour cells. Microscope images were taken at 40x of magnification.

Figure 4.3 below shows a Western blot of normal (N) and tumour (T) tissues obtained from the ErbB2-overexpressing N202 model investigated for γ-synuclein expression. The normal mammary gland tissue samples showed considerably high levels of the protein (~18 kDa monomer) as they are made up mostly of adipocytes which are known to express high levels of γ-synuclein. The tumour tissues, however, had no or very little expression of the monomer protein as they are made up almost exclusively of highly dividing epithelial tissue. However, an interesting observation was the consistent appearance of bands at ~30 kDa size that were much more intense in the tumour than in the normal tissues. As already noted in the previous chapter, the nature of these bands is not known but based on molecular weight it may be a result of γ-synuclein protein dimerization, although post-translational modifications and splice variation could not be excluded.

The appearance of this presumably dimer form of γ-synuclein has been reported in a study by Zhang and co-workers investigating a role of the protein in microtubule regulation. They reported significant amounts of the dimer form in their *in vitro* assays that demonstrated the ability of γ-synuclein to promote tubulin polymerization and to bind preformed microtubules. This study showed that γ-synuclein may act as a microtubule-associated protein and suggested that it may crosslink individual microtubules into bundles by dimerizing. Endogenous γ-synuclein was also found to exist as dimers and monomers to different extents, mostly as a monomer in the cell lysate of A2780 human ovarian cancer line and mostly as a dimer in mouse brain tissue lysate. In the cell lysate of T47D breast cancer line, oligomers (mostly trimers) of γ-synuclein were only detected in the assay pellet that contained the cytoskeleton,

but not in the supernatant which mainly represented the cytosolic cellular compartment where only monomers were detected (Zhang et al., 2010).

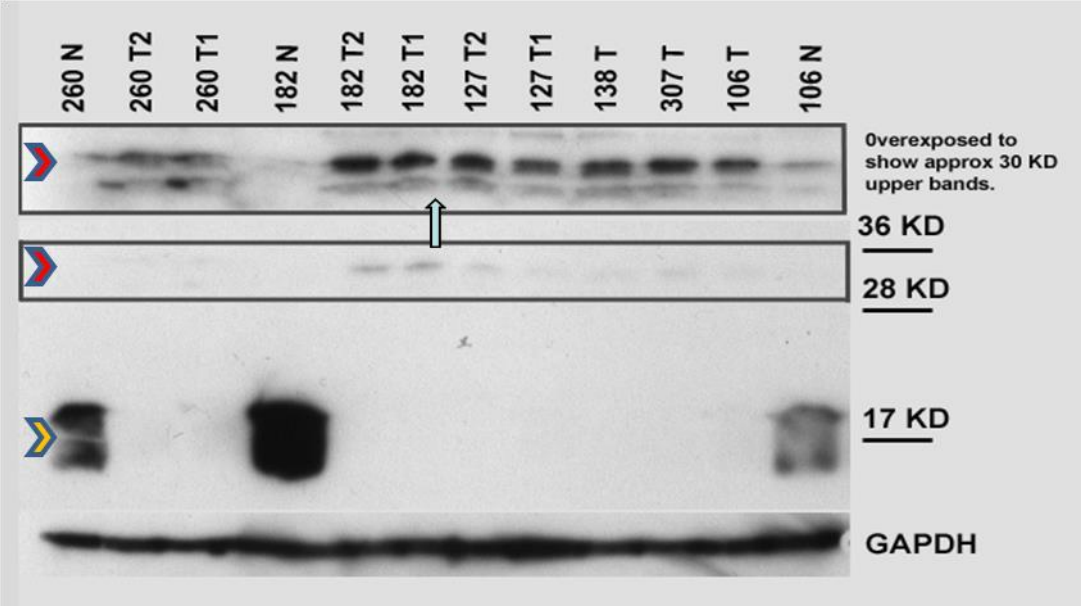

Figure 4.3. Immunodetection of γ-synuclein in tumour and normal mammary gland from N202 mouse model. Immunoblot showing γ-synuclein expression in normal (N) and tumour (T) mammary gland tissues: the upper rectangle box (aqua block arrow) shows longer exposure of the ~ 30 kDa (doublet) region of the same western blot. Orange and red arrow heads point to the monomer and doublet band positions, respectively.

It is probable that some of the expression detected in the tumour tissues came from the nerve fibers and endothelial cells of arterioles vascularizing the tumours, as well as from adipocytes that may have been included from adjacent adipose tissue. However, it is more likely to have come mostly from the tumourous epithelial cells since the immunoblot bands appear only at the dimer position, as in the ErbB2-positive N202A and N202E breast cancer cell lines (figure 3.2) that were actually derived from this N202 mouse model. Also, the presumable dimer bands are much more intense in the tumours than in the normal gland tissues. This is supported by the fact that in all 27 ErbB2-positive tumours γ-synuclein was detected only as a dimer, whereas in all normal mammary gland tissues it was detected mostly as a monomer which is the form seen in adipocytes.

This detection of γ-synuclein at the dimer position was also observed in 15 tumours isolated from the Blg-Cre^{+} BRCA2$^{fl/fl}$ p53$^{fl/fl}$ mutant mice, as can be seen in the representative figure 4.4 below. In 3 of these tumour tissues, however, γ-synuclein expression appeared very intense at the monomer band as well. This is probably due to inclusion of adjacent normal gland tissue, containing mostly adipocytes, during tumour harvest. However, this pattern of expression at both monomer and dimer states was also observed in some of the human breast cancer cell lines already presented in chapter 2 where expression was detected at either or both bands.

In an attempt to investigate the nature of the presumably dimer form, γ-synuclein protein was isolated from the breast cancer cell line SKBR3, which expresses the protein mostly as a dimer. The protein was purified, as outlined in the Materials and Methods chapter, and then subjected to enzymatic reaction tests for N-linked

glycosylation and phosphorylation. As can be seen in figure 4.5, the tests failed to detect any change in the electrophoretic mobility of γ-synuclein, thus suggesting that the two post-translational modification processes are not responsible for the doublet band. This result further supports the notion of dimerization and suggests that dimerization might be a functional aspect of the small, cytoplasmic γ-synuclein protein. In brief, aberrant expression of γ-synuclein was detected in mammary tumour tissues isolated from both ErbB2-positive models (N202 and NK) as well as from Blg-Cre^{+} BRCA2$^{fl/fl}$ p53$^{fl/fl}$ breast cancer model, with γ-synuclein expressed mostly as a dimer appearing at the ~30 kDa position in the Western blots.

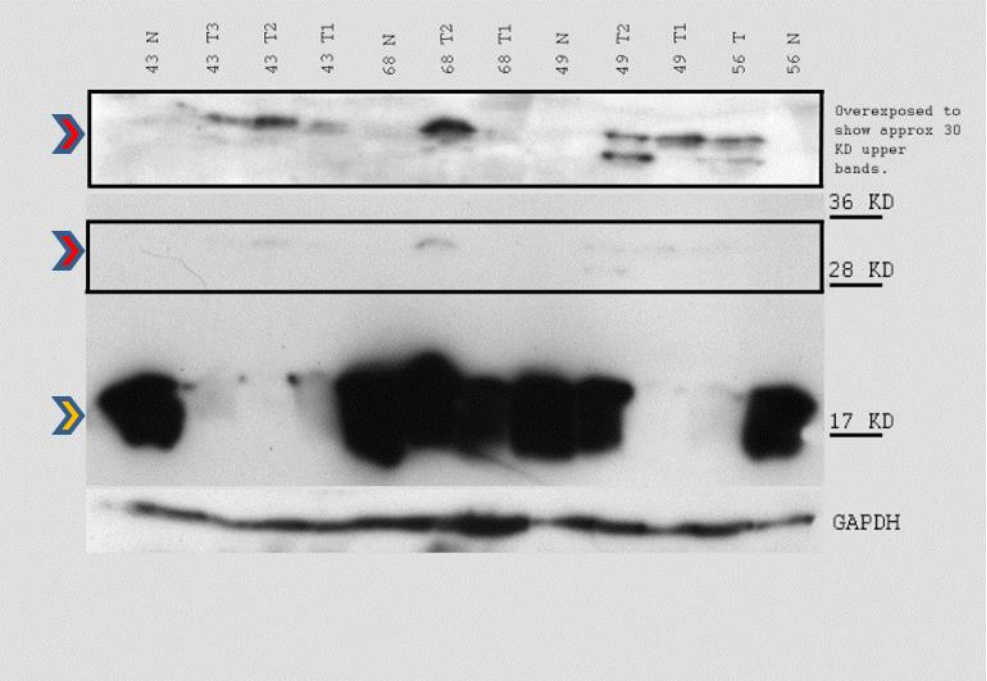

Figure 4.4. Immunodetection of γ-synuclein in tumour and normal mammary glands from Blg-Cre^{+} BRCA2$^{fl/fl}$ p53$^{fl/fl}$ double mutant mouse model. Immunoblot showing γ-synuclein expression in normal (N) and tumour (T) mammary gland tissue: the upper rectangle box (blue block arrow) shows longer exposure of the doublet region of the same Western blot. Orange and red arrow heads point to the monomer and doublet band positions, respectively.

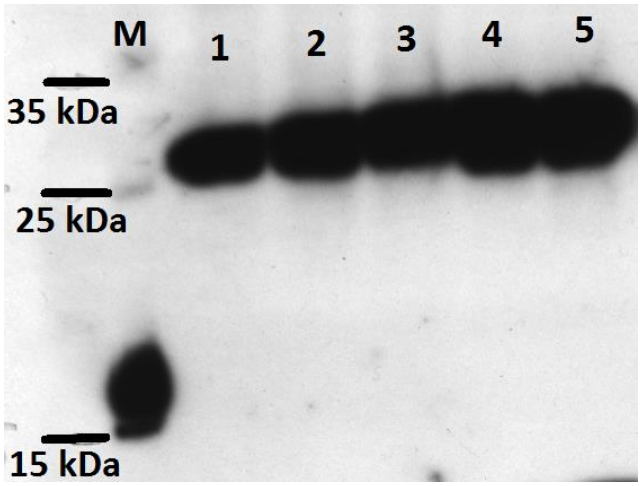

Figure 4.5. Immunoblot detection of purified γ-synuclein before and after reactions of enzymatic dephosphorylation and deglycosylation tests. M: protein from T47D cell line with mostly monomer, but also dimer and trimer forms, used as a marker. 1: purified γ-synuclein from SKBR3 cell line (reaction substrate source) loaded as control. 2 and 3: γ-synuclein after incubation with reaction components at 37 °C for 1 hour without (2) and with (3) PNGase F amidase enzyme. No difference was observed in SDS-PAGE electrophoretic mobility as protein was detected in the presumable dimer form, thus suggesting exclusion of N-linked glycosylation as a post-translational modification. 4 and 5: γ-synuclein detected before (4) and after (5) alkaline phosphatase treatment, with no resultant change in SDS-PAGE electrophoretic mobility.

Chapter 5. Effect of γ-synuclein gene deletion on the normal development of mouse mammary gland

5.1. Introduction

To investigate any possible role of γ-synuclein in mammary gland tumourigenesis it is imperative to explore its effect on the normal development of mammary gland. To this end, a subset of the FVB γ-synuclein KO and Wt mice generated at the end of stage I of breeding of the experimental cohorts (figure 2.1-control groups) were multiplied and used to investigate the effect of γ-synuclein deletion on the normal development of the mammary gland. Virgin females at 2, 3 and 13 months of age were sacrificed and the abdominal pair (L4 and R4) of mammary glands were dissected, one used for whole mount investigation and the other for H&E-stained section histological investigation. 6 females of each genotype (Wt and KO) were sacrificed per developmental time point. This would show any effect of γ-synuclein ablation on the dynamic process of ductal branching morphogenesis as this process begins mostly with the onset of puberty, which takes place at about 3-4 weeks of age. Whole mount and H&E-stained section histological investigations were also carried out on 14.5 day-gestating mammary glands obtained from females at 16 weeks of age. This would reveal any effect of γ-synuclein ablation on lobuloalveolar development, a stage that holds massive tissue remodelling involving extensive proliferation of the epithelial ducts and differentiation of alveoli.

5.2. Results and discussion

γ-synuclein was reported to play a role in efficient ER-α signalling. It was shown to be a component of the heat shock protein (Hsp)-ER-α complex, and that it enhanced the affinity of ER-α to estrogen as it activated the ligand-dependent ER-α transcriptional activity (Jiang et al., 2004). In the context of mammary gland development it has also been reported that ER-α-null mice did not differ from Wt

mice up to puberty, at which time their ducts showed no TEBs and failed to invade the fatty stroma (Mallepell et al., 2006). Furthermore, mice with conditional KO of ER-α in the mammary epithelium at different developmental stages have revealed that ER-α signalling is required for both proper ductal branching during puberty and normal lobuloalveolar development during late gestation and lactation (Feng et al., 2007). Robust branching morphogenesis begins with the rising levels of serum estrogens at puberty which induce the formation of TEBs at the distal ends of ducts, the sites of active cellular proliferation and differentiation during ductal morphogenesis. TEBs respond to estrogens and proliferate to elongate the ducts and undergo a bifurcation process to form new primary branches (Hinck and Silberstein, 2005). This process of ductal elongation and branching continues until an age of about 8-10 weeks, when the margins of the fat pad are reached. Accordingly, it is plausible to presume that γ-synuclein might be involved in ER-α signalling in the TEBs and hence play a role in ductal branching morphogenesis. However, as can be seen in figure 5.1 below, investigations of whole mount and H&E-stained sections revealed no differences in the structure and extent of ductal branching between γ-synuclein KO and Wt glands of 8- and 12-week old virgin females. This indicates that γ-synuclein is not essential for the process of epithelial ductal elongation and branching, but does not necessarily mean that it has no role in the process. In fact, transgenic mice overexpressing γ-synuclein under the control of mouse mammary tumour virus (MMTV) promoter showed an effect on mammary gland development (Liu et al., 2007b). In their study, whole mount histological analysis showed that the transgenic mammary gland exhibited a significant increase in ductal branching morphology and terminal end bud density starting at 10 weeks of age. This indicated a highly proliferative capacity of epithelial cells at the terminal

end buds. This pregnancy-like phenotype was confirmed by H&E-stained sections which also showed hyperplasia-like structures in the transgenic mammary glands characterized by areas of multilayered epithelium. Therefore, γ-synuclein may be involved in the process of ductal branching morphogenesis as evidenced by the transgenic glands overexpressing the protein, but it is not essential for this process as its deletion had no effect as evidenced by the KO glands in this current study.

The same null effect of γ-synuclein gene ablation on mammary gland ductal elongation and branching morphogenesis was observed in 13 month-old virgin females. 13 months would be more than long enough to reveal any effects γ-synuclein gene ablation may have on ductal elongation and branching as this process occurs with each oestrus cycle in the mature virgin mammary gland (Sternlicht, 2006). As figure 5.2 clearly shows, no differences were seen in the extent of elongation and ductal branching between the γ-synuclein KO and Wt mammary glands as revealed by whole mount and H&E-stained section histological investigations.

A gestating mammary gland undergoes a massive tissue remodelling process involving extensive proliferation of the epithelial ducts and differentiation of alveoli. Concomitant with this massive proliferation of epithelia, and to make room for such development, remodelling features the dedifferentiation of adipocytes whereby they lose their lipid droplets and become long projections scattered among the lobuloalveoli. As this stage represents the most extensive development of the mammary gland, it would be more likely to detect any effect of γ-synuclein deletion on the normal development at this stage. Also, studies of mouse mammary gland transcriptional profiles during gestation/lactation/involution cycle demonstrated that

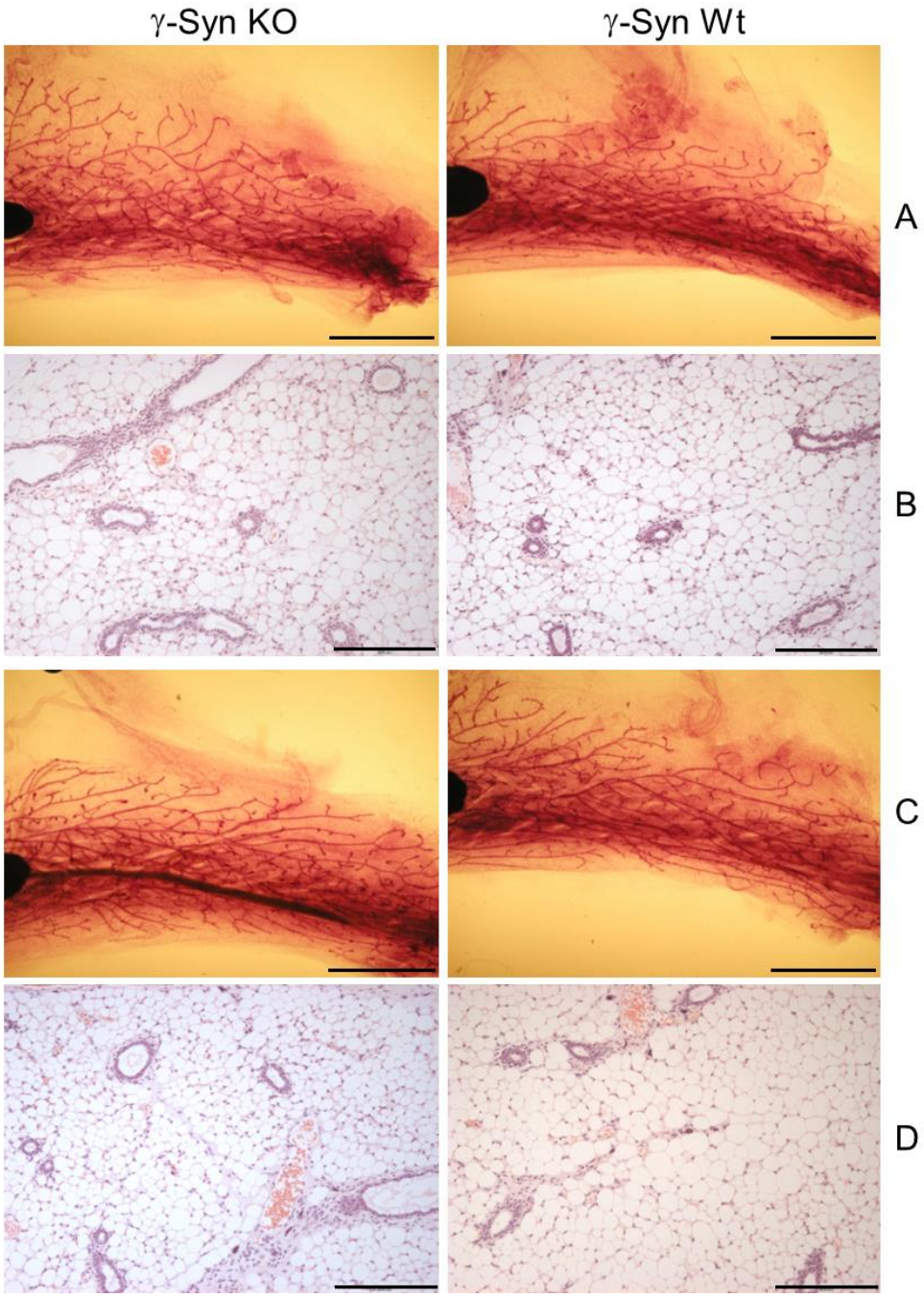

Figure 5.1. Effect of γ-synuclein gene deletion on elongation and ductal branching morphogenesis in mammary glands at 8 and 12 weeks of age. Representative microphotographs of whole mounts (12.5x; scale bars = 4 mm) and H&E-stained histological sections (100x; scale bars = 200 µm) of mammary glands obtained from FVB γ-synuclein KO and Wt virgin female mice at 8 weeks of age (A & B) and 12 weeks of age (C & D) (N = 6 animals/genotype/developmental point). No differences in the structure and extent of elongation and ductal branching morphology were observed.

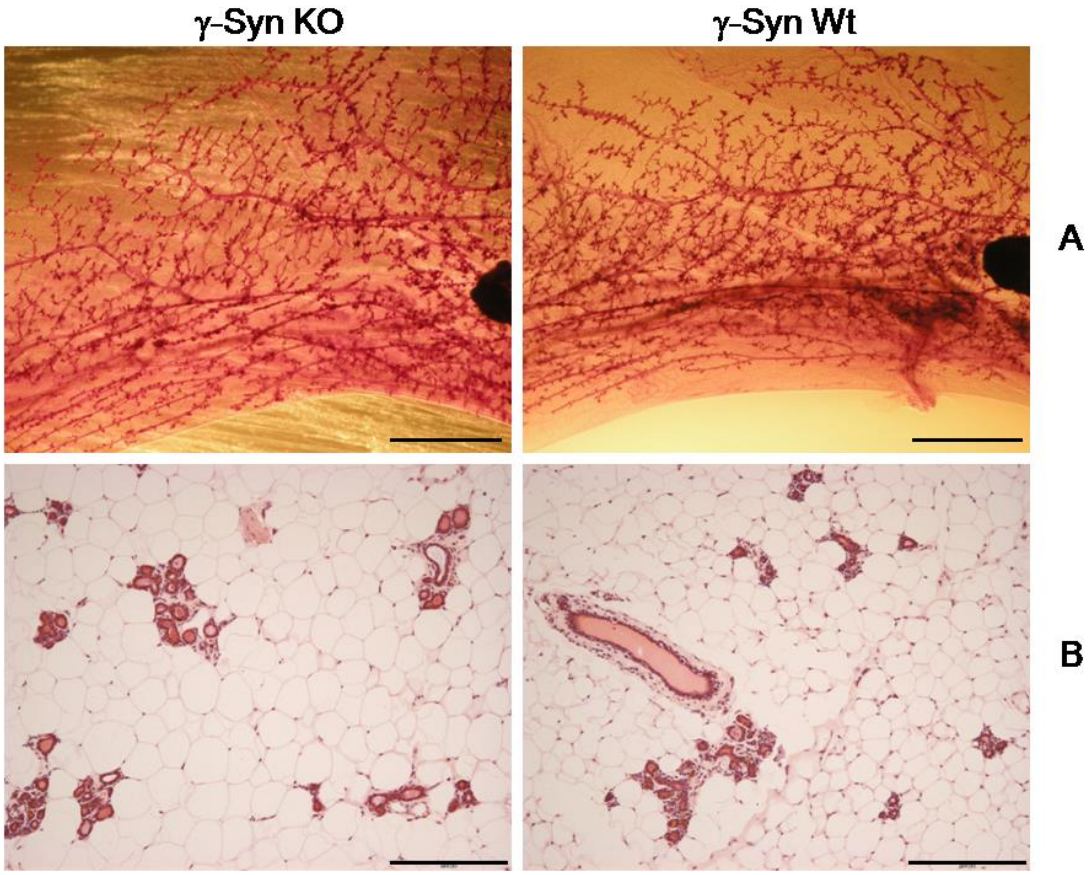

Figure 5.2. Effect of γ-synuclein gene deletion on elongation and ductal branching morphogenesis in mammary glands at 13 months of age. Representative microphotographs of A: whole mounts (12.5x; scale bars = 4 mm) and B: H&E-stained histological sections (100x; scale bars = 200 µm) of mammary glands obtained from FVB γ-synuclein KO and Wt virgin female mice at 13 months of age (N = 6 animals/genotype). No differences in the structure and extent of elongation and ductal branching morphology were observed.

the transcriptional levels of γ-synuclein decrease significantly and concurrently with dedifferentiation of mature adipocytes which express high levels of γ-synuclein. This decline proceeds until about day 7-8 of gestation where they reach over 50% of the original prepregnant state. Then, despite the continuing dedifferentiation of mature adipocytes, the levels start rising until around day 12-13 where they almost reach the original levels. They then decrease again significantly to about 4-11% of the prepregnant levels and remain so until they start rising back to the original levels with the onset of involution and redifferentiation of adipocytes (Clarkson and Watson, 2003). This intermittent rise between about days 7-13 of gestation might involve a role of γ-synuclein in this remodelling process.

Nevertheless, and as can be seen in figure 5.3, it appears that the deletion of γ-synuclein had no effect on the extent of ductal branching and differentiation of lobuloalveoli as the morphology of both KO and Wt glands changes very similarly during gestation. Moreover, γ-synuclein gene deletion did not produce any effects on the differentiation and function of alveoli during gestation and lactation. The γ-synuclein KO females developed normally lactating mammary glands: they produced milk and nursed their pups to grow as normal as the wild types. Both γ-synuclein KO and Wt mammary glands underwent normal gestation/lactation/involution cycle. In brief, deletion of γ-synuclein had no effect on the normal development of the mammary gland.

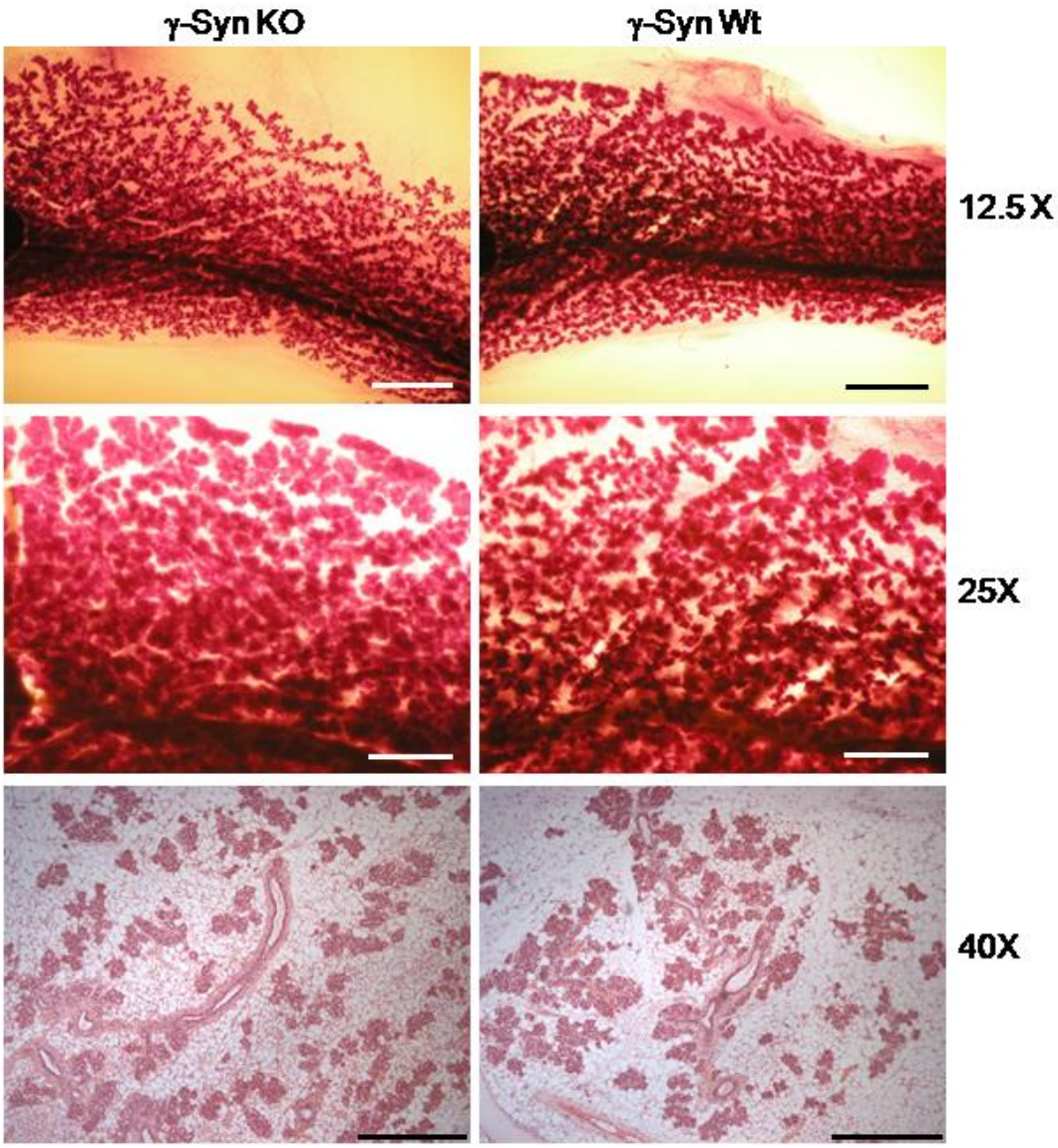

Figure 5.3. Effect of γ-synuclein gene deletion on ductal branching and lobuloalveolar development in gestating mammary glands. Upper two panels: whole mount microphotographs of 14.5-day gestating mammary glands (L4) obtained from FVB γ-synuclein KO and Wt female mice at 16 weeks of age (N = 6 animals/genotype): No differences were found in the structure, ductal branching and lobuloalveolar development in the gestating glands (12.5x: scale bars = 2 mm and 25x: scale bars = 1 mm). Lower panel: H&E-stained sections of a mammary gland (R4) from the same animal confirming no differences in the extent of ductal branching and differentiation of lobuloalveoli (scale bars = 500 μm).

Chapter 6. Effect of γ-synuclein gene deletion on ErbB2-induced mammary gland tumourigenesis

6.1. Introduction

As described in the General Introduction (Chapter 1), γ-synuclein has been claimed to play a role in mammary gland tumourigenesis. Its overexpression was reported to stimulate the growth and proliferation of cancer cells, promote the survival of cancer cells and inhibit apoptosis, inhibit the mitotic check point function and thereby increase chromosomal instability, and enhance breast cancer cell motility and metastasis. The above effects were obtained largely through cell culture systems utilizing breast cancer cell lines. In transgenic mice, aberrant expression of γ-synuclein stimulated ligand-dependent ER-α signalling, leading to a highly proliferative pregnancy-like phenotype of mammary epithelial cells and branching morphology. Therefore, if γ-synuclein indeed had an essential role in the development of mammary gland tumourigenesis and/or enhancing its progression, then abrogation of its expression would be expected to prevent the formation or retard the progression of mammary tumours. If such a result was realized then more serious efforts would be directed towards exploring the use of γ-synuclein as a biomarker of breast cancer progression and prognosis, and certainly as a target for treatment. However, the role of endogenous γ-synuclein in mammary gland tumourigenesis has not been studied in an appropriate *in vivo* model, and our research programme is the first attempt to demonstrate directly whether γ-synuclein is required for the development and/or progression of ErbB2-induced mammary tumours.

As mentioned in chapter 3, the choice of the transgenic ErbB2 model came as a result of a previous observation in our lab correlating the expression of γ-synuclein with that of ErbB2 receptor tyrosine kinase in the mouse mammary tumour cell line

MG1361. This cell line was originally established from a mammary adenocarcinoma isolated from the transgenic breast cancer mouse model FVB-Tg(MMTV-ErbB2)NK1Mul/J, (NK model) (Sacco et al., 1998). This transgenic mouse strain expresses a mutant form of the rat ErbB2 gene (activated ErbB2) under the regulation of the mouse mammary tumour virus promoter (MMTV). The mutation results in a single amino acid substitution at position 664 from valine to glutamic acid, rendering the receptor constitutively active. The transgene is expressed in a non-uniform and random fashion in the mammary epithelium leading to stochastic formation of multifocal tumours. These tumours develop with rapid kinetics, having a short latency of about 5 months, making this breast cancer model an aggressive one. Because the hypothesis we were going to test involved the prevention and/or retardment of tumour formation in the absence of γ-synuclein, this model seemed to be a good choice for this purpose.

To investigate the effect of γ-synuclein gene deletion on the development and progression of ErbB2-induced mammary tumours in the NK model, an intensive breeding work was undertaken in which γ-synuclein knockout mice on C57BL6 genetic background were backcrossed for several generations with FVB mice and finally intercrossed with mice of NK model, as outlined in the Materials and Methods chapter. This breeding work took approximately two years and produced 21 γ-synuclein Wt and 22 γ-synuclein KO experimental females carrying the activated ErbB2 transgene. Two control groups were also produced in the breeding work: a basic control group comprising 8 γ-synuclein Wt and 9 γ-synuclein KO females to control for the spontaneous incidence of mammary gland tumourigenesis; and a pregnancy passage control group comprising 11 γ-synuclein Wt and 14 γ-synuclein

KO females to control for any increased incidence of mammary tumours that may occur due to the proliferation of epithelial cells during gestation.

Animals from the experimental and pregnancy passage control groups were mated with non-experimental males at 7 weeks of age. This would further induce the transcription of the NK transgene in the experimental females as it is driven by an MMTV promoter that responds to elevated levels of progesterone during pregnancy. The female mothers were allowed to nurse pups for about 18-20 days. After weaning pups, females were monitored for tumour development by palpation 1-2 times weekly. The time of tumour detection was recorded, and thereupon measurements of tumours (2 perpendicular diameters) were recorded to monitor tumour growth. The basic and pregnancy passage control groups, lacking the activated ErbB2 transgene and showing no tumour development, were sacrificed at an age of 13.5 months. The experimental female animals, with the activated ErbB2 transgene, were sacrificed when the longer axis of the biggest palpable tumour reached 20 mm, as required by the Home Office regulations. Moreover, the following animal parameters were recorded: age at parity (taken as estimated onset of gestation = age at birth giving – 20 days), age at sacrifice (when the longer axis of the largest palpable tumour reached a length of 20 mm) and the number of palpable tumours formed. Upon sacrificing the animal, normal and tumourous mammary glands were dissected and harvested for histological investigations. Metastasis was investigated by visual inspection of body organs at sacrifice and by histological analysis of lung and kidney tissues.

6.2. Results and discussion

6.2.1. Deletion of γ-synuclein gene did not prevent formation of tumours in the mammary epithelium by activated ErbB2

Table 6.1 below shows summary description and tumour incidence in the γ-synuclein Wt and γ-synuclein KO female mice of the basic control, pregnancy passage control and experimental groups.

	Basic Control Group (No NK transgene; No pregnancy passage; sacrificed at 13.5 months of age)	Pregnancy Passage Control Group (No NK transgene; one pregnancy passage; sacrificed at 13.5 months of age)	Experimental Groups (Hemizygous NK transgene; one pregnancy passage; sacrificed when a tumour diameter reached 20 mm)
Wt	N = 8 No tumours developed	N = 11 No tumours developed	N = 21 All females developed tumours
KO	N = 9 No tumours developed	N = 14 Only 1 female developed tumours	N = 22 All females developed tumours

Table 6.1. Summary description and tumour incidence in γ-synuclein Wt and γ-synuclein KO female mice of the control and experimental cohorts.

In the basic control group, lacking the activated ErbB2 transgene and not passed through pregnancy, no tumours were formed in the mammary epithelium of both γ-synuclein Wt and γ-synuclein KO female mice during an observation time of 13.5 months. In the pregnancy passage control group, also lacking the activated ErbB2 transgene, none of the γ-synuclein Wt females developed any tumours and only 1/14 (7%) of the γ-synuclein KO females developed a mammary tumour which was detected at an age of 268 days. This incidence falls within the range of spontaneous mammary tumourigenesis in multiparous FVB mice which was recorded to be 14%, although spontaneous tumours were reported to be detected at an older age (> 300 days, mostly between 600-800 days of age) (Huang et al., 2008). Hence, the extensive proliferation of mammary epithelial cells during gestation (pregnancy passage) did not affect the spontaneous incidence of mammary tumours significantly, and this one incidence in the KO group may be considered negligible when comparing the effect of γ-synuclein deletion on mammary tumour formation by activated ErbB2 in the experimental females.

All experimental female cohorts harbouring the hemizygous activated ErbB2 transgene (21 γ-synuclein Wt and 22 γ-synuclein KO females) developed mammary tumours regardless of the presence or absence of the functional γ-synuclein gene. Thus, ablation of γ-synuclein did not prevent induction of mammary gland tumourigenesis by the activated ErbB2 transgene in mammary gland epithelium. Multifocal tumours were formed in the majority of the 5 pairs of mammary glands in most experimental female mice. This is a result of the pattern of expression of the activated ErbB2 transgene which is known to occur in a non-uniform and random fashion in the mammary epithelium (Muller et al., 1988). The experimental γ-

synuclein KO females developed more tumours than the γ-synuclein Wt ones, with a mean number of 12.8 and 10.6 mammary tumours/female mouse, respectively. This result is graphically presented in figure 6.1 below. This difference, however, was not significant (P = 0.30 using Wilcoxon's rank sum test). Generally, tumour tissue took a greyish white appearance, were mostly soft, had central areas of necrosis and contained blood-filled cysts. Figures 6.2 and 6.3 below show photographs of 4 representatives of each of the γ-synuclein KO and γ-synuclein Wt experimental females, respectively, dissected immediately upon sacrifice and showing mammary tumours at different stages of development in the different glands. Figure 6.4 below shows microphotographs of H&E-stained histological sections of some of these representative ErbB2-induced mammary tumours.

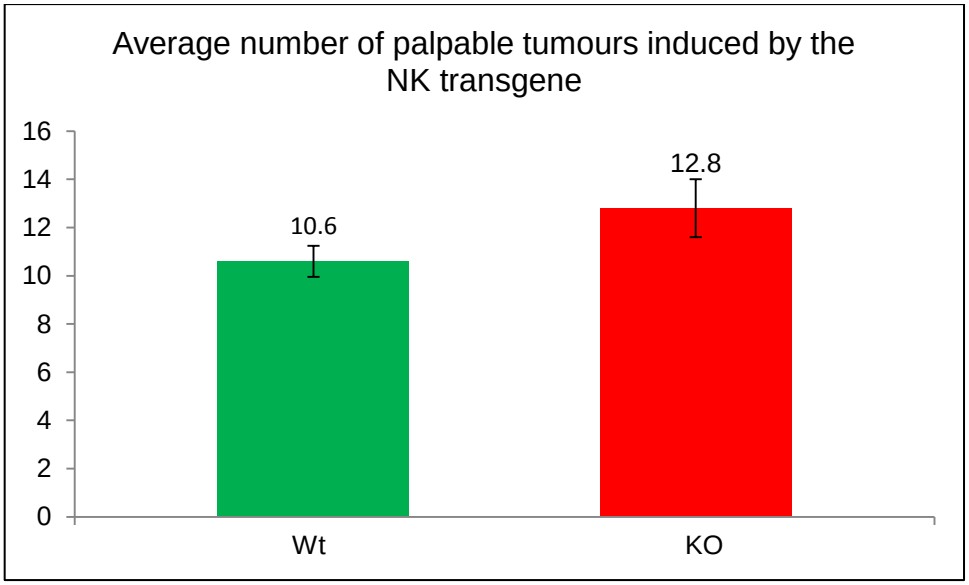

Figure 6.1. Average number of mammary tumours induced by activated ErbB2 transgene in the experimental female mice. The γ-synuclein KO group recorded a slightly, but not significantly, higher number of mammary tumours (P = 0.30 using Wilcoxon's rank sum test).

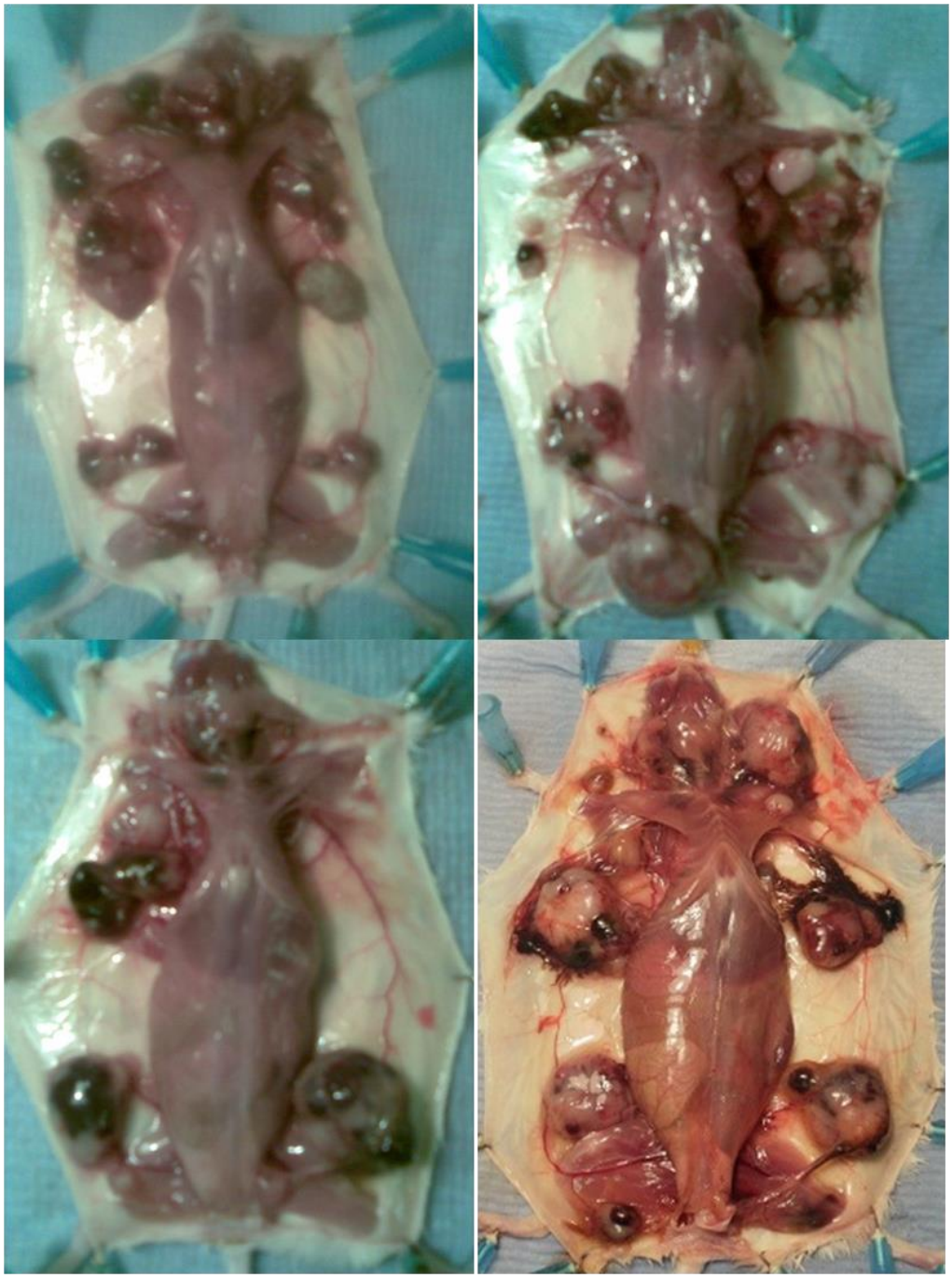

Figure 6.2. Photographs of dissected NK hemizygous, γ-synuclein KO females showing multifocal tumours induced by the activated ErbB2 transgene in the different mammary glands.

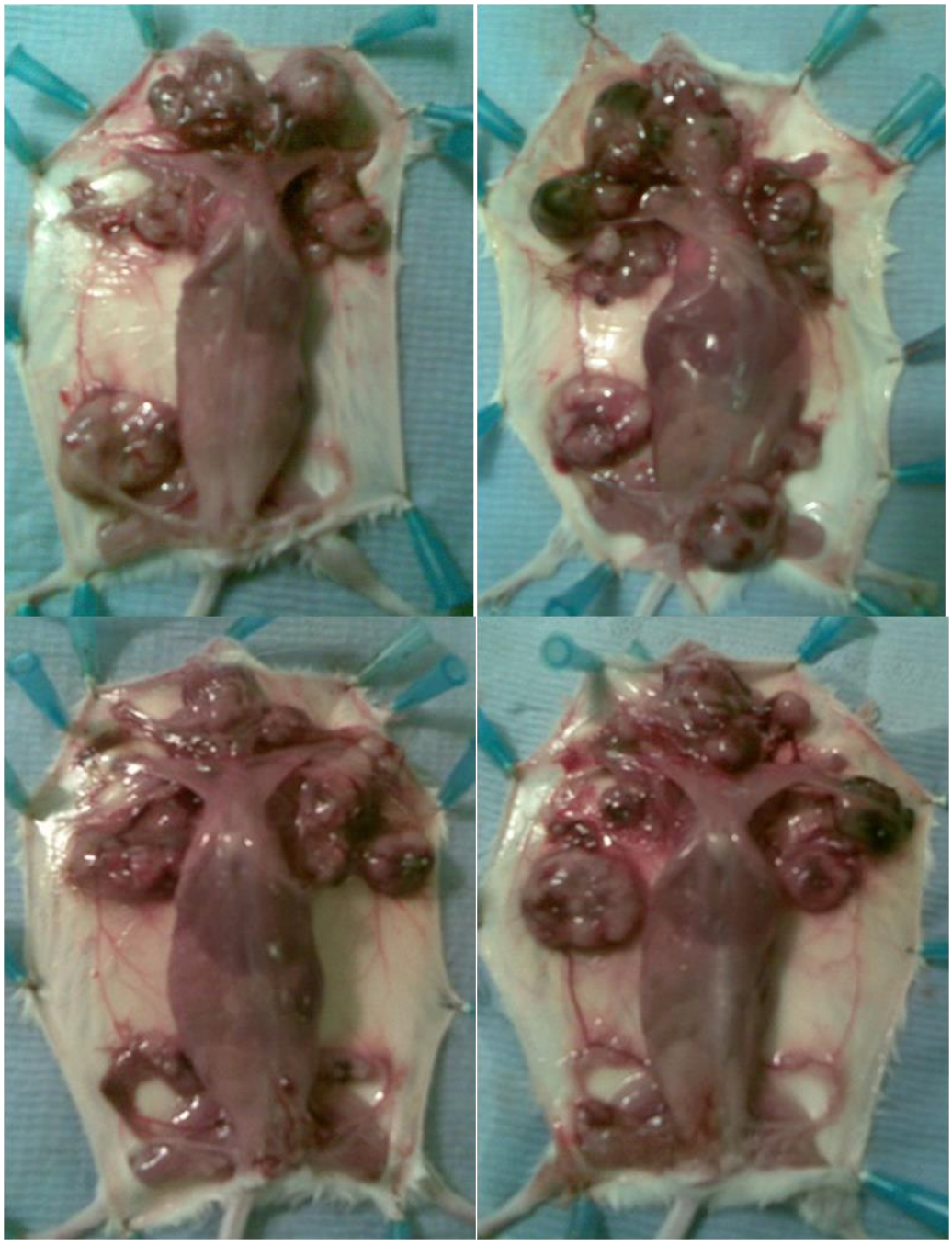

Figure 6.3. Photographs of dissected NK hemizygous, γ-synuclein Wt females showing multifocal tumours induced by the activated ErbB2 transgene in the different mammary glands.

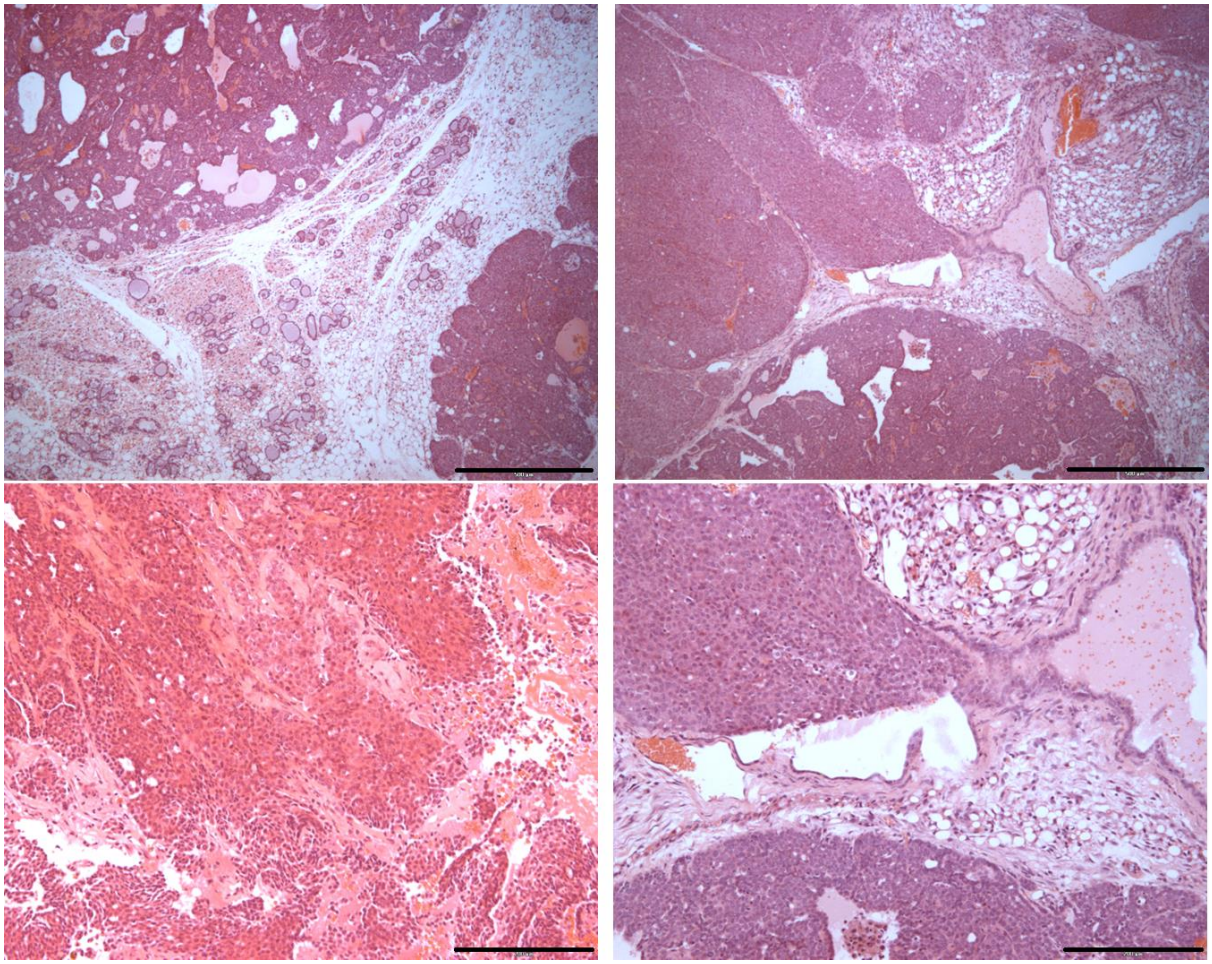

Figure 6.4. Microphotographs of H&E-stained histological sections of representative ErbB2-induced mammary tumours. Right two panels: γ-synuclein Wt mammary gland showing multifocal tumour with epithelia-derived tumour cells and little adjacent normal tissue; Scale bars = 500 µm for upper panel and 200 µm for lower inset panel. Left upper panel: γ-synuclein KO mammary gland showing multifocal tumour with epithelia-derived tumour cells and adjacent normal tissue; Scale bar = 500 µm. Left lower panel: γ-synuclein KO epithelia-derived tumour cells with no normal mammary tissue; Scale bar = 200 µm.

As transcription of the NK transgene is driven by an MMTV promoter that responds to elevated levels of progesterone during pregnancy, and to avoid any possible confounding effect of age on the levels of circulating progesterone and on the induction of mammary tumours by activated ErbB2, age at parity in the γ-synuclein Wt and γ-synuclein KO experimental females was compared. As can be seen in figure 6.5 below, the average age at parity was almost equal, being 79 days in the γ-synuclein Wt and 78 days in the γ-synuclein KO experimental females. Non-parametric statistical analysis was still carried out to confirm that there was no significant difference between the two genotypes (P = 0.94 using Wilcoxon's rank sum test).

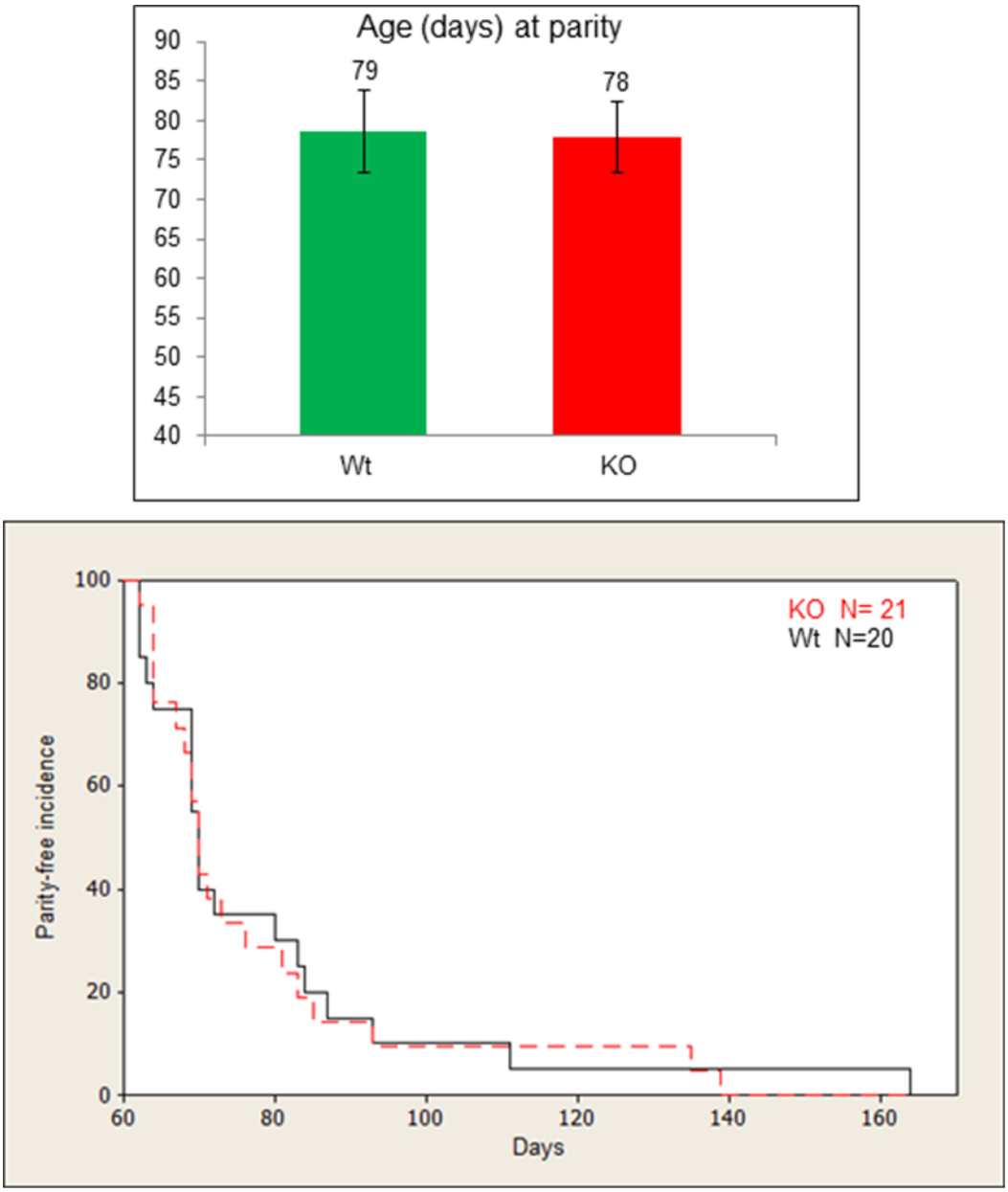

Figure 6.5. Age at parity in the γ-synuclein Wt and γ-synuclein KO experimental female mice. Upper panel: average age at parity in the γ-synuclein Wt and γ-synuclein KO experimental female mice. Lower panel: non-parametric "survival" plot with the Kaplan-Meier method for age at parity in the γ-synuclein Wt and γ-synuclein KO experimental females. No significant difference in age at parity between the two genotypes was found (P = 0.94 using Wilcoxon's rank sum test).

6.2.2. γ-synuclein KO mammary glands exhibited accelerated onset of tumours induced by activated ErbB2 transgene

As tumour incidence was 100% in both γ-synuclein Wt and KO experimental females, concluding that γ-synuclein is not essential for the induction of mammary tumours by activated ErbB2, the timing of tumour onset was next investigated. Mammary tumours were detected by palpation starting at an age of 116 days in the γ-synuclein KO experimental females and at an age of 131 days in the γ-synuclein Wt females. Considering the age at which the first palpable tumour was detected in each experimental animal, no statistically significant difference was seen between γ-synuclein KO and γ-synuclein Wt experimental groups (P = 0.20 using Wilcoxon's rank sum test). The median age (at which 50% of the first palpable tumours were already detected) was 149 and 151 days, and the mean age was 147 and 155 days, respectively. However, as can be seen in figure 6.6 the Kaplan-Meier curves show a trend for the first palpable tumours in the γ-synuclein KO females to be detected at an earlier age compared to the first palpable tumours in the γ-synuclein Wt females.

When all palpable tumours (including the first palpable ones) in all animals in each group were taken into account, the median age at which tumours were detected was significantly lower in the γ-synuclein KO animals (P = 0.01 using Wilcoxon's rank sum test; N = 132 and 118, respectively). Tumour latency (median), defined here as the age at which 50% of the formed tumours in the group were detected, was 165 days in the γ-synuclein KO females and 179 days in the γ-synuclein Wt females, and the mean age was 172 and 178 days, respectively. This accelerated latency can be graphically seen in figure 6.7 where the Kaplan-Meier curves appear separated for the most part, especially at the earlier events.

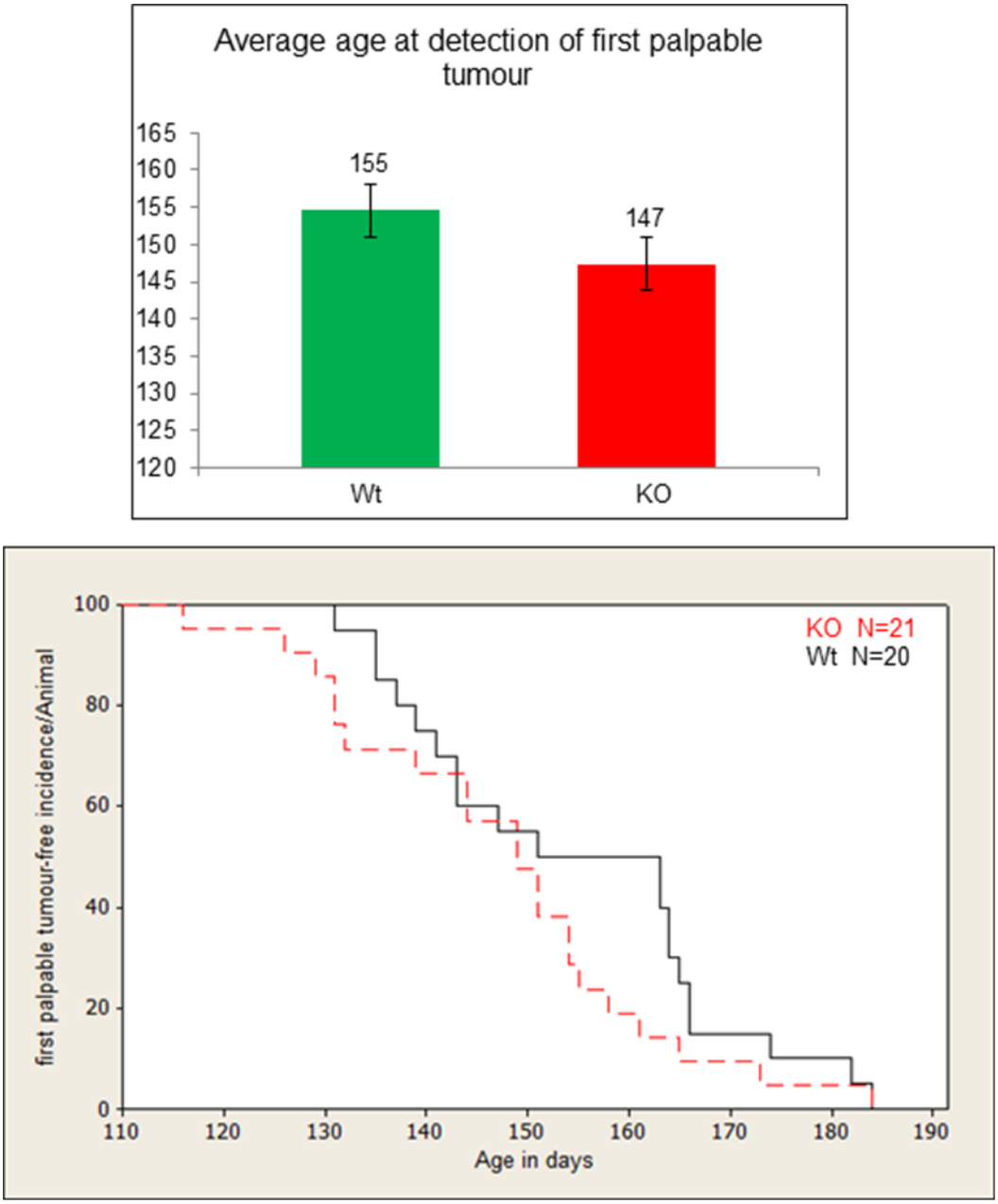

Figure 6.6. Age at detection of the first palpable tumour. Upper panel: average age at which the first palpable tumours were detected in the γ-synuclein Wt and γ-synuclein KO experimental female mice. Lower panel: non-parametric "survival" plot with the Kaplan-Meier method for the incidence of age at detection of first palpable tumour in the γ-synuclein Wt and γ-synuclein KO experimental females. Although no statistically significant difference between the two groups was found (P = 0.20 using Wilcoxon's rank sum test), the first palpable tumours in the KO group tended to occur earlier as seen by the red curve.

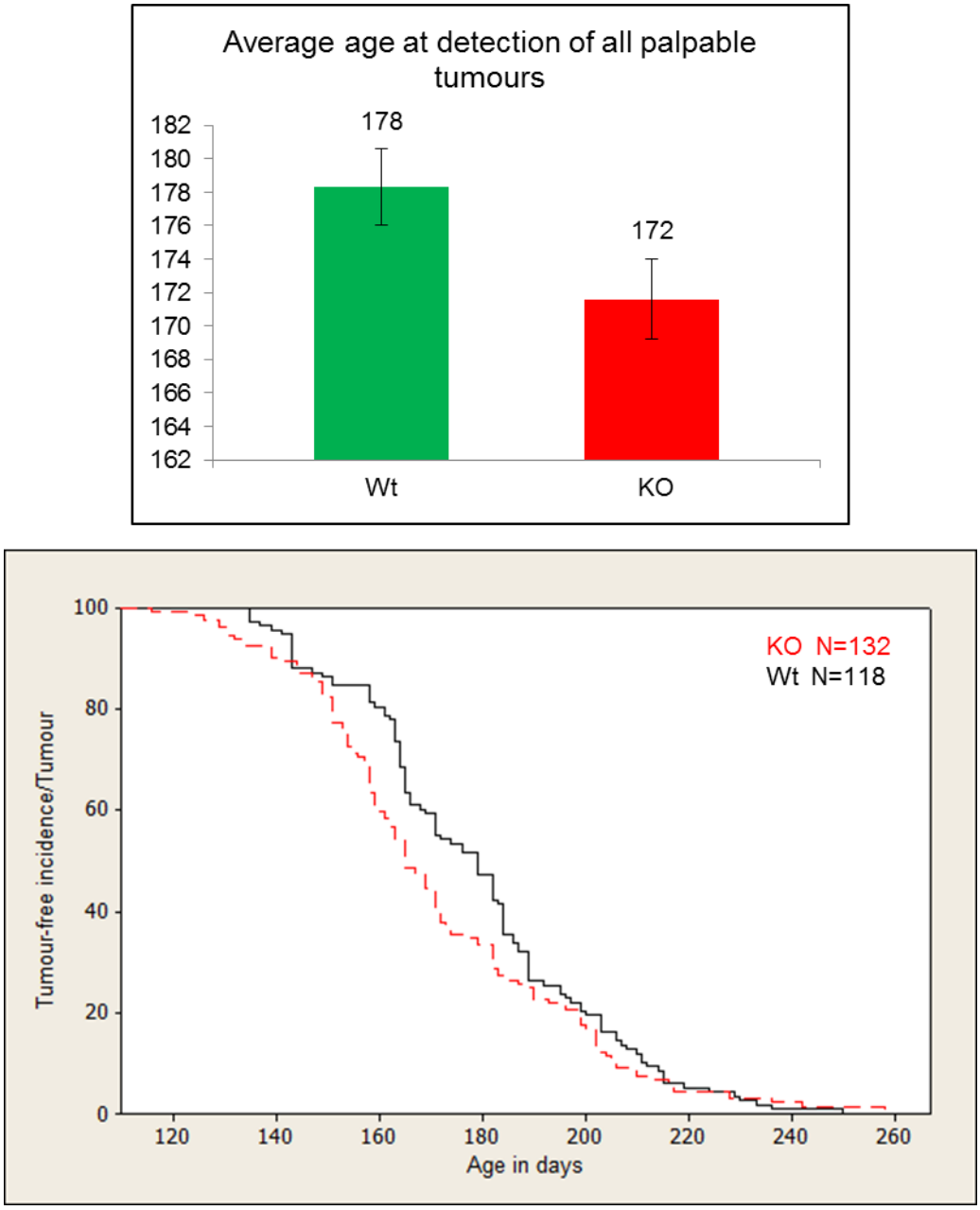

Figure 6.7. Age at detection of all palpable tumours. Upper panel: average age at which palpable tumours were detected in the γ-synuclein Wt and γ-synuclein KO experimental female mice. Lower panel: non-parametric "survival" plot with the Kaplan-Meier method for age at tumour detection in the γ-synuclein Wt and γ-synuclein KO experimental females. A highly significant difference in tumour latency was found between the two genotypes (P=0.01 using Wilcoxon's rank sum test), with the KO tumours being detected significantly earlier than the Wt ones.

This interesting result of γ-synuclein gene deletion accelerating the timing of tumour onset was not actually anticipated. This was in light of the available reports on the positive effect of γ-synuclein overexpression on stimulation of cancer cell growth, proliferation, survival, motility and metastasis, which inclined us to expect deletion of the gene to retard the development and progression of mammary tumours. Therefore, the previously highlighted positive correlation between ErbB2 and γ-synuclein expression, observed in both human and mouse mammary tumour tissue and cell lines, might suggest a possible involvement of γ-synuclein in some sort of negative regulation of the process of ErbB2-induced mammary gland tumourigenesis. A similar effect was reported in a study by Zhou and colleagues in which γ-synuclein expression was reported to be downregulated in approximately 60% (16/27) of human esophageal squamous cell carcinoma (ESCC) samples while it was upregulated in only 22% (6/27) of the samples and was not changed in 5 samples (Zhou et al., 2003). They further ectopically overexpressed γ-synuclein in ESCC 9706 cell line and found it to retard the growth rate in either low or high serum medium and to inhibit the transformation ability of the cells growing in soft agar. Their findings led to the conclusion that γ-synuclein may act as a negative regulator in human ESCC development. In the current study, knocking out γ-synuclein may have resulted in the lifting of some kind of negative regulation imposed upon the process of ErbB2-induced tumourigenesis, leading ultimately to the acceleration of the process and the observed earlier onset of mammary tumours. In brief, the definite genetic effect of γ-synuclein gene deletion on an FVB genetic background was the acceleration of the timing onset of mammary tumours induced by the activated ErbB2 receptor tyrosine kinase in the mammary epithelium.

6.2.3. Deletion of γ-synuclein gene had no significant effect on the growth of ErbB2-induced mammary tumours

As seen above, deletion of γ-synuclein gene did not prevent the formation of mammary tumours by activated ErbB2 transgene but rather unexpectedly accelerated the timing of tumour onset. To investigate whether deletion of γ-synuclein gene affected tumour growth, the age at which tumours reached a size of 250 mm^3 was considered. Many tumours included in the above investigations were not included in this analysis as they were smaller than 250 mm^3 at the time the animal had to be sacrificed. Figure 6.8 below shows that ErbB2-induced tumours in the γ-synuclein KO experimental females reached this tumour size when females were on average 192 days of age, compared to an average age of 201 days in the γ-synuclein Wt females. This difference was "marginally" significant (at the verge of statistical significance) ($P = 0.08$ using Wilcoxon's rank sum test; $N = 76$ and 69, respectively). This may have biological significance as the Kaplan-Meier curves show clear separation for the most part, pointing to a slightly faster growth of the γ-synuclein KO tumours.

However, as this result may include an effect of an earlier tumour onset in the γ-synuclein KO mammary epithelium, assuming tumour induction/formation and tumour growth to be two separate processes, the time it took for tumours to grow from a size of 250 mm^3 to a size of 1500 mm^3 was considered. These sizes were chosen as they allowed inclusion of the largest size span and tumour numbers possible: most formed tumours could not be included in this analysis because adjacent tumours fused after reaching a size of 250 mm^3 and many other tumours contained large blood-filled cysts that did not represent growth of tumour tissue. As a

result, only 9 KO and 8 Wt tumours were available for this tumour size growth analysis. Figure 6.9 below presents this result graphically. The γ-synuclein KO and γ-synuclein Wt experimental groups did not differ, with almost equal number of days (21 and 22, respectively) required for their tumours to grow from a size of 250 mm^3 to a size of 1500 mm^3 (P = 0.77 using Wilcoxon's rank sum test). Thus, deletion of γ-synuclein gene seems to have no effect on the growth of formed ErbB2-induced mammary tumours, although this result must be treated with caution as it is based on a rather small sample size.

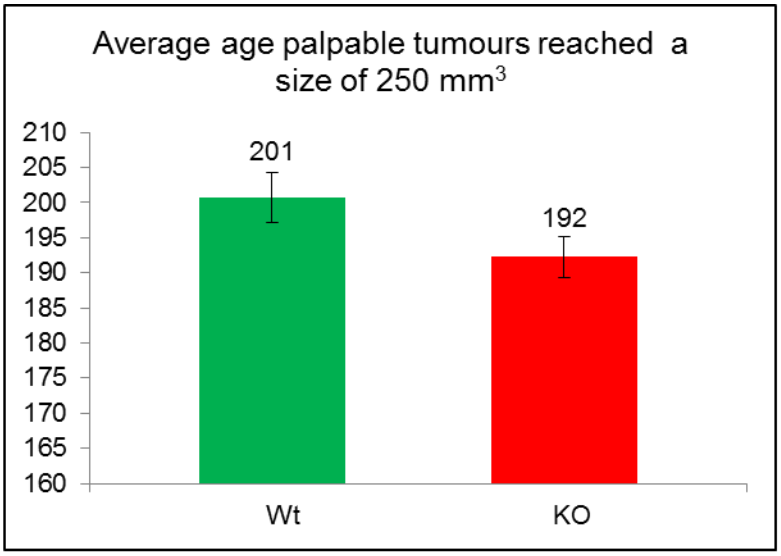

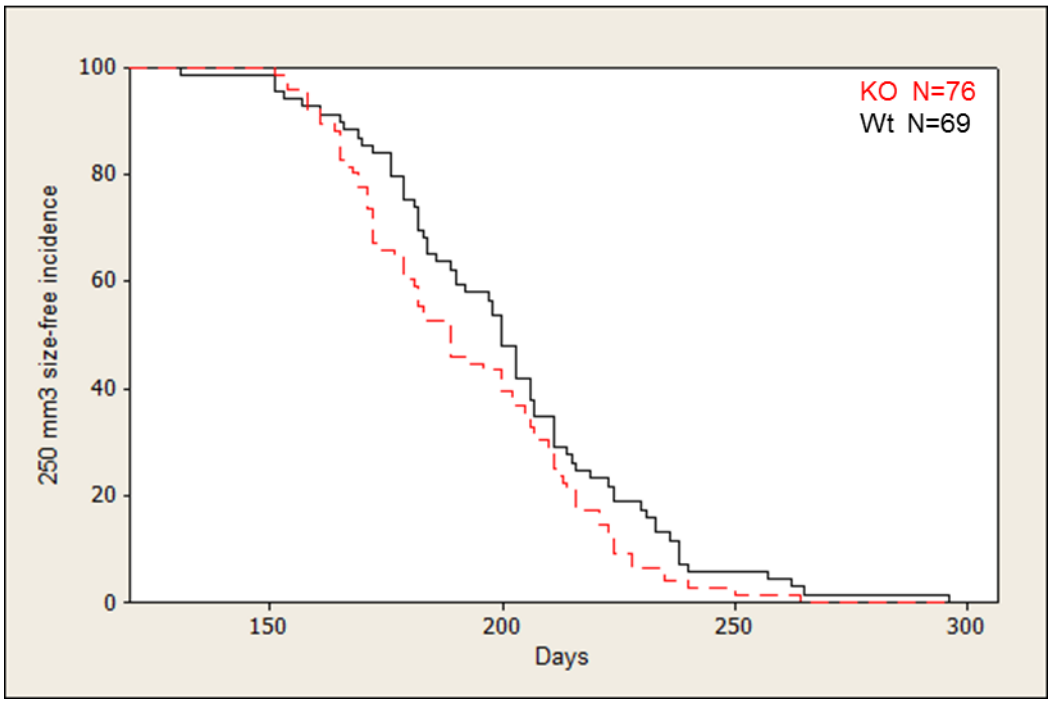

Figure 6.8. Age at which palpable tumours reached a size of 250 mm^3. Upper panel: average age at which palpable tumours reached a size of 250 mm^3 in the γ-synuclein Wt and γ-synuclein KO experimental female mice. Lower panel: non-parametric "survival" plot with the Kaplan-Meier method for age at reaching a 250 mm^3 size in the γ-synuclein Wt and γ-synuclein KO experimental females: a "marginally" significant difference between the two genotypes was observed (P = 0.08 using Wilcoxon's rank sum test; N = 69 and 76, respectively).

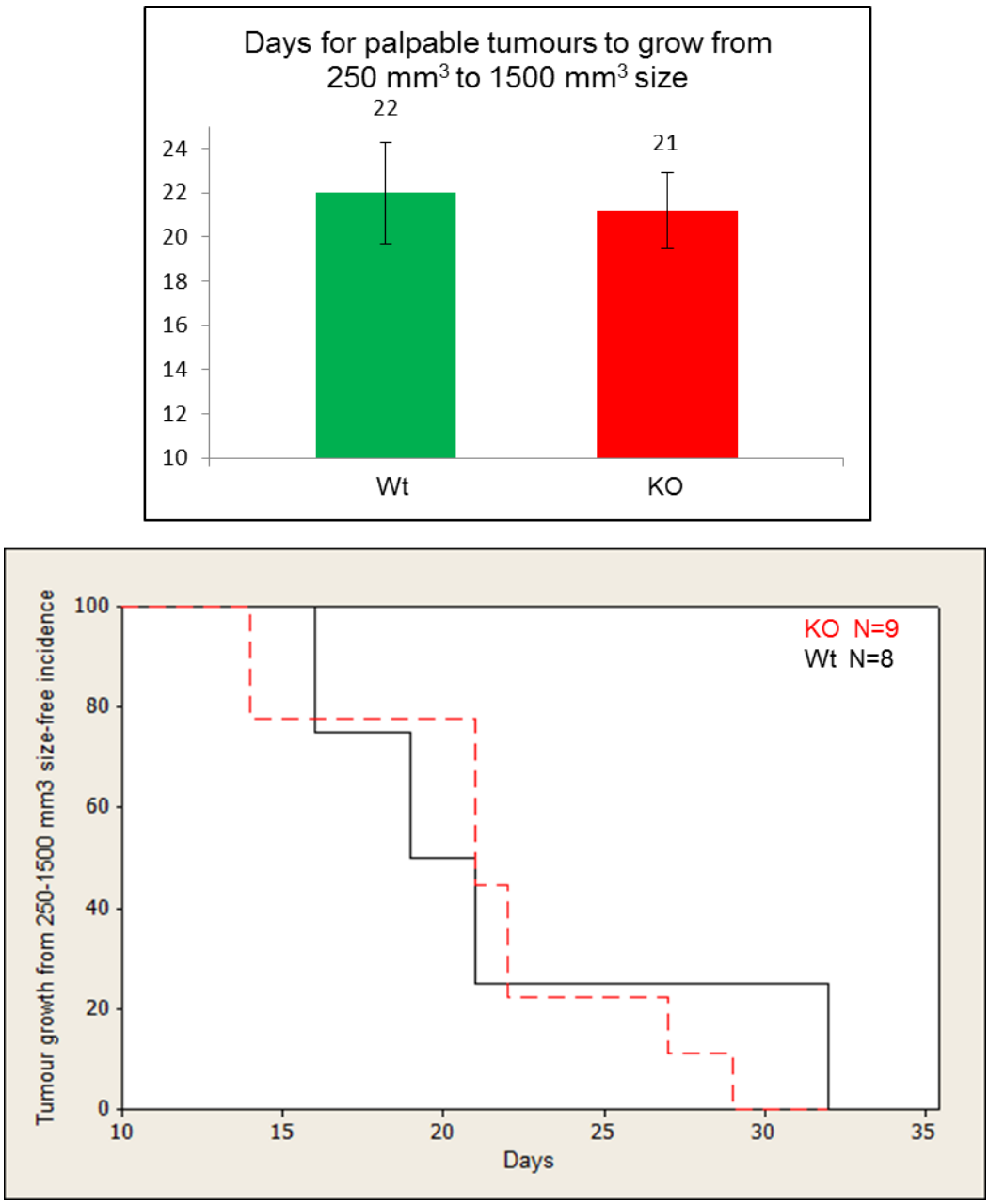

Figure 6.9. Effect of γ-synuclein gene deletion on tumour growth. Upper panel: average number of days required for palpable tumours induced in the γ-synuclein Wt and γ-synuclein KO experimental female mice to grow from a size of 250 mm^3 to a size of 1500 mm^3. Lower panel: non-parametric "survival" plot with the Kaplan-Meier method for number of days required for tumours from γ-synuclein Wt and γ-synuclein KO experimental females to grow from a size of 250 mm^3 to a size of 1500 mm^3: no significant difference between the two genotypes was found (P = 0.77 using Wilcoxon's rank sum test; N = 8 and 9, respectively).

6.2.4. Metastasis and animal survival are not affected by deletion of γ-synuclein gene in the NK model

Metastasis is a crucial aspect of cancer progression and is the main cause of death in cancer patients. A strong correlation between aberrant expression of γ-synuclein in primary tumours and progression to distant metastases in patients with different cancer types was reported (Liu et al., 2005). Further studies, particularly in breast cancer (Guo et al., 2007; Wu et al., 2007; Wu et al., 2003), and in liver cancer (Zhao et al., 2006), confirmed the late stage-specific aberrant expression of γ-synuclein in tumours and its correlation to metastasis. The positive role of γ-synuclein overexpression in invasion and metastasis of breast cancer cells was shown both *in vitro* and *in vivo* (Jia et al., 1999).

In the current study, the effect of γ-synuclein gene deletion on metastasis in the NK mouse model was investigated by visual inspection of body organs upon animal sacrifice and by histological investigations of kidney and lung tissues. No signs of lumps or tumour tissue were seen in the different organs inspected visually. H&E-stained histological sections of liver did not reveal any metastasis either. However, histological investigations of H&E-stained histological sections of the lungs confirmed metastasis to have occurred in both γ-synuclein KO and γ-synuclein Wt experimental females with approximately equal proportions, 12/21 (57 %) and 13/21 (62 %), respectively. Figure 6.10 below shows metastases in H&E-stained histological sections of lungs from both genotypes. Thus, deletion of γ-synuclein gene had no effect on metastasis of mammary tumour cells induced by activated ErbB2 in the NK mouse model.

In this study, survival of the experimental females was conditional upon tumour growth to a diameter of 20 mm, as required by the Home Office regulations. The age at which the animals had to be sacrificed was then largely dependent on the overall processes of tumour development, including timing of tumour onset, growth and progression. Figure 6.11 below shows the average age at sacrifice and a survival plot for the γ-synuclein KO and γ-synuclein Wt experimental females. The γ-synuclein KO experimental females had a slightly younger age at sacrifice than the γ-synuclein Wt experimental ones, averaging 216 and 224 days of age, respectively. However, this 8 day-difference was not statistically significant (P = 0.34 using Wilcoxon's rank sum test). In fact, the median age at which 50% of the animals had to be sacrificed was almost equal, being 218 and 219 days, respectively. Therefore, deletion of γ-synuclein gene had no effect on the overall development and progression of mammary gland tumourigenesis induced by the activated ErbB2 transgene on an FVB genetic background.

In conclusion, results of our study presented in this chapter clearly demonstrate that endogenous γ-synuclein is not required for development, growth and metastasis of mammary tumours. Moreover, all used endpoints demonstrated a trend for accelerated tumourigenesis in the absence of γ-synuclein. Thus we proved that a widely accepted idea about a role of this protein as a trigger and/or promoter of tumourigenesis and metastasis is not necessarily true. It is feasible that the increased levels of γ-synuclein observed in advance-stage tumours and metastases might reflect activation of pathways that retard rather than promote these processes. Further studies are required to clarify the role of γ-synuclein in these tumours. Looking retrospectively on the design of the *in vivo* experiments, one can conclude

that the used model of activated ErbB2-dependent mammary gland tumourigenesis was not the optimal choice for this study. Taking into account the potential acceleration of tumour development and growth in the absence of γ-synuclein, it would be preferable to employ a less aggressive model, for instance transgenic mice of the “N202” line (expressing unmodified ErbB2 receptor) that develop smaller and less tumours with significantly later onset and smaller growth rate. This might emphasise the effect of γ-synuclein depletion on at least some of the studied endpoints and produce clear evidence that endogenous γ-synuclein has a negative effect on mammary gland tumourigenesis.

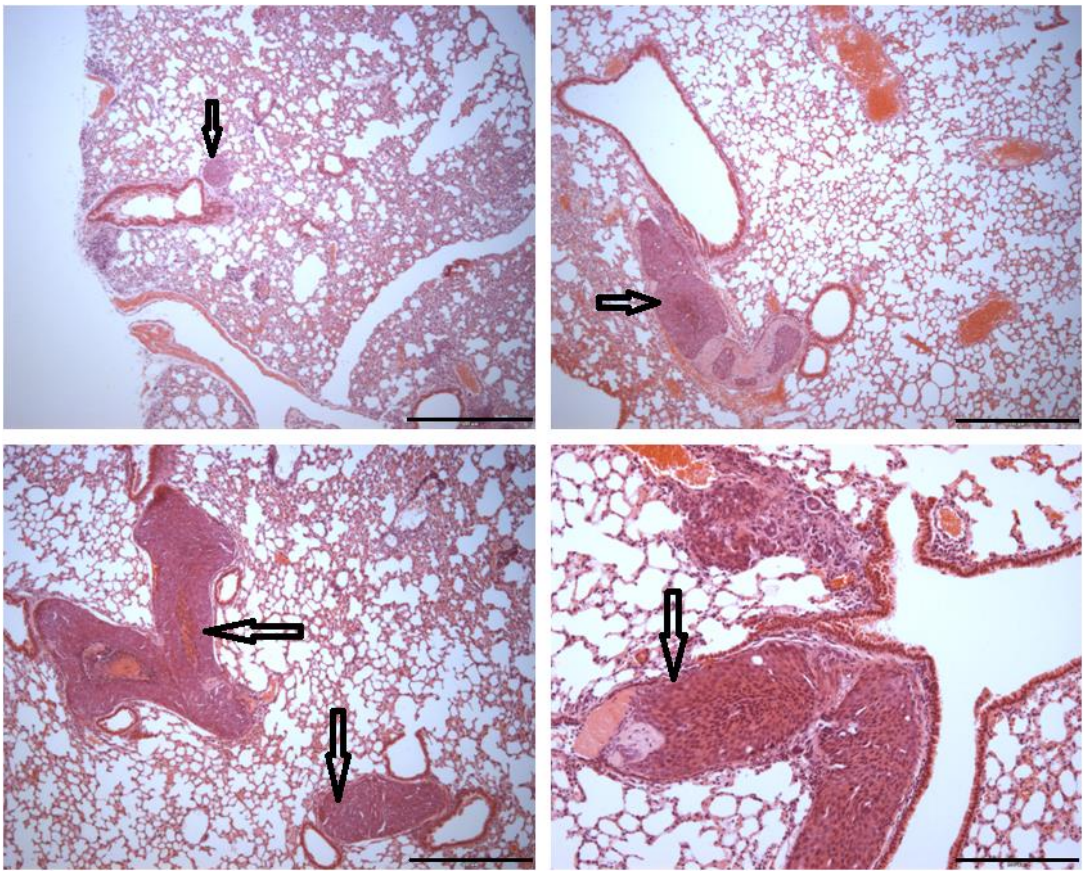

Figure 6.10. Effect of γ-synuclein gene deletion on tumour metastasis. Metastases to the lungs were observed in both γ-synuclein KO and γ-synuclein Wt experimental females with approximately equal proportions. Left two panels: arrows indicate metastases in γ-synuclein KO female lungs; scale bars = 500 µm. Right two panels: arrows indicate metastases in γ-synuclein Wt female lungs; scale bar = 500 µm in the upper panel and 200 µm in the lower panel.

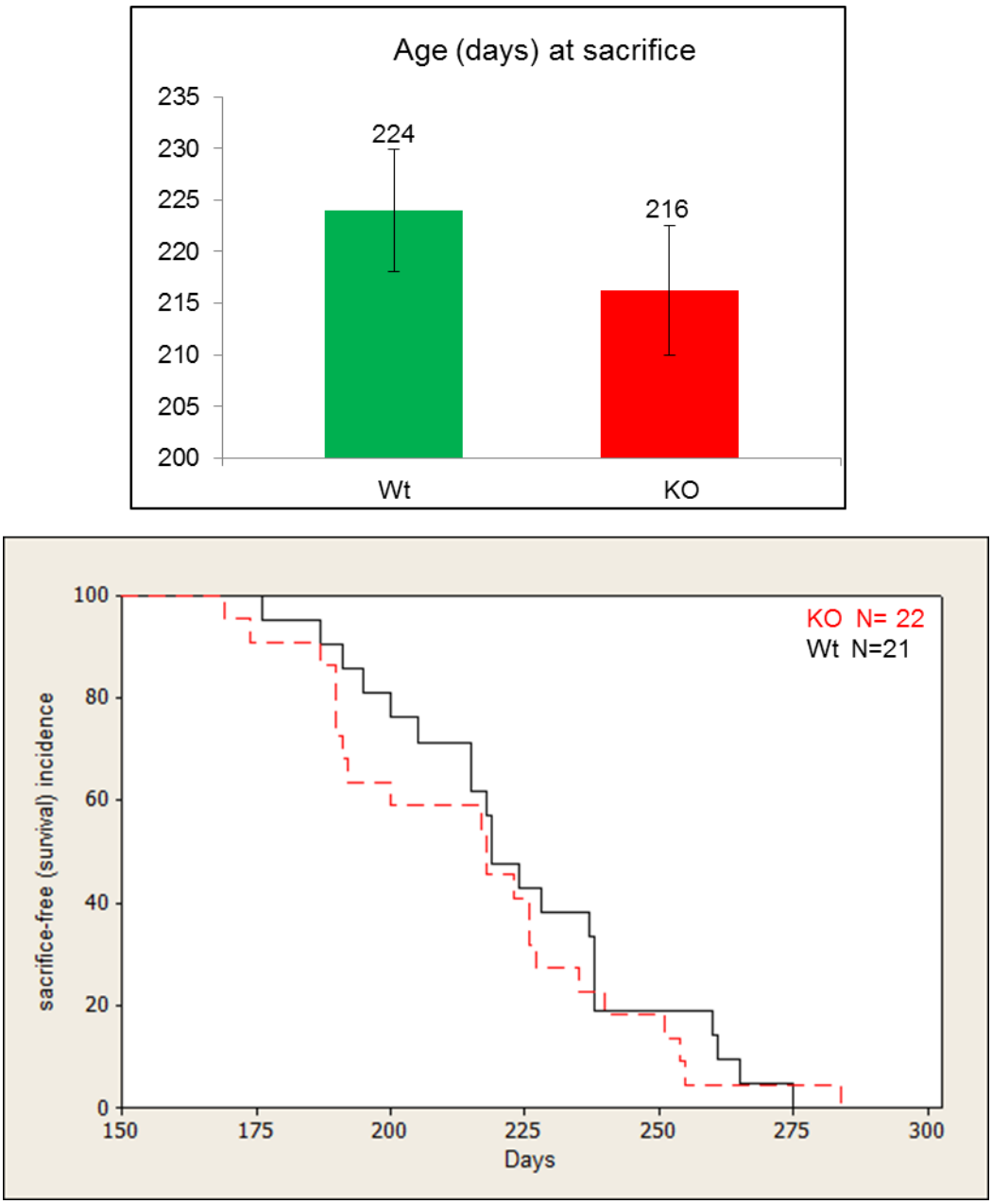

Figure 6.11. Effect of γ-synuclein gene deletion on survival. Upper panel: average age of γ-synuclein Wt and γ-synuclein KO experimental female mice at sacrifice (an animal was sacrificed when the longer tumour diameter reached 20 mm). Lower panel: non-parametric survival plot with the Kaplan-Meier method for age at sacrifice in the γ-synuclein Wt and γ-synuclein KO experimental females: no significant difference was found between the two genotypes (P = 0.34 using Wilcoxon's rank sum test; N = 21 and 22, respectively).

Chapter 7. General discussion and conclusions

Breast cancer is the most common cancer in women worldwide. In the year 2010, approximately 1.5 million people were diagnosed with the disease, amounting to nearly 16% of all female cancers. In the same year, the disease killed 11556 women and 77 men in the UK alone (CancerResearchUK, 2012). Despite the availability of some anti-cancer drugs, only moderate success has been achieved in the overall survival rates. This is because most patients undergo recurrence largely due to resistance that tumours eventually develop to drugs used for treatment. Success in improving the existing treatments and developing more effective ones would ultimately come from increased knowledge of the disease, especially at the cellular and molecular levels.

γ-synuclein has been claimed to play a role in mammary gland tumourigenesis. Its overexpression in cancer cells was shown to inhibit apoptosis and stimulate growth, proliferation, survival, motility and metastasis. In transgenic mice, aberrant expression of γ-synuclein stimulated ligand-dependent ER-α signalling, leading to a highly proliferative pregnancy-like phenotype of mammary epithelial cells and branching morphology. However, the role of endogenous γ-synuclein in mammary gland tumourigenesis has not been studied in an appropriate *in vivo* model. Previously in our lab, an observation was made correlating the expression of γ-synuclein with that of ErbB2 receptor tyrosine kinase in the mouse mammary tumour cell line MG1361. This cell line was originally established from a mammary adenocarcinoma isolated from the transgenic breast cancer mouse line FVB-Tg(MMTV-ErbB2)NK1Mul/J (NK model) chosen for this project. The question was thus raised whether γ-synuclein was required for the development and/or progression of ErbB2-induced mammary gland tumourigenesis. To this end, γ-synuclein knockout mice on C57BL6 genetic background were backcrossed for

several generations with FVB mice and finally intercrossed with mice of NK model to investigate the effect of γ-synuclein gene deletion on the development and progression of ErbB2-induced mammary tumours. In parallel, the effect of γ-synuclein gene deletion on the normal development of mammary gland was investigated in both virgin glands as well as 14.5 day gestating mammary glands.

To further investigate the observed correlation between the expression of γ-synuclein and that of ErbB2, mouse and human mammary tumour cell lines that are known to be either positive or negative for the ErbB2 protooncogene were investigated for γ-synuclein expression. The results of these investigations supported a previous suggestion that γ-synuclein expression is positively correlated with that of ErbB2 at both the mRNA and protein levels. According to molecular weight, γ-synuclein was detected mostly as a monomer, a dimer or both, although trimer forms were seen in some cell lines but at much lower levels. Furthermore, aberrant expression of γ-synuclein was detected in mammary tumour tissues isolated from both ErbB2-positive models (N202 and NK) as well as from Blg-Cre^{+} BRCA2$^{fl/fl}$ p53$^{fl/fl}$ breast cancer model, with γ-synuclein expressed mostly as a presumable dimer. This notion of oligomerization was further supported when enzymatic tests for N-linked glycosylation and phosphorylation failed to detect any change in electrophoretic mobility of γ-synuclein protein. This suggests that dimerization might be a functional aspect of the small, cytoplasmic γ-synuclein protein.

As few reports claimed that the protein may localize to various subcellular structures including centrosomes, mitotic spindle fibers and midbody, and that it may even translocate to the nucleus under stress conditions, the subcellular localization of γ-synuclein in the cell line MG1361 was investigated using highly specific, affinity

purified antibody previously produced and characterised in our laboratory. This cell line was selected because it was originally established from the same NK mouse model used for *in vivo* experiments in the current study. The results showed that γ-synuclein had cytoplasmic localization and in line with the majority of previous reports, it appeared to co-localize neither with γ-tubulin at the centrosomal region of dividing cells nor with β-actin in the cultured cells. Moreover, it was not seen co-localized with α-tubulin in the microtubule spindle fibers, nor was it observed associated with α-tubulin at the midbody during cytokinesis of dividing cells. The different results from the few reports above could be due to different behaviours of γ-synuclein in different cell types and/or to different conditions of cell growth, or to non-specific binding of antibodies used to certain intracellular structures, which is a known phenomenon for poorly purified antibodies with low specificity.

Investigations of γ-synuclein protein in normal FVB mouse mammary glands did not detect any expression in the epithelium lining the mammary ducts, indicating that it is not expressed in the normal epithelial cells of the mammary gland. However, the protein was detected in endothelial cells of small blood vessels, in autonomic nerve fibers innervating the gland and in the narrow cytoplasmic strips of white adipocytes making up most of the mammary gland stroma. Deletion of γ-synuclein gene did not have any effect on the normal development of the mammary gland. The extent of epithelial ducts' elongation and branching morphology was not affected during puberty, nor was the development and differentiation of lobuloalveoli during gestation. The γ-synuclein KO mammary glands produced normal amounts of milk as evidenced by the nursed pups that developed as normal as pups of Wt mothers. Thus, gestation/lactation/involution cycle in the γ-synuclein KO mammary glands

proceeded normally. These results indicate that γ-synuclein is not required for the biological processes governing the normal development of the mammary gland at any developmental stage - embryonic, pubertal or reproductive.

Ablation of γ-synuclein did not prevent induction of mammary gland tumours by activated ErbB2 transgene in mammary gland epithelium. Multifocal tumours were formed in the majority of the 5 pairs of mammary glands in most experimental female mice. The experimental ErbB2 hemizygous, γ-synuclein KO females developed slightly, but not significantly, more tumours than the ErbB2 hemizygous, γ-synuclein Wt littermates, demonstrating that γ-synuclein is not essential for the induction of mammary tumours by activated ErbB2. However, tumour latency was significantly shorter in the γ-synuclein KO animals than in the γ-synuclein Wt females, being 165 days and 179 days, respectively ($P = 0.01$ using Wilcoxon's test). This accelerated tumour onset suggests that the observed correlation between γ-synuclein and ErbB2 expression in human and mouse mammary tumour cell lines and tissues might underlie a negative regulation imposed by γ-synuclein on the process of ErbB2-induced mammary gland tumourigenesis. A similar result was observed by Zhou and co-workers in human esophageal squamous cell carcinoma samples where γ-synuclein was downregulated, and when ectopically overexpressed in ESCC 9706 cell line it retarded the growth rate and inhibited the transformation ability of the cancer cells.

Despite accelerating tumour onset, γ-synuclein gene deletion seems to have no significant effect on the growth rate of formed ErbB2-induced mammary tumours as both KO and Wt tumours required about the same number of days to advance from a size of 250 mm^3 to a size of 1500 mm^3, 21 and 22 days, respectively, although this

result must be treated with caution as it is based on a rather small sample size, N = 9 and 8, respectively. Similarly, metastasis of mammary tumour cells induced by activated ErbB2 in the NK mouse model was not significantly affected by the absence of γ-synuclein. The γ-synuclein KO experimental females had a slightly, but not significantly, younger age at sacrifice than the γ-synuclein Wt experimental ones, averaging 216 and 224 days of age, respectively.

In conclusion, our results clearly demonstrate that endogenous γ-synuclein is not required for induction, growth and progression of mammary tumours. Rather, all used endpoints demonstrated a trend for accelerated tumourigenesis in the absence of γ-synuclein in the NK model. It is feasible that the aberrant expression of γ-synuclein reported in advance-stage tumours and metastases reflects activation of pathways and mechanisms aimed at repressing rather than enhancing tumourigenesis. Hence, the widely accepted idea of γ-synuclein protein having an oncogenic property is not necessarily true, at least regarding ErbB2-induced tumourigenesis. Further studies are required to clarify the role of γ-synuclein in these tumours. Considering the observed trend towards accelerating the process of tumourigenesis, we recommend utilizing a less aggressive ErbB2 model to better reveal any significant effects γ-synuclein ablation may have on the process. This may include the “N202” mouse model (expressing Wt ErbB2 receptor) which induces less and smaller tumours with significantly later onset and smaller growth rate. This might emphasise the effect of γ-synuclein depletion on at least some of the studied endpoints and produce clear evidence that endogenous γ-synuclein may negatively regulate the process of mammary gland tumourigenesis.

Future prospects

As γ-synuclein was reported to have a positive effect on proliferation, migration, metastasis and survival of breast cancer cells, we anticipated the loss of its function to retard development of mammary tumours. Unexpectedly, however, its absence led to rather slightly accelerated mammary gland tumourigenesis induced by the constitutively active mutant ErbB2. We pursue conducting the same line of investigation but utilizing a less aggressive ErbB2 tyrosine kinase form for mammary tumour induction, that of the N202 model. This might emphasise the effect of γ-synuclein depletion on tumour growth rate, metastasis and survival, and produce clear evidence that endogenous γ-synuclein may negatively regulate the process of mammary gland tumourigenesis.

The results obtained in this study will be published as two different papers. One paper will report the observed null effect of deleting γ-synuclein gene on the normal development of mammary gland. It will highlight the fact that both wild type and knockout females underwent similar developmental changes of mammary gland at all stages, fetal, pubertal and reproductive. The second paper will report the unexpected effect of slight acceleration of ErbB2-induced mammary gland tumourigenesis upon deletion of γ-synuclein gene, revealing the significantly shorter tumour latency and slightly shorter survival.

Bibliography

ABELIOVICH, A., SCHMITZ, Y., FARINAS, I., CHOI-LUNDBERG, D., HO, W. H., CASTILLO, P. E., SHINSKY, N., VERDUGO, J. M., ARMANINI, M., RYAN, A., HYNES, M., PHILLIPS, H., SULZER, D. & ROSENTHAL, A. 2000. Mice lacking alpha-synuclein display functional deficits in the nigrostriatal dopamine system. *Neuron,* 25**,** 239-52.

AHMAD, M., ATTOUB, S., SINGH, M. N., MARTIN, F. L. & EL-AGNAF, O. M. 2007. Gamma-synuclein and the progression of cancer. *FASEB J,* 21**,** 3419-30.

AKOPIAN, A. N. & WOOD, J. N. 1995. Peripheral nervous system-specific genes identified by subtractive cDNA cloning. *J Biol Chem,* 270**,** 21264-70.

AL-WANDI, A., NINKINA, N., MILLERSHIP, S., WILLIAMSON, S. J., JONES, P. A. & BUCHMAN, V. L. 2010. Absence of alpha-synuclein affects dopamine metabolism and synaptic markers in the striatum of aging mice. *Neurobiol Aging,* 31**,** 796-804.

ANDERSON, S. M., RUDOLPH, M. C., MCMANAMAN, J. L. & NEVILLE, M. C. 2007. Key stages in mammary gland development. Secretory activation in the mammary gland: it's not just about milk protein synthesis! *Breast Cancer Res,* 9**,** 204.

ANWAR, S., PETERS, O., MILLERSHIP, S., NINKINA, N., DOIG, N., CONNOR-ROBSON, N., THRELFELL, S., KOONER, G., DEACON, R. M., BANNERMAN, D. M., BOLAM, J. P., CHANDRA, S. S., CRAGG, S. J., WADE-MARTINS, R. & BUCHMAN, V. L. 2011. Functional alterations to the nigrostriatal system in mice lacking all three members of the synuclein family. *J Neurosci,* 31**,** 7264-74.

ASSELIN-LABAT, M. L., SUTHERLAND, K. D., BARKER, H., THOMAS, R., SHACKLETON, M., FORREST, N. C., HARTLEY, L., ROBB, L., GROSVELD, F. G., VAN DER WEES, J., LINDEMAN, G. J. & VISVADER, J. E. 2007. Gata-3 is an essential regulator of mammary-gland morphogenesis and luminal-cell differentiation. *Nat Cell Biol,* 9**,** 201-9.

ATABAI, K., FERNANDEZ, R., HUANG, X., UEKI, I., KLINE, A., LI, Y., SADATMANSOORI, S., SMITH-STEINHART, C., ZHU, W., PYTELA, R.,

WERB, Z. & SHEPPARD, D. 2005. Mfge8 is critical for mammary gland remodeling during involution. *Mol Biol Cell,* 16**,** 5528-37.

BAXTER, F. O., CAME, P. J., ABELL, K., KEDJOUAR, B., HUTH, M., RAJEWSKY, K., PASPARAKIS, M. & WATSON, C. J. 2006. IKKbeta/2 induces TWEAK and apoptosis in mammary epithelial cells. *Development,* 133**,** 3485-94.

BOST, F., AOUADI, M., CARON, L. & BINETRUY, B. 2005. The role of MAPKs in adipocyte differentiation and obesity. *Biochimie,* 87**,** 51-6.

BOSTROM, P., ANDERSSON, L., RUTBERG, M., PERMAN, J., LIDBERG, U., JOHANSSON, B. R., FERNANDEZ-RODRIGUEZ, J., ERICSON, J., NILSSON, T., BOREN, J. & OLOFSSON, S. O. 2007. SNARE proteins mediate fusion between cytosolic lipid droplets and are implicated in insulin sensitivity. *Nat Cell Biol,* 9**,** 1286-93.

BOYER, F. & DREYER, J. L. 2008. The role of gamma-synuclein in cocaine-induced behaviour in rats. *Eur J Neurosci,* 27**,** 2938-51.

BRISKEN, C., AYYANNAN, A., NGUYEN, C., HEINEMAN, A., REINHARDT, F., TAN, J., DEY, S. K., DOTTO, G. P. & WEINBERG, R. A. 2002. IGF-2 is a mediator of prolactin-induced morphogenesis in the breast. *Dev Cell,* 3**,** 877-87.

BRISKEN, C., KAUR, S., CHAVARRIA, T. E., BINART, N., SUTHERLAND, R. L., WEINBERG, R. A., KELLY, P. A. & ORMANDY, C. J. 1999. Prolactin controls mammary gland development via direct and indirect mechanisms. *Dev Biol,* 210**,** 96-106.

BRISKEN, C., PARK, S., VASS, T., LYDON, J. P., O'MALLEY, B. W. & WEINBERG, R. A. 1998. A paracrine role for the epithelial progesterone receptor in mammary gland development. *Proc Natl Acad Sci U S A,* 95**,** 5076-81.

BROSE, N. 2008. For better or for worse: complexins regulate SNARE function and vesicle fusion. *Traffic,* 9**,** 1403-13.

BRUENING, W., GIASSON, B. I., KLEIN-SZANTO, A. J., LEE, V. M., TROJANOWSKI, J. Q. & GODWIN, A. K. 2000. Synucleins are expressed in the majority of breast and ovarian carcinomas and in preneoplastic lesions of the ovary. *Cancer,* 88**,** 2154-63.

BUCHMAN, V. L., ADU, J., PINON, L. G., NINKINA, N. N. & DAVIES, A. M. 1998a. Persyn, a member of the synuclein family, influences neurofilament network integrity. *Nat Neurosci,* 1**,** 101-3.

BUCHMAN, V. L., HUNTER, H. J., PINON, L. G., THOMPSON, J., PRIVALOVA, E. M., NINKINA, N. N. & DAVIES, A. M. 1998b. Persyn, a member of the synuclein family, has a distinct pattern of expression in the developing nervous system. *J Neurosci,* 18**,** 9335-41.

BUONO, K. D., ROBINSON, G. W., MARTIN, C., SHI, S., STANLEY, P., TANIGAKI, K., HONJO, T. & HENNIGHAUSEN, L. 2006. The canonical Notch/RBP-J signaling pathway controls the balance of cell lineages in mammary epithelium during pregnancy. *Dev Biol,* 293**,** 565-80.

BURRE, J., SHARMA, M., TSETSENIS, T., BUCHMAN, V., ETHERTON, M. R. & SUDHOF, T. C. 2010. Alpha-synuclein promotes SNARE-complex assembly in vivo and in vitro. *Science,* 329**,** 1663-7.

CABIN, D. E., SHIMAZU, K., MURPHY, D., COLE, N. B., GOTTSCHALK, W., MCILWAIN, K. L., ORRISON, B., CHEN, A., ELLIS, C. E., PAYLOR, R., LU, B. & NUSSBAUM, R. L. 2002. Synaptic vesicle depletion correlates with attenuated synaptic responses to prolonged repetitive stimulation in mice lacking alpha-synuclein. *J Neurosci,* 22**,** 8797-807.

CANCERRESEARCHUK. 2012. *Cancer Statistics* [Online]. Cancer Research UK. Available: www.cancerresearchuk.org.

CHANDRA, S., FORNAI, F., KWON, H. B., YAZDANI, U., ATASOY, D., LIU, X., HAMMER, R. E., BATTAGLIA, G., GERMAN, D. C., CASTILLO, P. E. & SUDHOF, T. C. 2004. Double-knockout mice for alpha- and beta-synucleins: effect on synaptic functions. *Proc Natl Acad Sci U S A,* 101**,** 14966-71.

CHANDRA, S., GALLARDO, G., FERNANDEZ-CHACON, R., SCHLUTER, O. M. & SUDHOF, T. C. 2005. Alpha-synuclein cooperates with CSPalpha in preventing neurodegeneration. *Cell,* 123**,** 383-96.

CHAPMAN, R. S., LOURENCO, P. C., TONNER, E., FLINT, D. J., SELBERT, S., TAKEDA, K., AKIRA, S., CLARKE, A. R. & WATSON, C. J. 1999. Suppression of epithelial apoptosis and delayed mammary gland involution in mice with a conditional knockout of Stat3. *Genes Dev,* 13**,** 2604-16.

CHARTIER-HARLIN, M. C., KACHERGUS, J., ROUMIER, C., MOUROUX, V., DOUAY, X., LINCOLN, S., LEVECQUE, C., LARVOR, L., ANDRIEUX, J., HULIHAN, M., WAUCQUIER, N., DEFEBVRE, L., AMOUYEL, P., FARRER, M. & DESTEE, A. 2004. Alpha-synuclein locus duplication as a cause of familial Parkinson's disease. *Lancet,* 364**,** 1167-9.

CHEN, X., DE SILVA, H. A., PETTENATI, M. J., RAO, P. N., ST GEORGE-HYSLOP, P., ROSES, A. D., XIA, Y., HORSBURGH, K., UEDA, K. & SAITOH, T. 1995. The human NACP/alpha-synuclein gene: chromosome assignment to 4q21.3-q22 and TaqI RFLP analysis. *Genomics,* 26**,** 425-7.

CLARKSON, R. W. & WATSON, C. J. 2003. Microarray analysis of the involution switch. *J Mammary Gland Biol Neoplasia,* 8**,** 309-19.

CLAYTON, D. F. & GEORGE, J. M. 1998. The synucleins: a family of proteins involved in synaptic function, plasticity, neurodegeneration and disease. *Trends in Neurosciences,* 21**,** 249-254.

COULDREY, C., MOITRA, J., VINSON, C., ANVER, M., NAGASHIMA, K. & GREEN, J. 2002. Adipose tissue: a vital in vivo role in mammary gland development but not differentiation. *Dev Dyn,* 223**,** 459-68.

DAVIDSON, W. S., JONAS, A., CLAYTON, D. F. & GEORGE, J. M. 1998. Stabilization of alpha-synuclein secondary structure upon binding to synthetic membranes. *J Biol Chem,* 273**,** 9443-9.

EDWARDS, T. L., SCOTT, W. K., ALMONTE, C., BURT, A., POWELL, E. H., BEECHAM, G. W., WANG, L., ZUCHNER, S., KONIDARI, I., WANG, G., SINGER, C., NAHAB, F., SCOTT, B., STAJICH, J. M., PERICAK-VANCE, M., HAINES, J., VANCE, J. M. & MARTIN, E. R. 2010. Genome-wide association study confirms SNPs in SNCA and the MAPT region as common risk factors for Parkinson disease. *Ann Hum Genet,* 74**,** 97-109.

FATA, J. E., KONG, Y. Y., LI, J., SASAKI, T., IRIE-SASAKI, J., MOOREHEAD, R. A., ELLIOTT, R., SCULLY, S., VOURA, E. B., LACEY, D. L., BOYLE, W. J., KHOKHA, R. & PENNINGER, J. M. 2000. The osteoclast differentiation factor osteoprotegerin-ligand is essential for mammary gland development. *Cell,* 103**,** 41-50.

FATA, J. E., MORI, H., EWALD, A. J., ZHANG, H., YAO, E., WERB, Z. & BISSELL, M. J. 2007. The MAPK(ERK-1,2) pathway integrates distinct and antagonistic signals from TGFalpha and FGF7 in morphogenesis of mouse mammary epithelium. *Dev Biol,* 306**,** 193-207.

FATA, J. E., WERB, Z. & BISSELL, M. J. 2004. Regulation of mammary gland branching morphogenesis by the extracellular matrix and its remodeling enzymes. *Breast Cancer Res,* 6**,** 1-11.

FENG, Y., MANKA, D., WAGNER, K. U. & KHAN, S. A. 2007. Estrogen receptor-alpha expression in the mammary epithelium is required for ductal and alveolar morphogenesis in mice. *Proc Natl Acad Sci U S A,* 104**,** 14718-23.

GEORGE, J. M. 2002. The synucleins. *Genome Biol,* 3**,** REVIEWS3002.

GIASSON, B. I., DUDA, J. E., FORMAN, M. S., LEE, V. M. & TROJANOWSKI, J. Q. 2001. Prominent perikaryal expression of alpha- and beta-synuclein in neurons of dorsal root ganglion and in medullary neurons. *Exp Neurol,* 172**,** 354-62.

GOLEBIEWSKA, U., GUO, Y., KHALIKAPRASAD, N., ZURAWSKY, C., YERRAMILLI, V. S. & SCARLATA, S. 2012. gamma-Synuclein Interacts with Phospholipase Cbeta2 to Modulate G Protein Activation. *PLoS One,* 7**,** e41067.

GRUNDKER, C., SCHLOTAWA, L., VIERECK, V. & EMONS, G. 2001. Protein kinase C-independent stimulation of activator protein-1 and c-Jun N-terminal kinase activity in human endometrial cancer cells by the LHRH agonist triptorelin. *Eur J Endocrinol,* 145**,** 651-8.

GUO, J., SHOU, C., MENG, L., JIANG, B., DONG, B., YAO, L., XIE, Y., ZHANG, J., CHEN, Y., BUDMAN, D. R. & SHI, Y. E. 2007. Neuronal protein synuclein gamma predicts poor clinical outcome in breast cancer. *Int J Cancer,* 121**,** 1296-305.

GUPTA, A., GODWIN, A. K., VANDERVEER, L., LU, A. & LIU, J. 2003a. Hypomethylation of the synuclein gamma gene CpG island promotes its aberrant expression in breast carcinoma and ovarian carcinoma. *Cancer Res,* 63**,** 664-73.

GUPTA, A., INABA, S., WONG, O. K., FANG, G. & LIU, J. 2003b. Breast cancer-specific gene 1 interacts with the mitotic checkpoint kinase BubR1. *Oncogene,* 22**,** 7593-9.

GUSCHINA, I., MILLERSHIP, S., O'DONNELL, V., NINKINA, N., HARWOOD, J. & BUCHMAN, V. 2010. Lipid classes and fatty acid patterns are altered in the brain of gamma-synuclein null mutant mice. *Lipids,* 46**,** 121-30.

HASHIMOTO, M., ROCKENSTEIN, E., MANTE, M., MALLORY, M. & MASLIAH, E. 2001. beta-Synuclein inhibits alpha-synuclein aggregation: a possible role as an anti-parkinsonian factor. *Neuron,* 32**,** 213-23.

HENS, J. R. & WYSOLMERSKI, J. J. 2005. Key stages of mammary gland development: molecular mechanisms involved in the formation of the embryonic mammary gland. *Breast Cancer Res,* 7**,** 220-4.

HIBI, T., MORI, T., FUKUMA, M., YAMAZAKI, K., HASHIGUCHI, A., YAMADA, T., TANABE, M., AIURA, K., KAWAKAMI, T., OGIWARA, A., KOSUGE, T., KITAJIMA, M., KITAGAWA, Y. & SAKAMOTO, M. 2009. Synuclein-gamma is closely involved in perineural invasion and distant metastasis in mouse models and is a novel prognostic factor in pancreatic cancer. *Clin Cancer Res,* 15**,** 2864-71.

HINCK, L. & SILBERSTEIN, G. B. 2005. Key stages in mammary gland development: the mammary end bud as a motile organ. *Breast Cancer Res,* 7**,** 245-51.

HIREMATH, M., LYDON, J. P. & COWIN, P. 2007. The pattern of beta-catenin responsiveness within the mammary gland is regulated by progesterone receptor. *Development,* 134**,** 3703-12.

HUANG, P., DUDA, D. G., JAIN, R. K. & FUKUMURA, D. 2008. Histopathologic findings and establishment of novel tumor lines from spontaneous tumors in FVB/N mice. *Comp Med,* 58**,** 253-63.

IBANEZ, P., BONNET, A. M., DEBARGES, B., LOHMANN, E., TISON, F., POLLAK, P., AGID, Y., DURR, A. & BRICE, A. 2004. Causal relation between alpha-synuclein gene duplication and familial Parkinson's disease. *Lancet,* 364**,** 1169-71.

ICHIMURA, T., ISOBE, T., OKUYAMA, T., TAKAHASHI, N., ARAKI, K., KUWANO, R. & TAKAHASHI, Y. 1988. Molecular cloning of cDNA coding for brain-specific 14-3-3 protein, a protein kinase-dependent activator of tyrosine and tryptophan hydroxylases. *Proc Natl Acad Sci U S A,* 85**,** 7084-8.

INABA, S., LI, C., SHI, Y. E., SONG, D. Q., JIANG, J. D. & LIU, J. 2005. Synuclein gamma inhibits the mitotic checkpoint function and promotes chromosomal instability of breast cancer cells. *Breast Cancer Res Treat,* 94**,** 25-35.

IWAI, A., MASLIAH, E., YOSHIMOTO, M., GE, N., FLANAGAN, L., DE SILVA, H. A., KITTEL, A. & SAITOH, T. 1995. The precursor protein of non-A beta component of Alzheimer's disease amyloid is a presynaptic protein of the central nervous system. *Neuron,* 14**,** 467-75.

JAKES, R., SPILLANTINI, M. G. & GOEDERT, M. 1994. Identification of two distinct synucleins from human brain. *FEBS Lett,* 345**,** 27-32.

JEANNOTTE, A. M., MCCARTHY, J. G., REDEI, E. E. & SIDHU, A. 2009. Desipramine modulation of alpha-, gamma-synuclein, and the norepinephrine transporter in an animal model of depression. *Neuropsychopharmacology,* 34**,** 987-98.

JENCO, J. M., RAWLINGSON, A., DANIELS, B. & MORRIS, A. J. 1998. Regulation of phospholipase D2: selective inhibition of mammalian phospholipase D isoenzymes by alpha- and beta-synucleins. *Biochemistry,* 37**,** 4901-9.

JI, H., LIU, Y. E., JIA, T., WANG, M., LIU, J., XIAO, G., JOSEPH, B. K., ROSEN, C. & SHI, Y. E. 1997. Identification of a breast cancer-specific gene, BCSG1, by direct differential cDNA sequencing. *Cancer Res,* 57**,** 759-64.

JIA, T., LIU, Y. E., LIU, J. & SHI, Y. E. 1999. Stimulation of breast cancer invasion and metastasis by synuclein gamma. *Cancer Res,* 59**,** 742-7.

JIANG, Y., LIU, Y. E., GOLDBERG, I. D. & SHI, Y. E. 2004. Gamma synuclein, a novel heat-shock protein-associated chaperone, stimulates ligand-dependent estrogen receptor alpha signaling and mammary tumorigenesis. *Cancer Res,* 64**,** 4539-46.

JIANG, Y., LIU, Y. E., LU, A., GUPTA, A., GOLDBERG, I. D., LIU, J. & SHI, Y. E. 2003. Stimulation of estrogen receptor signaling by gamma synuclein. *Cancer Res,* 63**,** 3899-903.

JONES, F. E. & STERN, D. F. 1999. Expression of dominant-negative ErbB2 in the mammary gland of transgenic mice reveals a role in lobuloalveolar development and lactation. *Oncogene,* 18**,** 3481-90.

KHALED, W. T., READ, E. K., NICHOLSON, S. E., BAXTER, F. O., BRENNAN, A. J., CAME, P. J., SPRIGG, N., MCKENZIE, A. N. & WATSON, C. J. 2007. The IL-4/IL-13/Stat6 signalling pathway promotes luminal mammary epithelial cell development. *Development,* 134**,** 2739-50.

KRITIKOU, E. A., SHARKEY, A., ABELL, K., CAME, P. J., ANDERSON, E., CLARKSON, R. W. & WATSON, C. J. 2003. A dual, non-redundant, role for LIF as a regulator of development and STAT3-mediated cell death in mammary gland. *Development,* 130**,** 3459-68.

KRUGER, R., KUHN, W., MULLER, T., WOITALLA, D., GRAEBER, M., KOSEL, S., PRZUNTEK, H., EPPLEN, J. T., SCHOLS, L. & RIESS, O. 1998. Ala30Pro

mutation in the gene encoding alpha-synuclein in Parkinson's disease. *Nat Genet,* 18**,** 106-8.

LAVEDAN, C. 1998. The synuclein family. *Genome Res,* 8**,** 871-80.

LAVEDAN, C., LEROY, E., DEHEJIA, A., BUCHHOLTZ, S., DUTRA, A., NUSSBAUM, R. L. & POLYMEROPOULOS, M. H. 1998. Identification, localization and characterization of the human gamma-synuclein gene. *Hum Genet,* 103**,** 106-12.

LEE, F. J., LIU, F., PRISTUPA, Z. B. & NIZNIK, H. B. 2001. Direct binding and functional coupling of alpha-synuclein to the dopamine transporters accelerate dopamine-induced apoptosis. *FASEB J,* 15**,** 916-26.

LI, J. Y., HENNING JENSEN, P. & DAHLSTROM, A. 2002a. Differential localization of alpha-, beta- and gamma-synucleins in the rat CNS. *Neuroscience,* 113**,** 463-78.

LI, L., CLEARY, S., MANDARANO, M. A., LONG, W., BIRCHMEIER, C. & JONES, F. E. 2002b. The breast proto-oncogene, HRGalpha regulates epithelial proliferation and lobuloalveolar development in the mouse mammary gland. *Oncogene,* 21**,** 4900-7.

LI, M., LIU, X., ROBINSON, G., BAR-PELED, U., WAGNER, K. U., YOUNG, W. S., HENNIGHAUSEN, L. & FURTH, P. A. 1997. Mammary-derived signals activate programmed cell death during the first stage of mammary gland involution. *Proc Natl Acad Sci U S A,* 94**,** 3425-30.

LIU, H., LIU, W., WU, Y., ZHOU, Y., XUE, R., LUO, C., WANG, L., ZHAO, W., JIANG, J. D. & LIU, J. 2005. Loss of epigenetic control of synuclein-gamma gene as a molecular indicator of metastasis in a wide range of human cancers. *Cancer Res,* 65**,** 7635-43.

LIU, H., ZHOU, Y., BOGGS, S. E., BELINSKY, S. A. & LIU, J. 2007a. Cigarette smoke induces demethylation of prometastatic oncogene synuclein-gamma in lung cancer cells by downregulation of DNMT3B. *Oncogene,* 26**,** 5900-10.

LIU, J., SPENCE, M. J., ZHANG, Y. L., JIANG, Y., LIU, Y. E. & SHI, Y. E. 2000. Transcriptional suppression of synuclein gamma (SNCG) expression in human breast cancer cells by the growth inhibitory cytokine oncostatin M. *Breast Cancer Res Treat,* 62**,** 99-107.

LIU, Y. E., PU, W., JIANG, Y., SHI, D., DACKOUR, R. & SHI, Y. E. 2007b. Chaperoning of estrogen receptor and induction of mammary gland proliferation by neuronal protein synuclein gamma. *Oncogene,* 26**,** 2115-25.

LONG, W., WAGNER, K. U., LLOYD, K. C., BINART, N., SHILLINGFORD, J. M., HENNIGHAUSEN, L. & JONES, F. E. 2003. Impaired differentiation and lactational failure of Erbb4-deficient mammary glands identify ERBB4 as an obligate mediator of STAT5. *Development,* 130**,** 5257-68.

LU, A., GUPTA, A., LI, C., AHLBORN, T. E., MA, Y., SHI, E. Y. & LIU, J. 2001. Molecular mechanisms for aberrant expression of the human breast cancer specific gene 1 in breast cancer cells: control of transcription by DNA methylation and intronic sequences. *Oncogene,* 20**,** 5173-85.

LU, A., ZHANG, F., GUPTA, A. & LIU, J. 2002. Blockade of AP1 transactivation abrogates the abnormal expression of breast cancer-specific gene 1 in breast cancer cells. *J Biol Chem,* 277**,** 31364-72.

MAILLEUX, A. A., OVERHOLTZER, M., SCHMELZLE, T., BOUILLET, P., STRASSER, A. & BRUGGE, J. S. 2007. BIM regulates apoptosis during mammary ductal morphogenesis, and its absence reveals alternative cell death mechanisms. *Dev Cell,* 12**,** 221-34.

MALLEPELL, S., KRUST, A., CHAMBON, P. & BRISKEN, C. 2006. Paracrine signaling through the epithelial estrogen receptor alpha is required for proliferation and morphogenesis in the mammary gland. *Proc Natl Acad Sci U S A,* 103**,** 2196-201.

MANNA, T., SARKAR, T., PODDAR, A., ROYCHOWDHURY, M., DAS, K. P. & BHATTACHARYYA, B. 2001. Chaperone-like activity of tubulin. binding and reactivation of unfolded substrate enzymes. *J Biol Chem,* 276**,** 39742-7.

MAROTEAUX, L., CAMPANELLI, J. T. & SCHELLER, R. H. 1988. Synuclein: a neuron-specific protein localized to the nucleus and presynaptic nerve terminal. *J Neurosci,* 8**,** 2804-15.

MCDANIEL, S. M., RUMER, K. K., BIROC, S. L., METZ, R. P., SINGH, M., PORTER, W. & SCHEDIN, P. 2006. Remodeling of the mammary microenvironment after lactation promotes breast tumor cell metastasis. *Am J Pathol,* 168**,** 608-20.

MILLERSHIP, S. J., NINKINA, N., GUSCHINA, I. A., NORTON, J., BRAMBILLA, R.,

OORT, P. J., ADAMA, S. H., DENNIS, R. J., VOSHOL, P. J., ROCHFORD, J. J. & BUCHMAN, V. L. 2012. Increased lipolysis and altered lipid homeostasis protect γ-synuclein-null mutant mice from diet-induced obesity. *Proc Natl Acad Sci U S A,* 109**,** 20943-48.

MORI, F., TANJI, K., YOSHIMOTO, M., TAKAHASHI, H. & WAKABAYASHI, K. 2002. Immunohistochemical comparison of alpha- and beta-synuclein in adult rat central nervous system. *Brain Res,* 941**,** 118-26.

MOZZI, R., BURATTA, S. & GORACCI, G. 2003. Metabolism and functions of phosphatidylserine in mammalian brain. *Neurochem Res,* 28**,** 195-214.

MULLER, W. J., SINN, E., PATTENGALE, P. K., WALLACE, R. & LEDER, P. 1988. Single-step induction of mammary adenocarcinoma in transgenic mice bearing the activated c-neu oncogene. *Cell,* 54**,** 105-115.

MURPHY, D. D., RUETER, S. M., TROJANOWSKI, J. Q. & LEE, V. M. 2000. Synucleins are developmentally expressed, and alpha-synuclein regulates the size of the presynaptic vesicular pool in primary hippocampal neurons. *J Neurosci,* 20**,** 3214-20.

NAKAJO, S., OMATA, K., AIUCHI, T., SHIBAYAMA, T., OKAHASHI, I., OCHIAI, H., NAKAI, Y., NAKAYA, K. & NAKAMURA, Y. 1990. Purification and characterization of a novel brain-specific 14-kDa protein. *J Neurochem,* 55**,** 2031-8.

NAKAJO, S., TSUKADA, K., OMATA, K., NAKAMURA, Y. & NAKAYA, K. 1993. A new brain-specific 14-kDa protein is a phosphoprotein. Its complete amino acid sequence and evidence for phosphorylation. *Eur J Biochem,* 217**,** 1057-63.

NAYLOR, M. J., LI, N., CHEUNG, J., LOWE, E. T., LAMBERT, E., MARLOW, R., WANG, P., SCHATZMANN, F., WINTERMANTEL, T., SCHUETZ, G., CLARKE, A. R., MUELLER, U., HYNES, N. E. & STREULI, C. H. 2005. Ablation of beta1 integrin in mammary epithelium reveals a key role for integrin in glandular morphogenesis and differentiation. *J Cell Biol,* 171**,** 717-28.

NELSON, C. M., VANDUIJN, M. M., INMAN, J. L., FLETCHER, D. A. & BISSELL, M. J. 2006. Tissue geometry determines sites of mammary branching morphogenesis in organotypic cultures. *Science,* 314**,** 298-300.

NGUYEN, A. V. & POLLARD, J. W. 2000. Transforming growth factor beta3 induces cell death during the first stage of mammary gland involution. *Development,* 127**,** 3107-18.

NINKINA, N., PAPACHRONI, K., ROBERTSON, D. C., SCHMIDT, O., DELANEY, L., O'NEILL, F., COURT, F., ROSENTHAL, A., FLEETWOOD-WALKER, S. M., DAVIES, A. M. & BUCHMAN, V. L. 2003. Neurons expressing the highest levels of gamma-synuclein are unaffected by targeted inactivation of the gene. *Mol Cell Biol,* 23**,** 8233-45.

NINKINA, N. N., ALIMOVA-KOST, M. V., PATERSON, J. W., DELANEY, L., COHEN, B. B., IMREH, S., GNUCHEV, N. V., DAVIES, A. M. & BUCHMAN, V. L. 1998. Organization, expression and polymorphism of the human persyn gene. *Hum Mol Genet,* 7**,** 1417-24.

NINKINA, N. N., PRIVALOVA, E. M., PINŃ, L. G. P., DAVIES, A. M. & BUCHMAN, V. L. 1999. Developmentally Regulated Expression of Persyn, a Member of the Synuclein Family, in Skin. *Experimental Cell Research,* 246**,** 308-311.

OAKES, S. R., HILTON, H. N. & ORMANDY, C. J. 2006. The alveolar switch: coordinating the proliferative cues and cell fate decisions that drive the formation of lobuloalveoli from ductal epithelium. *Breast Cancer Res,* 8**,** 207.

OAKS, A. W. & SIDHU, A. 2011. Synuclein modulation of monoamine transporters. *FEBS Lett*.

OFTEDAL, O. T. 2002. The origin of lactation as a water source for parchment-shelled eggs. *J Mammary Gland Biol Neoplasia,* 7**,** 253-66.

OORT, P. J., KNOTTS, T. A., GRINO, M., NAOUR, N., BASTARD, J. P., CLEMENT, K., NINKINA, N., BUCHMAN, V. L., PERMANA, P. A., LUO, X., PAN, G., DUNN, T. N. & ADAMS, S. H. 2008. Gamma-synuclein is an adipocyte-neuron gene coordinately expressed with leptin and increased in human obesity. *J Nutr,* 138**,** 841-8.

ORMANDY, C. J., NAYLOR, M., HARRIS, J., ROBERTSON, F., HORSEMAN, N. D., LINDEMAN, G. J., VISVADER, J. & KELLY, P. A. 2003. Investigation of the transcriptional changes underlying functional defects in the mammary glands of prolactin receptor knockout mice. *Recent Prog Horm Res,* 58**,** 297-323.

OSTREROVA, N., PETRUCELLI, L., FARRER, M., MEHTA, N., CHOI, P., HARDY, J. & WOLOZIN, B. 1999. alpha-Synuclein shares physical and functional homology with 14-3-3 proteins. *J Neurosci,* 19**,** 5782-91.

PALS, P., LINCOLN, S., MANNING, J., HECKMAN, M., SKIPPER, L., HULIHAN, M., VAN DEN BROECK, M., DE POOTER, T., CRAS, P., CROOK, J., VAN BROECKHOVEN, C. & FARRER, M. J. 2004. alpha-Synuclein promoter confers susceptibility to Parkinson's disease. *Ann Neurol,* 56**,** 591-5.

PAN, Z. Z., BRUENING, W., GIASSON, B. I., LEE, V. M. & GODWIN, A. K. 2002. Gamma-synuclein promotes cancer cell survival and inhibits stress- and chemotherapy drug-induced apoptosis by modulating MAPK pathways. *J Biol Chem,* 277**,** 35050-60.

PAN, Z. Z., BRUENING, W. & GODWIN, A. K. 2006. Involvement of RHO GTPases and ERK in synuclein-gamma enhanced cancer cell motility. *Int J Oncol,* 29**,** 1201-5.

PANKRATZ, N., WILK, J. B., LATOURELLE, J. C., DESTEFANO, A. L., HALTER, C., PUGH, E. W., DOHENY, K. F., GUSELLA, J. F., NICHOLS, W. C., FOROUD, T. & MYERS, R. H. 2009. Genomewide association study for susceptibility genes contributing to familial Parkinson disease. *Hum Genet,* 124**,** 593-605.

PARK, J. Y. & LANSBURY, P. T., JR. 2003. Beta-synuclein inhibits formation of alpha-synuclein protofibrils: a possible therapeutic strategy against Parkinson's disease. *Biochemistry,* 42**,** 3696-700.

PEAKER, M. 2002. The mammary gland in mammalian evolution: a brief commentary on some of the concepts. *J Mammary Gland Biol Neoplasia,* 7**,** 347-53.

PEREZ, R. G., WAYMIRE, J. C., LIN, E., LIU, J. J., GUO, F. & ZIGMOND, M. J. 2002. A role for alpha-synuclein in the regulation of dopamine biosynthesis. *J Neurosci,* 22**,** 3090-9.

PERRIN, R. J., WOODS, W. S., CLAYTON, D. F. & GEORGE, J. M. 2000. Interaction of human alpha-Synuclein and Parkinson's disease variants with phospholipids. Structural analysis using site-directed mutagenesis. *J Biol Chem,* 275**,** 34393-8.

POLYMEROPOULOS, M. H., LAVEDAN, C., LEROY, E., IDE, S. E., DEHEJIA, A., DUTRA, A., PIKE, B., ROOT, H., RUBENSTEIN, J., BOYER, R., STENROOS, E. S., CHANDRASEKHARAPPA, S., ATHANASSIADOU, A., PAPAPETROPOULOS, T., JOHNSON, W. G., LAZZARINI, A. M., DUVOISIN, R. C., DI IORIO, G., GOLBE, L. I. & NUSSBAUM, R. L. 1997. Mutation in the

alpha-synuclein gene identified in families with Parkinson's disease. *Science,* 276**,** 2045-7.

PRONIN, A. N., MORRIS, A. J., SURGUCHOV, A. & BENOVIC, J. L. 2000. Synucleins are a novel class of substrates for G protein-coupled receptor kinases. *J Biol Chem,* 275**,** 26515-22.

QUAGLINO, A., SALIERNO, M., PELLEGROTTI, J., RUBINSTEIN, N. & KORDON, E. C. 2009. Mechanical strain induces involution-associated events in mammary epithelial cells. *BMC Cell Biol,* 10**,** 55.

RALPH, R. J., PAULUS, M. P. & GEYER, M. A. 2001. Strain-specific effects of amphetamine on prepulse inhibition and patterns of locomotor behavior in mice. *J Pharmacol Exp Ther,* 298**,** 148-55.

REIM, K., MANSOUR, M., VAROQUEAUX, F., MCMAHON, H. T., SUDHOF, T. C., BROSE, N. & ROSENMUND, C. 2001. Complexins regulate a late step in Ca2+-dependent neurotransmitter release. *Cell,* 104**,** 71-81.

SACCO, M. G., GRIBALDO, L., BARBIERI, O., TURCHI, G., ZUCCHI, I., COLLOTTA, A., BAGNASCO, L., BARONE, D., MONTAGNA, C., VILLA, A., MARAFANTE, E. & VEZZONI, P. 1998. Establishment and characterization of a new mammary adenocarcinoma cell line derived from MMTV neu transgenic mice. *Breast Cancer Res Treat,* 47**,** 171-80.

SAID, T. K., CONNEELY, O. M., MEDINA, D., O'MALLEY, B. W. & LYDON, J. P. 1997. Progesterone, in addition to estrogen, induces cyclin D1 expression in the murine mammary epithelial cell, in vivo. *Endocrinology,* 138**,** 3933-9.

SATAKE, W., NAKABAYASHI, Y., MIZUTA, I., HIROTA, Y., ITO, C., KUBO, M., KAWAGUCHI, T., TSUNODA, T., WATANABE, M., TAKEDA, A., TOMIYAMA, H., NAKASHIMA, K., HASEGAWA, K., OBATA, F., YOSHIKAWA, T., KAWAKAMI, H., SAKODA, S., YAMAMOTO, M., HATTORI, N., MURATA, M., NAKAMURA, Y. & TODA, T. 2009. Genome-wide association study identifies common variants at four loci as genetic risk factors for Parkinson's disease. *Nat Genet,* 41**,** 1303-7.

SCHORR, K., LI, M., BAR-PELED, U., LEWIS, A., HEREDIA, A., LEWIS, B., KNUDSON, C. M., KORSMEYER, S. J., JAGER, R., WEIHER, H. & FURTH, P. A. 1999. Gain of Bcl-2 is more potent than bax loss in regulating mammary epithelial cell survival in vivo. *Cancer Res,* 59**,** 2541-5.

SEAGROVES, T. N., KRNACIK, S., RAUGHT, B., GAY, J., BURGESS-BEUSSE, B., DARLINGTON, G. J. & ROSEN, J. M. 1998. C/EBPbeta, but not C/EBPalpha, is essential for ductal morphogenesis, lobuloalveolar proliferation, and functional differentiation in the mouse mammary gland. *Genes Dev,* 12**,** 1917-28.

SHEN, P. H., FAN, Q. X., LI, Y. W., ZHANG, W., HE, X. K., WANG, Z. & ZHANG, Y. H. 2011. SNCG shRNA suppressed breast cancer cell xenograft formation and growth in nude mice. *Chin Med J (Engl),* 124**,** 1524-8.

SIMON-SANCHEZ, J., SCHULTE, C., BRAS, J. M., SHARMA, M., GIBBS, J. R., BERG, D., PAISAN-RUIZ, C., LICHTNER, P., SCHOLZ, S. W., HERNANDEZ, D. G., KRUGER, R., FEDEROFF, M., KLEIN, C., GOATE, A., PERLMUTTER, J., BONIN, M., NALLS, M. A., ILLIG, T., GIEGER, C., HOULDEN, H., STEFFENS, M., OKUN, M. S., RACETTE, B. A., COOKSON, M. R., FOOTE, K. D., FERNANDEZ, H. H., TRAYNOR, B. J., SCHREIBER, S., AREPALLI, S., ZONOZI, R., GWINN, K., VAN DER BRUG, M., LOPEZ, G., CHANOCK, S. J., SCHATZKIN, A., PARK, Y., HOLLENBECK, A., GAO, J., HUANG, X., WOOD, N. W., LORENZ, D., DEUSCHL, G., CHEN, H., RIESS, O., HARDY, J. A., SINGLETON, A. B. & GASSER, T. 2009. Genome-wide association study reveals genetic risk underlying Parkinson's disease. *Nat Genet,* 41**,** 1308-12.

SINGH, V. K., ZHOU, Y., MARSH, J. A., UVERSKY, V. N., FORMAN-KAY, J. D., LIU, J. & JIA, Z. 2007. Synuclein-gamma targeting peptide inhibitor that enhances sensitivity of breast cancer cells to antimicrotubule drugs. *Cancer Res,* 67**,** 626-33.

SINGLETON, A., GWINN-HARDY, K., SHARABI, Y., LI, S. T., HOLMES, C., DENDI, R., HARDY, J., CRAWLEY, A. & GOLDSTEIN, D. S. 2004. Association between cardiac denervation and parkinsonism caused by alpha-synuclein gene triplication. *Brain,* 127**,** 768-72.

SMULDERS, R., CARVER, J. A., LINDNER, R. A., VAN BOEKEL, M. A., BLOEMENDAL, H. & DE JONG, W. W. 1996. Immobilization of the C-terminal extension of bovine alphaA-crystallin reduces chaperone-like activity. *J Biol Chem,* 271**,** 29060-6.

SOHN, B. H., MOON, H. B., KIM, T. Y., KANG, H. S., BAE, Y. S., LEE, K. K. & KIM, S. J. 2001. Interleukin-10 up-regulates tumour-necrosis-factor-alpha-related

apoptosis-inducing ligand (TRAIL) gene expression in mammary epithelial cells at the involution stage. *Biochem J,* 360**,** 31-8.

SONG, J., SAPI, E., BROWN, W., NILSEN, J., TARTARO, K., KACINSKI, B. M., CRAFT, J., NAFTOLIN, F. & MOR, G. 2000. Roles of Fas and Fas ligand during mammary gland remodeling. *J Clin Invest,* 106**,** 1209-20.

SONG, M. S., PARK, Y. K., LEE, J. H. & PARK, K. 2001. Induction of glucose-regulated protein 78 by chronic hypoxia in human gastric tumor cells through a protein kinase C-epsilon/ERK/AP-1 signaling cascade. *Cancer Res,* 61**,** 8322-30.

SOUZA, J. M., GIASSON, B. I., LEE, V. M. & ISCHIROPOULOS, H. 2000. Chaperone-like activity of synucleins. *FEBS Lett,* 474**,** 116-9.

SPECHT, C. G., TIGARET, C. M., RAST, G. F., THALHAMMER, A., RUDHARD, Y. & SCHOEPFER, R. 2005. Subcellular localisation of recombinant alpha- and gamma-synuclein. *Mol Cell Neurosci,* 28**,** 326-34.

SPILLANTINI, M. G., DIVANE, A. & GOEDERT, M. 1995. Assignment of human alpha-synuclein (SNCA) and beta-synuclein (SNCB) genes to chromosomes 4q21 and 5q35. *Genomics,* 27**,** 379-81.

SPILLANTINI, M. G., SCHMIDT, M. L., LEE, V. M., TROJANOWSKI, J. Q., JAKES, R. & GOEDERT, M. 1997. Alpha-synuclein in Lewy bodies. *Nature,* 388**,** 839-40.

STERN, D. F. 2003. ErbBs in mammary development. *Experimental Cell Research,* 284**,** 89-98.

STERNLICHT, M. D. 2006. Key stages in mammary gland development: the cues that regulate ductal branching morphogenesis. *Breast Cancer Res,* 8**,** 201.

STERNLICHT, M. D., KOUROS-MEHR, H., LU, P. & WERB, Z. 2006. Hormonal and local control of mammary branching morphogenesis. *Differentiation,* 74**,** 365-81.

STRICKLAND, P., SHIN, G. C., PLUMP, A., TESSIER-LAVIGNE, M. & HINCK, L. 2006. Slit2 and netrin 1 act synergistically as adhesive cues to generate tubular bi-layers during ductal morphogenesis. *Development,* 133**,** 823-32.

SUNG, Y. H. & ELIEZER, D. 2007. Residual structure, backbone dynamics, and interactions within the synuclein family. *J Mol Biol,* 372**,** 689-707.

SURGUCHEVA, I., MCMAHON, B. & SURGUCHOV, A. 2006. gamma-synuclein has a dynamic intracellular localization. *Cell Motil Cytoskeleton,* 63**,** 447-58.

SURGUCHEVA, I. & SURGUCHOV, A. 2008. Gamma-synuclein: cell-type-specific promoter activity and binding to transcription factors. *J Mol Neurosci,* 35**,** 267-71.

SURGUCHOV, A., PALAZZO, R. E. & SURGUCHEVA, I. 2001. Gamma synuclein: subcellular localization in neuronal and non-neuronal cells and effect on signal transduction. *Cell Motil Cytoskeleton,* 49**,** 218-28.

SURGUCHOV, A., SURGUCHEVA, I., SOLESSIO, E. & BAEHR, W. 1999. Synoretin--A new protein belonging to the synuclein family. *Mol Cell Neurosci,* 13**,** 95-103.

TEULIERE, J., FARALDO, M. M., DEUGNIER, M. A., SHTUTMAN, M., BEN-ZE'EV, A., THIERY, J. P. & GLUKHOVA, M. A. 2005. Targeted activation of beta-catenin signaling in basal mammary epithelial cells affects mammary development and leads to hyperplasia. *Development,* 132**,** 267-77.

THANGARAJU, M., RUDELIUS, M., BIERIE, B., RAFFELD, M., SHARAN, S., HENNIGHAUSEN, L., HUANG, A. M. & STERNECK, E. 2005. C/EBPdelta is a crucial regulator of pro-apoptotic gene expression during mammary gland involution. *Development,* 132**,** 4675-85.

TOUCHMAN, J. W., DEHEJIA, A., CHIBA-FALEK, O., CABIN, D. E., SCHWARTZ, J. R., ORRISON, B. M., POLYMEROPOULOS, M. H. & NUSSBAUM, R. L. 2001. Human and mouse alpha-synuclein genes: comparative genomic sequence analysis and identification of a novel gene regulatory element. *Genome Res,* 11**,** 78-86.

UEDA, K., FUKUSHIMA, H., MASLIAH, E., XIA, Y., IWAI, A., YOSHIMOTO, M., OTERO, D. A., KONDO, J., IHARA, Y. & SAITOH, T. 1993. Molecular cloning of cDNA encoding an unrecognized component of amyloid in Alzheimer disease. *Proc Natl Acad Sci U S A,* 90**,** 11282-6.

UVERSKY, V. N., LI, J., SOUILLAC, P., MILLETT, I. S., DONIACH, S., JAKES, R., GOEDERT, M. & FINK, A. L. 2002. Biophysical properties of the synucleins and their propensities to fibrillate: inhibition of alpha-synuclein assembly by beta- and gamma-synucleins. *J Biol Chem,* 277**,** 11970-8.

VANHOUTEN, J., SULLIVAN, C., BAZINET, C., RYOO, T., CAMP, R., RIMM, D. L., CHUNG, G. & WYSOLMERSKI, J. 2010. PMCA2 regulates apoptosis during mammary gland involution and predicts outcome in breast cancer. *Proc Natl Acad Sci U S A,* 107**,** 11405-10.

WALCZEWSKA, A., STEPIEN, T., BEWICZ-BINKOWSKA, D. & ZGORZYNSKA, E. 2011. [The role of docosahexaenoic acid in neuronal function]. *Postepy Hig Med Dosw (Online),* 65**,** 314-27.

WALTON, K. D., WAGNER, K. U., RUCKER, E. B., 3RD, SHILLINGFORD, J. M., MIYOSHI, K. & HENNIGHAUSEN, L. 2001. Conditional deletion of the bcl-x gene from mouse mammary epithelium results in accelerated apoptosis during involution but does not compromise cell function during lactation. *Mech Dev,* 109**,** 281-93.

WATSON, C. J. & KHALED, W. T. 2008. Mammary development in the embryo and adult: a journey of morphogenesis and commitment. *Development,* 135**,** 995-1003.

WATSON, C. J. & KREUZALER, P. A. 2011. Remodeling mechanisms of the mammary gland during involution. *Int J Dev Biol,* 55**,** 757-62.

WERSINGER, C. & SIDHU, A. 2009. Partial regulation of serotonin transporter function by gamma-synuclein. *Neurosci Lett,* 453**,** 157-61.

WIDAKOWICH, C., DE AZAMBUJA, E., GIL, T., CARDOSO, F., DINH, P., AWADA, A. & PICCART-GEBHART, M. 2007. Molecular targeted therapies in breast cancer: where are we now? *Int J Biochem Cell Biol,* 39**,** 1375-87.

WU, K., QUAN, Z., WENG, Z., LI, F., ZHANG, Y., YAO, X., CHEN, Y., BUDMAN, D., GOLDBERG, I. D. & SHI, Y. E. 2007. Expression of neuronal protein synuclein gamma gene as a novel marker for breast cancer prognosis. *Breast Cancer Res Treat,* 101**,** 259-67.

WU, K., WENG, Z., TAO, Q., LIN, G., WU, X., QIAN, H., ZHANG, Y., DING, X., JIANG, Y. & SHI, Y. E. 2003. Stage-specific expression of breast cancer-specific gene gamma-synuclein. *Cancer Epidemiol Biomarkers Prev,* 12**,** 920-5.

XIA, Y., SAITOH, T., UEDA, K., TANAKA, S., CHEN, X., HASHIMOTO, M., HSU, L., CONRAD, C., SUNDSMO, M., YOSHIMOTO, M., THAL, L., KATZMAN, R. & MASLIAH, E. 2001. Characterization of the human alpha-synuclein gene: Genomic structure, transcription start site, promoter region and polymorphisms. *J Alzheimers Dis,* 3**,** 485-494.

ZARRANZ, J. J., ALEGRE, J., GOMEZ-ESTEBAN, J. C., LEZCANO, E., ROS, R., AMPUERO, I., VIDAL, L., HOENICKA, J., RODRIGUEZ, O., ATARES, B., LLORENS, V., GOMEZ TORTOSA, E., DEL SER, T., MUNOZ, D. G. & DE

YEBENES, J. G. 2004. The new mutation, E46K, of alpha-synuclein causes Parkinson and Lewy body dementia. *Ann Neurol,* 55**,** 164-73.

ZHANG, H., KOUADIO, A., CARTLEDGE, D. & GODWIN, A. K. 2010. Role of gamma-synuclein in microtubule regulation. *Exp Cell Res*.

ZHAO, W., LIU, H., LIU, W., WU, Y., CHEN, W., JIANG, B., ZHOU, Y., XUE, R., LUO, C., WANG, L., JIANG, J. D. & LIU, J. 2006. Abnormal activation of the synuclein-gamma gene in hepatocellular carcinomas by epigenetic alteration. *Int J Oncol,* 28**,** 1081-8.

ZHOU, C. Q., LIU, S., XUE, L. Y., WANG, Y. H., ZHU, H. X., LU, N. & XU, N. Z. 2003. Down-regulation of gamma-synuclein in human esophageal squamous cell carcinoma. *World J Gastroenterol,* 9**,** 1900-3.

ZHOU, Y., INABA, S. & LIU, J. 2006. Inhibition of synuclein-gamma expression increases the sensitivity of breast cancer cells to paclitaxel treatment. *Int J Oncol,* 29**,** 289-95.

Appendix

Appendix 1. Conventional PCR genotyping for selection of the breeders, control and experimental animals.

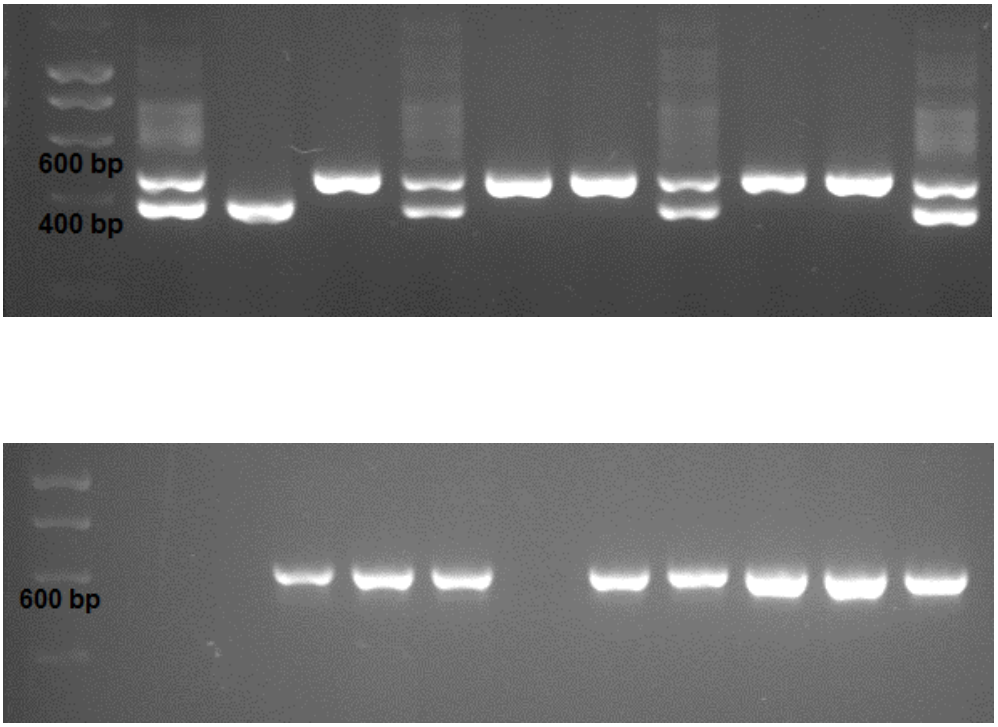

Upper panel: γ-synuclein genotyping for selection of breeder, control and experimental animals. Three primers, with a common upstream primer for both Wt and KO alleles and a specific downstream primer for each, produced two amplified fragments, a wild-type fragment of 480 bp and a knock-out one of 397 bp.

Lower panel: a 622 bp fragment amplified from NK transgene for selection of experimental females.

Appendix 2. qRT-PCR for selection of the NK homozygous male breeder parent used for generating the NK hemizygous experimental females.

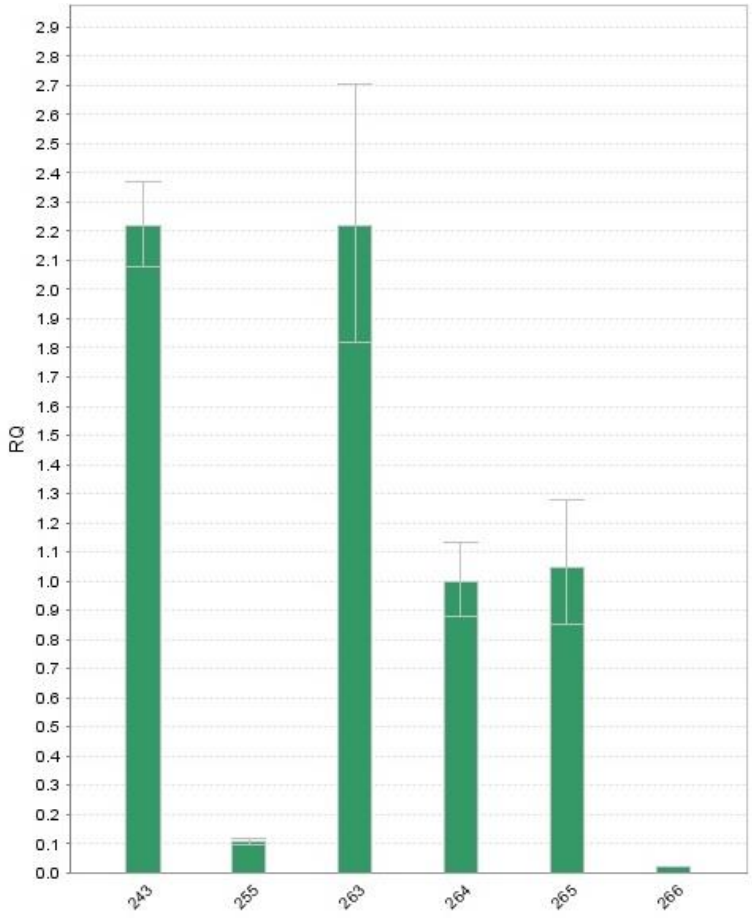

Real-time PCR utilizing CYBR Green chemistry was used to detect amplification of the NK transgene and the housekeeping gene GAPDH (for use as an internal control). 243/263, 264/265 and 255/266 represent NK transgene homozygous, NK transgene hemizygous and Wt genotypes, respectively. Fold change was calculated using the $2^{-\Delta\Delta Ct}$ comparative method. (RQ: relative quantification).